DOT/FAA/AR-06/45

Air Traffic Organization
Operations Planning
Office of Aviation Research and Development
Washington, DC 20591

Investigating the Thin-Film Versus Bulk Material Properties of Structural Adhesives

May 2008

Final Report

This document is available to the U.S. public through the National Technical Information Service (NTIS), Springfield, Virginia 22161.

U.S. Department of Transportation
Federal Aviation Administration

NOTICE

This document is disseminated under the sponsorship of the U.S. Department of Transportation in the interest of information exchange. The United States Government assumes no liability for the contents or use thereof. The United States Government does not endorse products or manufacturers. Trade or manufacturer's names appear herein solely because they are considered essential to the objective of this report. This document does not constitute FAA certification policy. Consult your local FAA aircraft certification office as to its use.

This report is available at the Federal Aviation Administration William J. Hughes Technical Center's Full-Text Technical Reports page: actlibrary.tc.faa.gov in Adobe Acrobat portable document format (PDF).

Technical Report Documentation Page

1. Report No.	2. Government Accession No.	3. Recipient's Catalog No.
DOT/FAA/AR-06/45		

4. Title and Subtitle	5. Report Date
INVESTIGATING THE THIN-FILM VERSUS BULK MATERIAL PROPERTIES OF STRUCTURAL ADHESIVES	May 2008
	6. Performing Organization Code
7. Author(s)	8. Performing Organization Report No.
Nicholas Burst and Daniel O. Adams	
9. Performing Organization Name and Address	10. Work Unit No. (TRAIS)
Department of Mechanical Engineering University of Utah Salt Lake City, Utah 84112	
	11. Contract or Grant No.
12. Sponsoring Agency Name and Address	13. Type of Report and Period Covered
U.S. Department of Transportation Federal Aviation Administration Air Traffic Organization Operations Planning Office of Aviation Research and Development Washington, DC 20591	Final Report
	14. Sponsoring Agency Code ACE-110

15. Supplementary Notes

The Federal Aviation Administration Airport and Aircraft Safety R&D Division Technical Monitor was Peter Shyprykevich.

6. Abstract

A combined experimental and computational investigation was performed to determine whether the material properties of structural adhesives differ between their thin-film in situ and bulk forms. Both shear and tensile tests were performed using bulk adhesive specimens as well as in situ adhesive specimens. Three aerospace-grade adhesives were used: Loctite EA 9394, EA 9392, and EA 9360. For in situ adhesive tests, three bondline thicknesses of 0.25 mm (0.01 in.), 1.27 mm (0.05 in.), and 2.54 mm (0.10 in.) were investigated. Shear tests focused on the use of the V-notched Iosipescu shear specimen, featuring a 120° notch angle for use with thin adhesive bondlines. Additionally, the thick adherend lap joint test configuration was evaluated for determining shear properties of adhesives. Tensile tests focused on adhesively bonded butt joint specimens as well as bulk adhesive bar specimens. The results from in situ and bulk adhesive shear tests suggest that the slight decrease in apparent shear strength with increasing bondline thickness was produced by slight changes in the adhesive stress state. Further, the shear strengths obtained from bulk adhesive tests were comparable to those from in situ tests. The results from moiré interferometry showed that no significant difference in adhesive shear modulus between the three thicknesses investigated. Combined, these results suggest that the shear strength and shear modulus of the adhesives investigated do not differ when tested in their thin-film in situ and bulk forms. Additionally, these results show that the Iosipescu shear test configuration is well suited for both in situ and bulk adhesive shear tests. Finite element analyses and moiré interferometry experiments performed for the thick adherend lap shear test showed a relatively nonuniform state of stress throughout the adhesive bondline, suggesting that the test results may not be representative of the actual adhesive shear properties. The results from butt tensile tests and analysis suggest that the apparent variation in tensile strength as a function of bondline thickness was a result of variations in the adhesive stress state, rather than the actual tensile strength of the adhesive. In total, the results of this investigation suggest that the adhesive properties obtained from bulk adhesive specimens are valid for use in structural analysis of in situ thin-film adhesives.

17. Key Words	18. Distribution Statement
Mechanical properties of adhesives, Adhesive bonding, Test methods	This document is available to the U.S. public through the National Technical Information Service (NTIS) Springfield, Virginia 22161

19. Security Classif. (of this report)	20. Security Classif. (of this page)	21. No. of Pages	22. Price
Unclassified	Unclassified	139	

Form DOT F1700.7 (8-72) Reproduction of completed page authorized

ACKNOWLEDGEMENTS

The authors acknowledge the assistance of Dr. Hal Gascoigne of the California Polytechnic State University, San Luis Obispo, California, particularly with the implementation of moiré interferometry in this investigation. Additionally, the authors acknowledge the guidance of Dr. Larry DeVries of the University of Utah. The authors are grateful for the assistance provided by these individuals.

TABLE OF CONTENTS

		Page
EXECUTIVE SUMMARY		xvii
1.	INTRODUCTION	1
2.	FINITE ELEMENT MODELING	3
2.1	Introduction	3
2.2	Analysis Methodology	4
2.3	Shear Test Analysis	4
2.3.1	Iosipescu Specimens	4
2.3.2	Bulk Adhesive Iosipescu Specimens	9
2.3.3	Thick Adherend Lap Joint Specimen	9
2.4	Butt Tensile Test Analysis	10
3.	RESULTS OF FINITE ELEMENT ANALYSIS	11
3.1	Results of Shear Specimen Analyses	11
3.2	Data Processing	12
3.3	Original Iosipescu V-Notched Specimen	13
3.3.1	Shear Stresses Original Iosipescu V-Notched Specimen	13
3.3.2	Normal Stresses for the Original Iosipescu V-Notched Specimens	15
3.3.3	von Mises Equivalent Stress	18
3.3.4	Conclusions for Original Iosipescu V-Notched Specimen	20
3.4	Iosipescu U-Notched Specimen	20
3.4.1	Shear Stresses for Iosipescu U-Notched Specimens	21
3.4.2	Normal Stresses for Iosipescu U-Notched Specimens	28
3.4.3	Combined Stresses for Iosipescu U-Notched Specimens	34
3.4.4	Conclusions for Iosipescu U-Notched Specimens	43
3.5	Iosipescu V-Notched Specimens With Variable Notch Angle	44
3.5.1	Shear Stresses for Variable Notch Angle Iosipescu V-Notch	44
3.5.2	Normal Stresses for the Iosipescu V-Notched Specimens	51
3.5.3	von Mises Stresses for Iosipescu V-Notched Specimens	58
3.5.4	Conclusions for Variable Angled Iosipescu V-Notched Specimens	66
3.6	Iosipescu V-Notched Specimens With Variable NDR	67

3.6.1 Shear Stress for Variable NDR Specimens 67

3.6.2 Normal Stresses for Iosipescu V-Notched Specimens With Variable NDR 70

3.6.3 Conclusions for Variable NDR Iosipescu V-Notched Specimens 70

3.7 Conclusions for Iosipescu Specimens 75
3.8 Thick Adherend Lap Joint Results 76

3.8.1 Shear Stresses in Thick Adherend Lap Joint 76
3.8.2 Normal Stresses in Thick Adherend Lap Joint 77

3.9 Butt Tensile Results 79

4. SPECIMEN FABRICATION AND TEST METHODOLOGIES 81

4.1 Introduction 81
4.2 Adhesives Tested 81
4.3 Bulk Adhesive Specimen Fabrication 81
4.4 Bonded Iosipescu Specimen Fabrication 84

4.4.1 Aluminum Surface Preparation 85
4.4.2 Bonding Procedures 86
4.4.3 Removal of Adhesive Flash 88

4.5 Butt Tensile Specimen Fabrication 88
4.6 Iosipescu Testing Methods 89

4.6.1 Bulk Iosipescu Tests 90
4.6.2 Bonded Iosipescu Tests 91

4.7 Tensile Test Methods 92

4.7.1 Bulk Adhesive Tensile Tests 92
4.7.2 Butt Tensile Tests 92

4.8 Moiré Interferometry 94

4.8.1 Moiré Interoferometry Background 94
4.8.2 Moiré Test Setup 95

5. RESULTS OF EXPERIMENTAL TESTS 97

5.1 Introduction 97
5.2 Results of Bulk Adhesive Iosipescu Shear Tests 97
5.3 Results of Bonded Iosipescu Specimens 100

5.4 Results of Bulk Adhesive Tensile Tests 103
5.5 Results of Butt Tensile Tests 106
5.6 Iosipescu Moiré Results 108
5.7 Thick Adherend Lap Joint Moiré Results 113

6. SUMMARY AND CONCLUSIONS 118

7. REFERENCES 119

LIST OF FIGURES

Figure		Page
1	Adhesive Joint Iosipescu Specimen	3
2	Schematic of Notch Geometries for Adhesive Joint Iosipescu Specimens	5
3	Boundary Conditions for the Iosipescu Model	5
4	Adhesively Bonded Original Iosipescu V-Notched Specimens	6
5	Iosipescu U-Notched Specimens With Varying Notch Radius	7
6	Variable Notch Angle Iosipescu V-Notched Specimens	8
7	Variable NDR Iosipescu V-Notched Specimens	9
8	Dimensions for Thick Adherend Lap Joint Finite Element Model	10
9	Geometry of Butt Tensile Specimen for Finite Element Model	11
10	Shear Stress Distributions in (a) Full Adhesive Bond and (b) Around Notch Tip for Original Iosipescu V-Notched Specimens (Normalized)	14
11	Shear Stress Distributions Along Adhesive Centerline for 90° V-Notched Iosipescu Specimens	15
12	Transverse Stress Distributions in (a) Full Adhesive Bond and (b) Around Notch Tip for Original Iosipescu V-Notched Specimens (Normalized)	16
13	Axial Stress Distributions in (a) Full Adhesive Bond and (b) Around Notch Tip for Original Iosipescu V-Notched Specimens (Normalized)	17
14	von Mises Stress Distributions in (a) Full Adhesive Bond and (b) Around Notch Tip for Original Iosipescu V-Notched Specimens (Normalized)	19
15	Shear Stress Distributions in (a) Full Adhesive Bond and (b) Around Notch Tip for Iosipescu U-Notched Specimens With 0.25-mm (0.01-in.) Bondline (Normalized)	22
16	Shear Stresses for Iosipescu U-Notched Specimens With 1.27-mm (0.05-in.) Bondline (Normalized)	23
17	Shear Stresses for Iosipescu U-Notched Specimens With 2.54-mm (0.10-in.) Bondline (Normalized)	23

18	Shear Stresses for Iosipescu U-Notched Bulk Adhesive Specimens (Normalized)	24
19	Shear Stresses Around Entire Notch for Adhesively Bonded Iosipescu U-Notched Specimens (Normalized)	25
20	Shear Stress Distribution Along Axial Centerline for Iosipescu U-Notched Specimens With Different Notch Radius Values, 0.25-mm (0.01-in.) Bondline	26
21	Shear Stress Distribution Along Axial Centerline for Iosipescu U-Notched Specimens With Different Notch Radius Values, 1.27-mm (0.05-in.) Bondline	26
22	Shear Stress Distribution Along Axial Centerline for Iosipescu U-Notched Specimens With Different Notch Radius Values, 2.54-mm (0.10-in.) Bondline	27
23	Shear Stress Distribution Along Axial Centerline for Iosipescu U-Notched Bulk Adhesive Specimens With Different Notch Radius Values	27
24	Transverse Stress Distributions in (a) Full Adhesive Bond and (b) Around Notch Tip for Iosipescu U-Notched Specimens With 0.25-mm (0.01-in.) Bondline (Normalized)	29
25	Axial Stress Distributions in (a) Full Adhesive Bondline and (b) Around Notch Tip for Iosipescu U-Notched Specimens With 0.25-mm (0.01-in.) Bondline (Normalized)	30
26	Transverse Stresses for Iosipescu U-Notched Specimens With 1.27-mm (0.05-in.) Bondline (Normalized)	31
27	Axial Stresses for Iosipescu U-Notched Specimens With 1.27-mm (0.05-in.) Bondline (Normalized)	31
28	Transverse Stresses for Iosipescu U-Notched With 2.54-mm (0.10-in.) Bondline (Normalized)	32
29	Axial Stresses for Iosipescu U-Notched With 2.54-mm (0.10-in.) Bondline (Normalized)	32
30	Transverse Stresses for Iosipescu U-Notched Bulk Adhesive (Normalized)	33
31	Axial Stresses for Iosipescu U-Notched Bulk Adhesive (Normalized)	33
32	von Mises Stress Distributions in (a) Full Adhesive Bondline and (b) Around Notch Tip for Iosipescu U-Notched Specimens With 0.25-mm (0.01-in.) Bondline (Normalized)	35

33 von Mises Stress Distributions in (a) Full Adhesive Bondline and (b) Around Notch Tip for Iosipescu U-Notched Specimens With 1.27-mm (0.05-in.) Bondline (Normalized) 36

34 von Mises Stresses for Iosipescu U-Notched Specimens With 2.54-mm (0.10-in.) Bondline (Normalized) 37

35 von Mises Stresses for Iosipescu U-Notched Bulk Adhesive Specimens (Normalized) 38

36 Locations of Maximum Values of Stress Components in Variable Notch Radius Iosipescu U-Notched Specimens With 0.25-mm (0.01-in.) Bondline 40

37 Maximum Values of Stress Components for Variable Notch Radius Iosipescu U-Notched Specimens With 0.25-mm (0.01-in.) Bondline (Normalized) 40

38 Locations of Maximum Values of Stress Components in Variable Notch Radius Iosipescu U-Notched Specimens With 1.27-mm (0.05-in.) Bondline 41

39 Maximum Values of Stress Components for Variable Notch Width Iosipescu U-Notched Specimens With 1.27-mm (0.05-in.) Bondline (Normalized) 41

40 Locations of Maximum Values of Stress Components in Variable Notch Radius Iosipescu U-Notched Specimens With 2.54-mm (0.10-in.) Bondline 42

41 Maximum Normalized Values of Stress Components for Variable Notch Width Iosipescu U-Notched Specimens With 2.54-mm (0.10-in.) Bondline 42

42 Maximum Normalized Values of Stress Components for Variable Notch Width Iosipescu U-Notched Bulk Adhesive Specimens 43

43 Shear Stress Distributions in (a) Full Adhesive Bondline and (b) Around Notch Tip for Variable Angle Iosipescu V-Notched Specimens With 0.25-mm (0.01-in.) Bondline (Normalized) 45

44 Shear Stress Distributions in (a) Full Adhesive Bondline and (b) Around Notch Tip for Variable Angle Iosipescu V-Notched Specimens With 1.27-mm (0.05-in.) Bondline (Normalized) 46

45 Shear Stress Distributions for Variable Angle Iosipescu V-Notched Specimens With 2.54-mm (0.10-in.) Bondline (Normalized) 47

46 Shear Stress Distributions for Bulk Adhesive Variable Angle Iosipescu V-Notched Specimens (Normalized) 48

47	Shear Stress Distribution Along Axial Centerline as a Function of Notch Angle for Iosipescu V-Notched Specimens With 0.254-mm (0.01-in.) Bondline	49
48	Shear Stress Distribution Along Axial Centerline as a Function of Notch Angle for Iosipescu V-Notched Specimens With 1.27-mm (0.05-in.) Bondline	49
49	Shear Stress Distribution Along Axial Centerline as a Function of Notch Angle for Iosipescu V-Notched Specimens With 2.54-mm (0.10-in.) Bondline	50
50	Shear Stress Distribution Along Axial Centerline as a Function of Notch Angle for Bulk Adhesive Iosipescu V-Notched Specimens	50
51	Transverse Stress Distributions in (a) Full Adhesive Bondline and (b) Around Notch Tip for Variable Angle Iosipescu V-Notched Specimens With 0.25-mm (0.01-in.) Bondline (Normalized)	52
52	Axial Stress Distributions in (a) Full Adhesive Bondline and (b) Around Notch Tip for Variable Angle Iosipescu V-Notched Specimens With 0.25-mm (0.01-in.) Bondline (Normalized)	53
53	Transverse Stress Distributions for Variable Angle Iosipescu V-Notched Specimens With 1.27-mm (0.05-in.) Bondline (Normalized)	54
54	Axial Stress Distributions for Variable Angle Iosipescu V-Notched Specimens With 1.27-mm (0.05-in.) Bondline (Normalized)	54
55	Transverse Stress Distributions for Variable Angle Iosipescu V-Notched Specimens With 2.54-mm (0.10-in.) Bondline (Normalized)	55
56	Axial Stress Distributions for Variable Angle Iosipescu V-Notched Specimens With 2.54-mm (0.10-in.) Bondline (Normalized)	55
57	Transverse Stress Distributions for Bulk Adhesive Variable Angle Iosipescu V-Notched Specimens (Normalized)	56
58	Axial Stress Distributions for Bulk Adhesive Variable Angle Iosipescu V-Notched Specimens (Normalized)	57
59	von Mises Stress Distributions in (a) Full Adhesive Bondline and (b) Around Notch Tip for Variable Angle Iosipescu V-Notched Specimens With 0.25-mm (0.01-in.) Bondline (Normalized)	59
60	von Mises Stress Distributions in (a) Full Adhesive Bondline and (b) Around Notch Tip for Variable Angle Iosipescu V-Notch Specimens With 1.27-mm (0.05-in.) Bondline	60

61 von Mises Stress Distributions for Variable Angle Iosipescu V-Notched Specimens With 2.54-mm (0.10-in.) Bondline (Normalized) 61

62 von Mises Stress Distributions for Bulk Adhesive Variable Angle Iosipescu V-Notched Specimens (Normalized) 62

63 Locations of Maximum Values of Stress Components in Adhesive Bondline for Iosipescu V-Notched Specimens With 0.25-mm (0.01-in.) Bondline 63

64 Maximum Normalized Values of Stress Components for Variable Notch Angle Iosipescu V-Notched Specimens With 0.25-mm (0.01-in.) Bondline 63

65 Locations of Maximum Values of Stress Components Adhesive Bondline for Iosipescu V-Notched Specimens With 1.27-mm (0.05-in.) Bondline 64

66 Maximum Normalized Values of Stress Components for Variable Notch Angle Iosipescu V-Notched Specimens With 1.27-mm (0.05-in.) Bondline 64

67 Locations of Maximum Values of Stress Components in Adhesive Bondline for Iosipescu V-Notched Specimens With 2.54-mm (0.10-in.) Bondline 65

68 Maximum Normalized Values of Stress Components for Variable Notch Angle Iosipescu V-Notched Specimens With 2.54-mm (0.10-in.) Bondline 65

69 Maximum Normalized Values of Stress Components for Variable Notch Angle Iosipescu V-Notched Bulk Adhesive Specimens 66

70 Shear Stress Distributions in (a) Full Adhesive Bondline and (b) Around Notch Tip for 120° Iosipescu V-Notched Specimens With 0.25-mm (0.01-in.) Bondline (Normalized) 68

71 Shear Stress Distributions in Adhesive Bondline for 120° Iosipescu V-Notched Specimens With 1.27-mm (0.05-in.) Bondline (Normalized) 69

72 Shear Stress Distributions in Adhesive Bondline for 120° Iosipescu V-Notched Specimens With 2.54-mm (0.10-in.) Bondline (Normalized) 70

73 Transverse Stress Distributions in (a) Full Adhesive Bondline and (b) Around Notch Tip for 120° Iosipescu V-Notched Specimens With 0.25-mm (0.01-in.) Bondline (Normalized) 71

74 Axial Stress Distributions in (a) Full Adhesive Bondline and (b) Around Notch Tip for 120° Iosipescu V-Notched Specimens With 0.25-mm (0.01-in.) Bondline (Normalized) 72

75 (a) Transverse and (b) Axial Stress Distributions in Adhesive Bond for 120° Iosipescu V-Notched Specimens With 1.27-mm (0.05-in.) Bondline (Normalized) 73

76 (a) Transverse and (b) Axial Stress Distributions in Adhesive Bondline for 120° Iosipescu V-Notched Specimens With 1.27-mm (0.05-in.) Bondline (Normalized) 74

77 Shear Stress Distributions Along Axial Centerlines for Bonded Iosipescu Specimens With 120° Notch Angle and Bulk Adhesive Iosipescu Specimens With 90° Notch Angle 75

78 Shear Stresses in the Adhesive Test Section of the Thick Adherend Lap Joint for Bondline Thicknesses (a) 0.25 mm (0.01 in.), (b) 1.27 mm (0.05 in.), and (c) 2.54 mm (0.10 in.) (Normalized) 76

79 Variation of Shear Stresses Along Adhesive Midplane for Three Bondline Thicknesses 77

80 Transverse (a) and Axial (b) Stresses in the Adhesive Test Section of the Thick Adherend Lap Joint for Bondline Thicknesses 0.25 mm (0.01 in.), 1.27 mm (0.05 in.), and 2.54 mm (0.10 in.), Respectively (Normalized) 78

81 Axial Normal Stresses in Butt Tensile Adhesive Bondlines 80

82 Vacuum Bell Jar for Adhesive Mixing and Degassing 82

83 Dimensions for Bulk Adhesive Tensile Specimens 82

84 Bulk Adhesive Iosipescu Specimens: Uncut Casting and Finished Specimens With 120° and 90° Notches, Respectively 83

85 Aluminum Adherend Dimensions for Bonded Iosipescu Specimens With Bondline Thicknesses of (a) 0.254 mm (0.01 in.), (b) 1.27 mm (0.05 in.), and (c) 2.54 mm (0.10 in.) 84

86 Bonded Iosipescu Specimen Dimensions 85

87 Anodizing Line Setup Consisting of (a) Alkaline Cleaner/Deoxidizer, Nitric Acid Bath and (b) Phosphoric Anodizing and Water Rinse Tanks 86

88 Bonding Fixture With Iosipescu Specimens 87

89 Static Mixer: (a) Fully Assembled Dispensing Gun and (b) Close-Up of Fluted Nozzle 88

90 Butt Tensile Adherend Dimensions 89

91	Butt Tensile Specimens With Three Adhesive Bondline Thicknesses	89
92	Bulk Adhesive Iosipescu Test Setup	90
93	Bonded Iosipescu Test Setup	92
94	Tensile Test Setups for (a) Bulk Adhesive and (b) Butt Tensile Specimens	93
95	Loading Setup for Bonded Iosipescu Moiré Interferometry	96
96	Loading Setup for Thick Adherend Lap Joint Moiré Interferometry	96
97	Complete Setup for Moiré Interferometry	97
98	Characteristic Shear Stress-Shear Strain Curves for Three Adhesives	98
99	Characteristic Failures of Bulk Iosipescu Specimens for all Three Adhesives	100
100	Apparent Shear Strength Versus Bondline Thickness for EA 9394	100
101	Apparent Shear Strength Versus Bondline Thickness for EA 9392	101
102	Apparent Shear Strength Versus Bondline Thickness for EA 9360	101
103	Characteristic Axial and Transverse Stress-Strain Curves for EA 9394	104
104	Characteristic Failures of Bulk Adhesive Tensile Specimens	106
105	Apparent Tensile Strength of EA 9394 Butt Tensile Specimens	107
106	Characteristic Failures of Butt Tensile Specimens	108
107	(a) U- and (b) V-Displacement Fields for Bonded Iosipescu Specimen With 0.27-mm (0.010-in.) Bondline. Inserts are Enlarged Views of the V-Field at (c) the Center and (d) Around the Notch Tip of the Adhesive Bond	110
108	(a) U- and (b) V-Displacement Fields for Bonded Iosipescu Specimen With 1.19-mm (0.047-in.) Bondline. Inserts are Enlarged Views of the V-Field at (c) the Center and (d) Around the Notch Tip of the Adhesive Bond	111
109	(a) U- and (b) V-Displacement Fields for Bonded Iosipescu Specimen With 2.54-mm (0.100-in.) Bondline. Inserts are Enlarged Views of the V-Field at (c) the Center and (d) Around the Notch Tip of the Adhesive Bond	112
110	Shear Strain Across Adhesive Bondline (Normalized With Respect to Adherend Shear Strain)	113

111 (a) U- and (b) V-Displacement Fields for Thick Adherend Lap Joint Specimen With 0.25-mm (0.010-in.) Bondline. Inserts are Enlarged Views of the U-Field at (c) the Center and (d) End of the Lap 115

112 (a) U- and (b) V-Displacement Fields for Thick Adherend Lap Joint Specimen With 1.27-mm (0.050-in.) Bondline. Inserts are Enlarged Views of the U-Field at (c) the Center and (d) End of the Lap 116

113 (a) U- and (b) V-Displacement Fields for Thick Adherend Lap Joint Specimen With 2.54-mm (0.100-in.) Bondline. Inserts are Enlarged Views of the U-Field at (c) the Center and (d) End of the Lap 117

LIST OF TABLES

Table		Page
1	Material Properties Used in Finite Element Analyses	4
2	Applied Fixture Displacement as a Function of Bondline Thickness	6
3	Maximum Values of Shear and Normal Stress Components for Original Iosipescu V-Notched Specimens	18
4	Maximum Values of von Mises Stresses for the Original Iosipescu V-Notched Specimen	20
5	Summary Results for Bulk Adhesive Iosipescu Tests	99
6	Summary Results for EA 9394 Bonded Iosipescu Tests	102
7	Summary Results for EA 9392 Bonded Iosipescu Tests	103
8	Summary Results for EA 9360 Bonded Iosipescu Tests	103
9	Summary Results for Bulk Adhesive Tensile Tests	105
10	Summary Results for Bulk Adhesive Shear Modulus Tests	105
11	Summary Results for EA 9394 Butt Tensile Tests	107

EXECUTIVE SUMMARY

A combined experimental and computational investigation was performed to determine whether the material properties of structural adhesives differ between their thin-film in situ and bulk forms. Both shear and tensile tests were performed using bulk adhesive specimens as well as in situ adhesive specimens. Three aerospace-grade adhesives were used: Loctite EA 9394, EA 9392, and EA 9360. For in situ adhesive tests, three bondline thicknesses of 0.25 mm (0.01 in.), 1.27 mm (0.05 in.), and 2.54 mm (0.10 in.) were investigated. Shear tests focused on the use of the V-notched Iosipescu shear specimen, featuring a 120° notch angle for use with thin adhesive bondlines. Additionally, the thick adherend lap joint test configuration was evaluated for determining shear properties of adhesives. Tensile tests focused on adhesively bonded butt joint specimens as well as bulk adhesive bar specimens.

The results from in situ and bulk adhesive shear tests suggest that the slight decrease in apparent shear strength with increasing bondline thickness was produced by slight changes in the adhesive stress state. Further, the shear strengths obtained from bulk adhesive tests were comparable to those from in situ tests. The results from moiré interferometry showed no significant difference in adhesive shear modulus between the three thicknesses investigated. Combined, these results suggest that the shear strength and shear modulus of the adhesives investigated do not differ when tested in their thin-film in situ and bulk forms. Additionally, these results show that the Iosipescu shear test configuration is well suited for both in situ and bulk adhesive shear tests. Finite element analyses and moiré interferometry experiments performed for the thick adherend lap shear test showed a relatively nonuniform state of stress throughout the adhesive bondline, suggesting that the test results may not be representative of the actual adhesive shear properties. The results from butt tensile tests and analysis suggest that the apparent variation in tensile strength as a function of bondline thickness was a result of variations in the adhesive stress state, rather than the actual tensile strength of the adhesive. In total, the results of this investigation suggest that the adhesive properties obtained from bulk adhesive specimens are valid for use in structural analysis of in situ thin-film adhesives.

1. INTRODUCTION.

One of the major trends in the overlapping fields of aviation and aerospace is the rise in use of adhesively bonded structures. Adhesive bonds are steadily replacing mechanical fasteners due to their many advantages, including significant weight savings, decreases in cost, decreases in manufacturing processes, and better load distribution. With the rising propensity to use adhesives comes the inherent necessity of understanding how an adhesively bonded joint will function under the intended operating conditions. For structural analysis purposes, it is necessary to have accurate mechanical properties, such as strength and modulus, for the adhesive. Currently, there appears to be considerable confusion and a lack of consensus on whether mechanical properties obtained from testing bulk adhesive specimens may be used in the design and analysis of thin-film adhesive joints. At the source of this confusion is the question of whether the mechanical properties of an adhesive are different in a relatively thin bondline, or in situ, versus in bulk form.

Certain adhesive test methods, such as the lap joint tests in ASTM D 1002 [1] and ASTM D 3165 [2], use the adhesive in its thin-film or in situ form. However, these lap joint tests are known to produce nonuniform states of stress in the adhesive bondline. Thus, these test methods do not provide a simple or straightforward measure of the stiffness or strength properties of the adhesive [3 and 4]. The thick adherend lap joint test, ASTM D 5656 [5], is believed to produce less variability in the shear stress distribution and lower peel stresses in the adhesive [4]. However, the lap joints with thick adherends, as in ASTM D 5656, will produce nonuniform shear stress distributions for some adhesive thicknesses and stiffnesses [6].

Another approach to determine the mechanical properties of an adhesive is through bulk adhesive tests, where an entire specimen is cast or machined from the adhesive material. Although no ASTM standard tests exist for bulk adhesive tests, many of the standards included in ASTM Volume 8 (Sections 1 through 4) for plastics or Volume 9 (Sections 1 and 2) for rubbers may be adapted to test the properties of bulk adhesives. Tensile tests of bulk adhesives are relatively straight-forward and may be performed using either cast or machined tensile specimens. Shear strength and shear modulus determinations of the bulk adhesive may be accomplished using several test methods, including solid rod torsion tests or using the V-notched Iosipescu shear test method, ASTM D 5379 [7], or the recently developed V-notched rail shear test method, ASTM D 7078 [8].

Although hundreds, if not thousands, of adhesives have been characterized in thin-film or in situ form and many test laboratories and researchers have performed bulk adhesive tests, there have been surprisingly few investigations that have addressed the thin-film versus bulk material properties of structural adhesives. A review of the open literature revealed that among the limited studies that have been published, there is considerable confusion and a lack of consensus on whether mechanical properties obtained from testing bulk adhesive specimens may be used in the design and analysis of thin-film adhesive joints. Dolev and Ishai [9] conducted torsion tests on bulk and in situ adhesive specimens to compare mechanical properties under different states of stress. Good correlation between in situ and bulk shear yield strength and elastic modulus was obtained. The authors concluded that elastic and strength properties of an in situ adhesive may be determined by bulk adhesive tests. In contrast, Chai [10] used the napkin-ring shear test to

show that the ultimate shear strain in a thin bondline was more than 30 times greater than the corresponding bulk material property. This was due to the supposed enhancement of mechanical properties when a material is stressed while under tight spatial constraint. Peretz [11] concluded that the in situ adhesive shear modulus increased with increasing adhesive thickness up to the bulk material shear modulus. The shear strengths obtained from thin adhesive layers were similar to those obtained from bulk tests. Lilleheden [12] used moiré interferometry to perform a detailed experimental investigation of modulus variations in adhesives for different adhesive thicknesses using a modified lap adherend specimen and found no difference in the measured moduli of the adhesive between the thin-film and bulk forms. Tomblin, et al. [13] investigated the effect of bondline thickness using three test methods: ASTM D 1002, D 3165, and D 5656. Bondline thicknesses ranging from 0.010 to 0.160 in. were investigated using three paste adhesives. Regardless of bondline thickness, the thin adherend tests (ASTM D 1002 and D 3165) produced lower apparent shear strengths than the thick adherend test (ASTM D 5656). The results from the thick adherend test showed a reduction in the apparent shear strength with increasing bondline thickness for all three adhesives tested. The shear modulus was also reported to decrease as the bondline thickness increased using the ASTM D 5656 test.

In summary, a review of the open literature reveals that there is currently no clear consensus on the equivalence of thin-film versus bulk adhesive tests. One explanation that has been offered for the existence of differences in mechanical properties of in situ versus bulk adhesive is the presence of a diffuse region or interphase at the boundary between the adhesive and adherend [14 and 15]. Others, however, have attributed differences in mechanical properties to factors such as variability in adhesive casting and curing conditions, lack of a well-defined state of stress, and inadequate methods of strain measurement [11]. Clearly, a complex state of stress is produced by the geometric discontinuities in many in situ test configurations and by the drastically different material properties of the adhesive and adherends. Thus, it is not clear whether differences in material properties are due to material-related differences or test/measurement-related differences. The goal of the present investigation is to determine conclusively whether the mechanical properties of structural adhesives differ when in thin-film (in situ) versus bulk forms. As a result, this report will address whether bulk adhesive properties are suited for use in the design and analysis of adhesively bonded structures.

A combined experimental and computational approach was employed to evaluate the thin-film versus bulk mechanical properties of structural adhesives. Both shear and tensile properties were evaluated with emphasis on the shear response. The adhesive joint Iosipescu specimen (figure 1) was selected as the primary method of evaluating shear properties. Based on the traditional Iosipescu shear specimen, several studies, including those by Wysherley, et al. [16], Grabovac and Morris [17], Ding, et al. [18], and Ignjatovic, et al. [19], found that the test induces a state of uniform shear stress in the adhesive bond. In addition, shear behavior was analyzed with the thick adherend lap joint specimen. Tensile properties were evaluated with simple bar specimens in uniaxial tension.

Extensive finite element analyses were conducted to determine the effect of specimen geometry and bondline thickness on the stress state in the adhesive bond. The majority of these analyses focused on the adhesively bonded Iosipescu specimen to find the optimal specimen geometry for a state of uniform shear and to determine the effect of bondline thickness on the stress state. A

finite element analysis was also used to evaluate the effect of bondline thickness in the thick adherend lap joint, the butt tensile specimen, and the state of stress in bulk adhesive specimens.

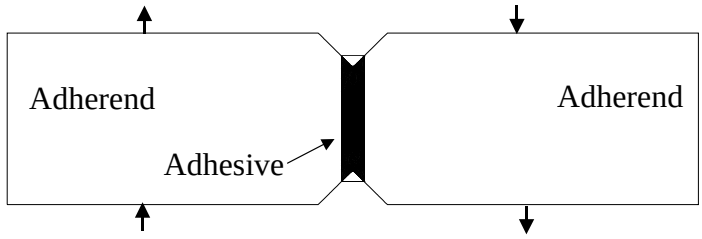

Figure 1. Adhesive Joint Iosipescu Specimen

Both bulk and in situ adhesive tests were performed using three different structural adhesives. One adhesive, Loctite EA 9394, was selected as the primary adhesive due to the extensive nature of past characterization using this adhesive. This adhesive was used in all bulk and in situ tests. Two additional adhesives, Loctite EA 9392 and Loctite EA 9360, were used as secondary adhesives and when more than one adhesive was investigated. Bulk adhesive tests were performed on Iosipescu shear specimens and bar tensile specimens. In situ tests for strength properties were performed primarily with adhesively bonded Iosipescu specimens and butt tensile specimens. Determination of modulus for thin adhesive bondlines was found to be a complicated endeavor. One of the most promising techniques for measuring bondline deformation is the use of moiré interferometry. The application of this optical experimental method to adhesive bondlines was documented by Asundi [20] and Post, et al. [21]. In this investigation, moiré interferometry was used to evaluate the adhesively bonded Iosipescu specimen and the thick adherend lap joint.

2. FINITE ELEMENT MODELING.

2.1 INTRODUCTION.

The finite element numerical method was used to quantitatively determine and compare the various states of stress and strain throughout the adhesive layer for several shear and tensile loading configurations and geometries. The primary shear specimen was the adhesively bonded Iosipescu specimen. Significant analysis was performed on this specimen in an effort to identify the specific geometry that produced the most uniform state of stress. Additionally, limited analysis was performed on the thick adherend lap joint and the butt tensile specimen. To determine the effect of bondline thickness on the adhesive stress state, each specimen configuration and geometry was modeled with three different adhesive bondline thicknesses. Analyses were also performed on bulk adhesive Iosipescu specimens.

Contour maps of specific stress and strain components were constructed to identify which configurations produced the most desirable stress state. For the shear test, the optimum configuration was the one that produced the most uniform state of shear stress with minimal normal (tensile and/or compressive) stresses in the adhesive. For the tensile test, the optimum

configuration was the one that produced the most uniform state of uniaxial tensile stress in the adhesive.

2.2 ANALYSIS METHODOLOGY.

All finite element modeling was performed with the software package ANSYS 6.0 [22]. The data produced by ANSYS was then normalized and used to create contour plots of stress and strain using the postprocessing plotting software package Surfer 7.04 [23].

Material properties used in the finite element analyses are listed in table 1. The adhesive properties were chosen to be representative of the paste adhesives used in this investigation. Both the aluminum adherends and the adhesive were modeled as linear-elastic isotropic materials. Thus, the analyses are valid only in the loading ranges in which these materials remain linear-elastic. Note that only aluminum adherends were considered.

Table 1. Material Properties Used in Finite Element Analyses

	E		ν
Material	GPa	Msi	
Aluminum	70.33	10.20	0.33
Adhesive	4.24	0.615	0.37

E = Modulus of elasticity
ν = Poisson's ratio

2.3 SHEAR TEST ANALYSIS.

The shear behavior of the adhesive was evaluated using configurations based on two shear tests: the Iosipescu shear test and the thick adherend lap joint test. Each of these shear tests is discussed individually in the following sections.

2.3.1 Iosipescu Specimens.

One method of investigating the shear response of adhesives is using the standard Iosipescu specimen (ASTM D 5379) modified to test adhesives by cutting the specimen between the notches and then adhesively bonding the two halves back together in a manner that retains the initial geometry. Three different types of adhesive joint Iosipescu specimens are shown in figure 2. Type A has no notch at all, Type B is notched but the notch does not extend into the adhesive, and Type C has a notch extending into the adhesive bondline. Previous research [18] has shown that Type A and Type B specimens have singular stresses at the adhesive/adherend interface corners [18]. Thus, all specimen variations considered in this study were of the Type C variety with the notch extending into the adhesive.

All Iosipescu specimens were modeled using a two-dimensional plane stress approximation with a constant thickness of 4.76 mm (0.1875 in.) to match the thickness of the aluminum adherends used in the experimental tests. The elements used were 8-noded isoparametric ANSYS PLANE82 elements.

Boundary conditions for the finite element model consisted of an applied displacement in the vertical, or y direction, applied to one half of the specimen while the other half was constrained against displacement in the vertical direction as shown in figure 3. Additionally, the top left corner of the specimen was constrained in the horizontal, or x direction, to prevent rigid-body motion.

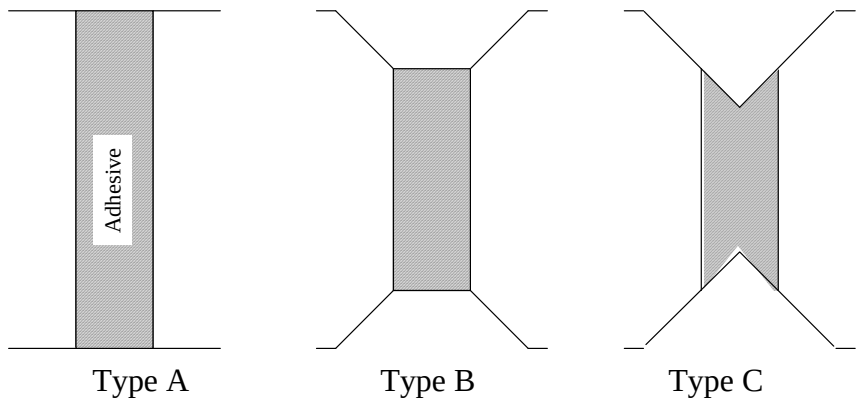

Figure 2. Schematic of Notch Geometries for Adhesive Joint Iosipescu Specimens

The contact areas of the fixture on the specimen (lengths a and b in figure 3) were determined such that both tensile σ_y stresses and penetrations (overlapping y displacements along the contact surfaces) were prevented. The magnitude of the applied displacement was chosen so that the average shear stress in the adhesive between the notch roots was approximately 27.5 MPa (4000 psi). To meet this criterion, it was necessary to change the displacement value for each of the three bondline thicknesses. For bondline thicknesses of 0.254 mm (0.01 in.), 1.27 mm (0.05 in.), and 2.54 mm (0.10 in.), displacements in the negative y direction of 0.038 mm (0.0015 in.), 0.063 mm (0.0025 in.), and 0.076 mm (0.003 in.), respectively, were used as shown in table 2.

Additionally, figure 3 defines the nomenclature transverse and axial directions that will be used throughout the remainder of this report. The transverse direction corresponds to the x direction and the axial direction corresponds to the y direction.

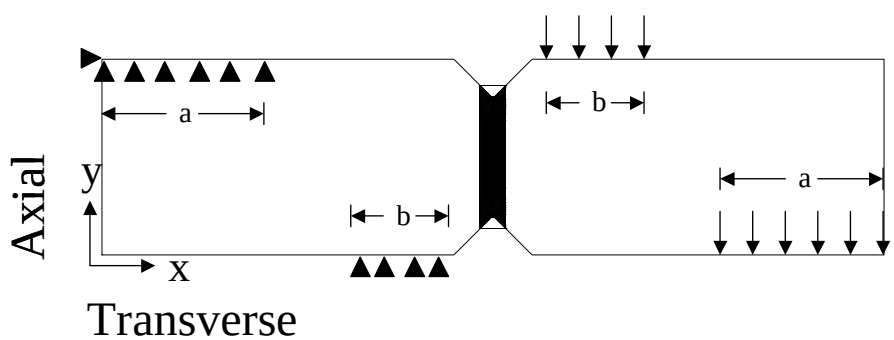

Figure 3. Boundary Conditions for the Iosipescu Model

Table 2. Applied Fixture Displacement as a Function of Bondline Thickness

Bondline Thickness, mm (in.)	Fixture Displacement, mm (in.)
0.254 (0.010)	0.038 (0.0015)
1.270 (0.050)	0.063 (0.0025)
2.540 (0.100)	0.076 (0.0030)

2.3.1.1 Original Iosipescu V-Notched Specimen.

For the present investigation, the adhesively bonded Iosipescu specimen that retains the same dimensions as the standard Iosipescu specimen is referred to as the original Iosipescu V-notched specimen. In this configuration, the overall dimensions of the specimen were kept at their standard values: the overall specimen length was maintained at 76 mm (3.0 in.) and the height was maintained at 19 mm (0.75 in.). Additionally, the original notch angle of 90° was also used. The two opposing notches each have a depth of 3.81 mm (0.15 in.), which is 0.20 times the total height of the specimen shown in figure 4.

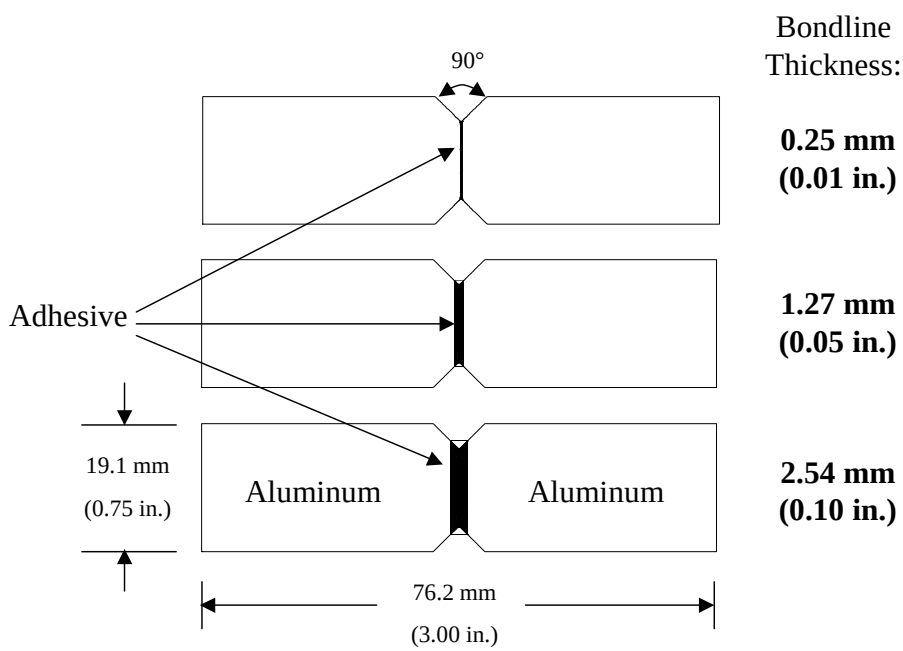

Figure 4. Adhesively Bonded Original Iosipescu V-Notched Specimens

2.3.1.2 Iosipescu U-Notched Specimens.

The 90° notch angle employed in the original Iosipescu V-notched specimen produced a relatively uniform state of shear stress in the center of the adhesive test section. However, it had an undesirable effect of large shear stress concentrations at the notch tips and even larger shear and normal stress concentrations at the side of the notch tips on the notch flank. In an effort to eliminate these stress concentrations, the sharp tip of the V-notch was replaced with a rounded

U-notch. The concept investigated was whether the more gradual notch transition of the U-notch would produce a more uniform state of stress than the more abrupt V-notch. The geometry of the Iosipescu U-notched specimen was consistent with the geometry of the original Iosipescu V-notched specimen. The overall height and length of the specimen as well as the notch depth remained unmodified.

The variable geometric feature of the Iosipescu U-notched specimen was the width of the notch. The notch width was modified over a range from 3.81 mm (0.15 in.) to 7.62 mm (0.30 in.). While the overall notch width is important, the notch radius is of greater interest since this dimension reflects the radius of curvature of the notch in the adhesive. Therefore, the radius of the notch, or half of the notch width, was used to identify the U-notched specimens. The notch radius varied from 1.27 mm (0.050 in.) to 3.81 mm (0.150 in.), with intermediate values of 1.91 mm (0.075 in.), 2.54 mm (0.100 in.), and 3.18 mm (0.125 in.), as shown in figure 5. The geometry of the notch consisted of parallel vertical sides with the curved bottom being semicircular. It is noteworthy that the 3.81-mm (0.15-in.) radius notch is entirely semicircular with no vertical sides. Similar to the 90° V-notched specimen, this configuration also has a notch width of 7.62 mm (0.30 in.).

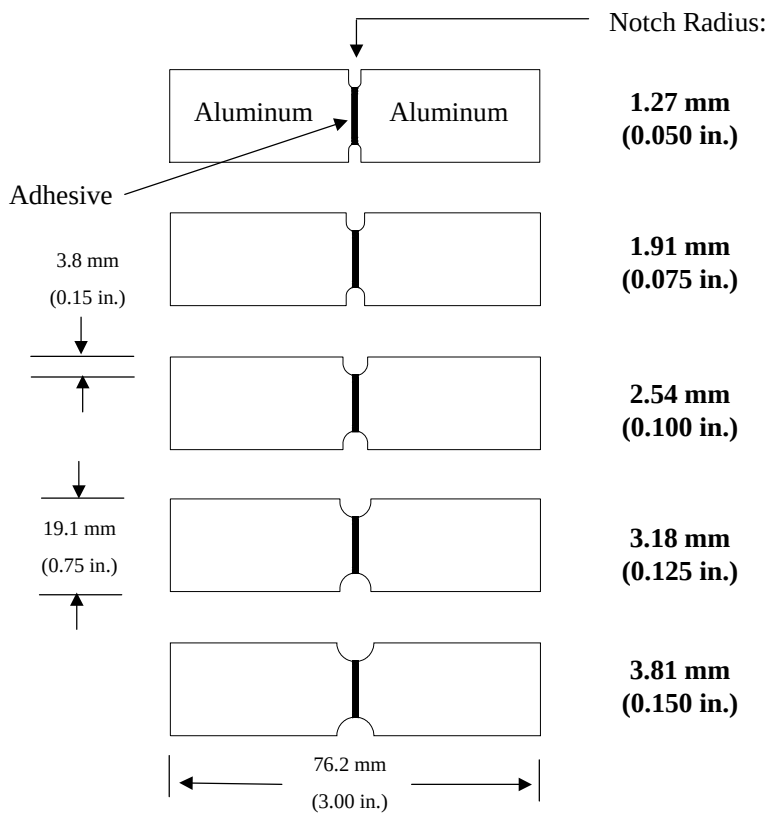

Figure 5. Iosipescu U-Notched Specimens With Varying Notch Radius

2.3.1.3 Variable Notch Angle Iosipescu V-Notched Specimens.

Another concept for reducing the stress concentrations in the original Iosipescu specimens was to vary the notch angle. The angle was reduced to 80° and 70°, but this only magnified the stress concentrations. The angle was then widened to 103° and 120°. The 103° angle was chosen due to a previous investigation [18] that indicated that the notch angle for producing an optimum state of uniform shear stress in an isotropic material is 102.6°. However, the evaluation of an initial set of notch angles showed that an angle of 120° gave the most favorable results. Thus, notch angles of 115° and 125° were added. Note that only the notch angle was changed from the original geometry and all other dimensions remained the same. The five notch angles modeled are shown in figure 6.

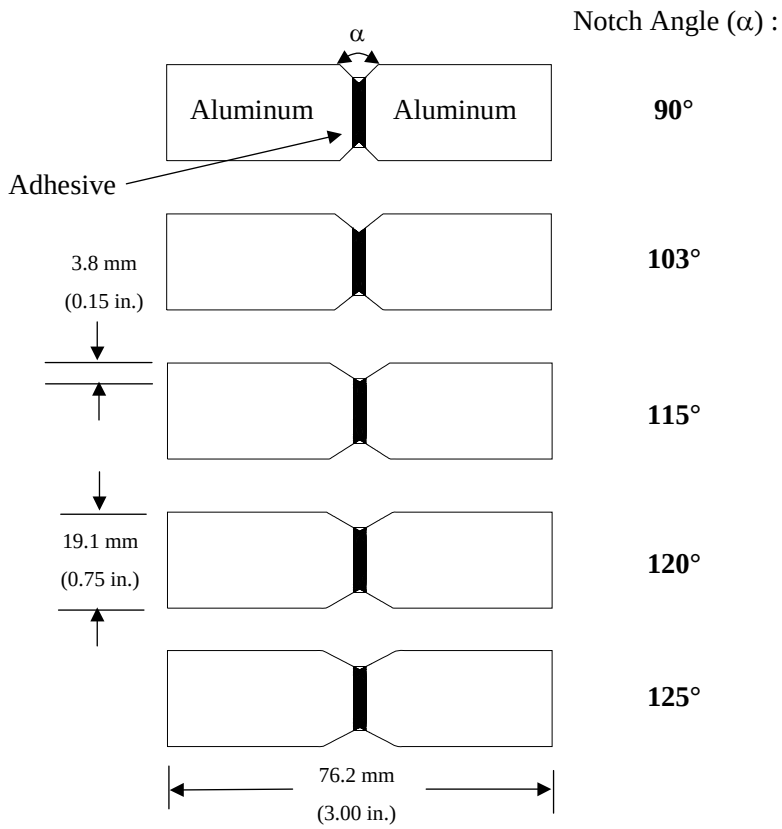

Figure 6. Variable Notch Angle Iosipescu V-Notched Specimens

2.3.1.4 Variable Notch Depth Ratio Iosipescu V-Notched Specimens.

The final variation on the Iosipescu specimen was to vary the notch depth. The original Iosipescu specimen had a notch depth of 3.81 mm (0.15 in.), producing a notch depth to a specimen height ratio of 0.20. In this study, the ratio of notch depth to specimen height is referred to as the notch depth ratio, or NDR. For the V-notched Iosipescu specimens, the NDR was increased to 0.225 and 0.250 and decreased to 0.175 and 0.150 for a total of five different NDRs. As with all other Iosipescu modifications, the motivation for changing the NDR was to

determine if the normal stress concentrations could be reduced while contributing to a more uniform state of shear stress throughout the entire adhesive section. Due to the results obtained from the previous geometric variations, the variable NDR specimen was modeled as a V-notched specimen with a notch angle of 120°. The specimens investigated with the five variable NDRs are shown in figure 7.

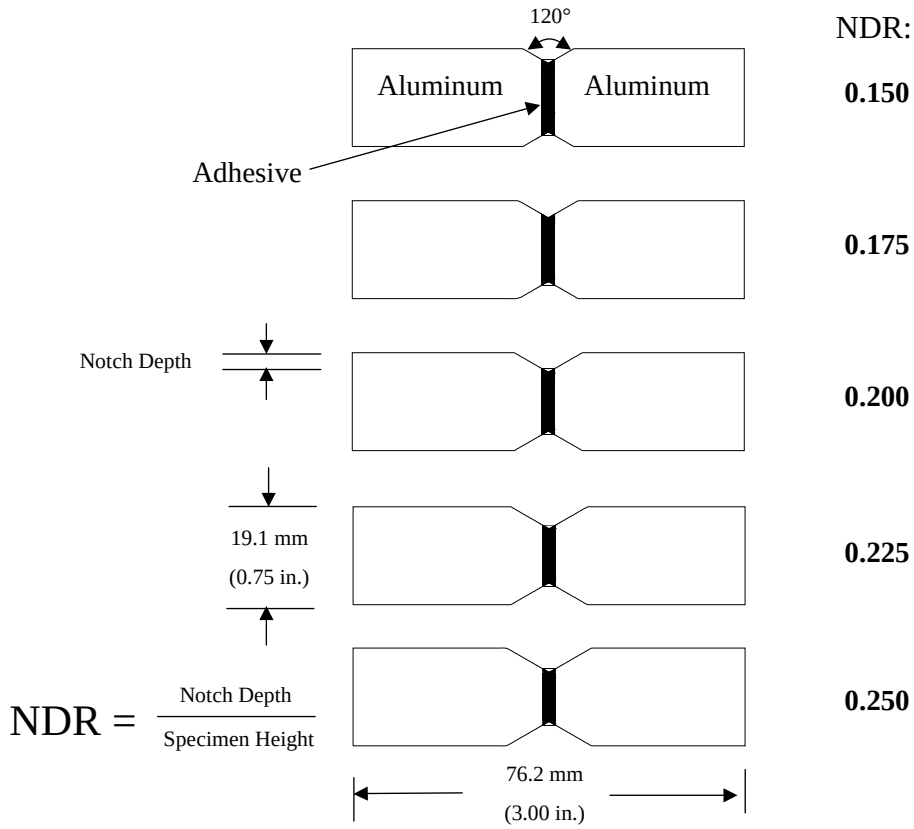

Figure 7. Variable NDR Iosipescu V-Notched Specimens

2.3.2 Bulk Adhesive Iosipescu Specimens.

A finite element analysis was also performed on bulk adhesive specimens to determine if properties obtained from bulk adhesive tests could be used to model in situ adhesive behavior. Finite element models of the bulk adhesive specimens were created by simply changing the material properties of the adherends in the bonded Iosipescu models from aluminum to adhesive. A bulk adhesive analysis was performed on all the Iosipescu specimens presented above.

2.3.3 Thick Adherend Lap Joint Specimen.

A commonly used adhesive shear test is the thick adherend lap shear test, ASTM D 5656 (figure 8). This test method is somewhat different from the Iosipescu tests in that the specimen is loaded

in tension and the lap configuration transfers a shear load to the adhesive test section. Two-dimensional plane stress finite element analyses were conducted on this test specimen for comparison with the bonded Iosipescu specimens. A uniaxial tensile load was applied to produce an average shear stress of 27.5 MPa (4000 psi) in the adhesive gage section. As with the Iosipescu analyses, bondline thicknesses of 0.25 mm (0.01 in.), 1.27 mm (0.05 in.), and 2.54 mm (0.10 in.) were modeled.

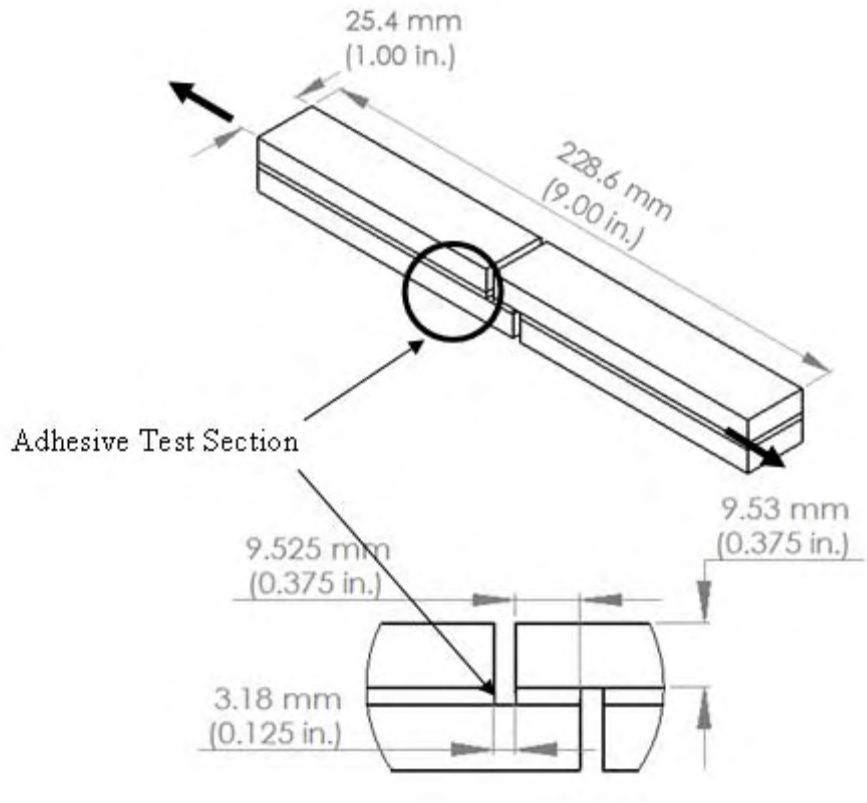

Figure 8. Dimensions for Thick Adherend Lap Joint Finite Element Model

2.4 BUTT TENSILE TEST ANALYSIS.

To observe the effect of bondline thickness on tensile properties, finite element analysis was performed on butt tensile specimens. The specimens modeled were based on ASTM D 2094 [24] and had a square cross-section measuring 12.7 mm (0.50 in.) on a side. The aluminum adherends each had a length of 38.1 mm (1.5 in.). Specimens were modeled with bondline thicknesses of 0.25 mm (0.01 in.), 1.27 mm (0.05 in.), and 2.54 mm (0.10 in.). The material properties used for both aluminum and adhesive were the same as the properties used in the shear tests.

Due to the square cross-section of the specimen, a plane stress analysis was deemed inappropriate, and thus, a three-dimensional analysis was performed. The rectangular geometry of the specimen allowed for the model to be simplified due to symmetry such that only 1/8 of the full specimen was modeled (see figure 9). A uniform pressure of 6.9 MPa (1000 psi) was

applied to the end of the adherend in the axial direction. Eight-noded ANSYS Solid45 brick elements were used.

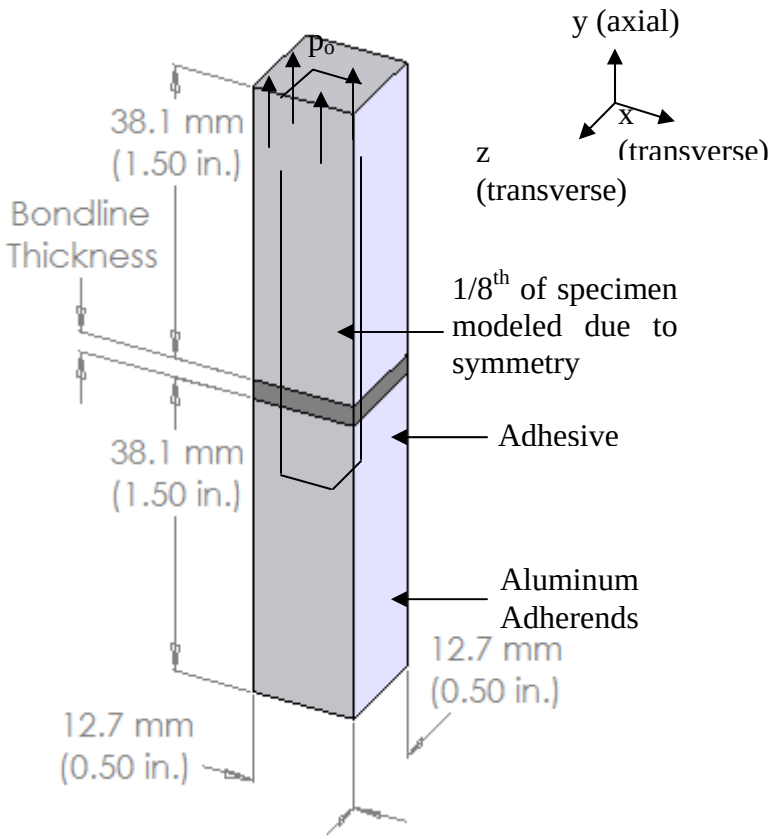

Figure 9. Geometry of Butt Tensile Specimen for Finite Element Model

3. RESULTS OF FINITE ELEMENT ANALYSIS.

3.1 RESULTS OF SHEAR SPECIMEN ANALYSES.

For each finite element model analyzed, values of transverse, axial, and shear stress were recorded at each node within the model. These stress component values were then normalized with respect to the average shear stress between the notches for the Iosipescu specimens and with respect to the average shear stress along the adhesive midplane for the thick adherend lap joint. The normalized stress values were plotted as contours of constant stress to illustrate stress variations throughout the specimen. Since the adhesive layer was of primary concern, most of the stress contour plots are of only the adhesive bondline. All analysis geometries were modeled using the three bondline thicknesses of 0.25 mm (0.01 in.), 1.27 mm (0.05 in.), and 2.54 mm (0.10 in.), as well as a bulk adhesive specimen of the given geometry (the thick adherend lap joint was not modeled in bulk adhesive form).

There were two main objectives of the finite element analyses. First, many different specimen geometries were modeled to determine the geometry that produced the most uniform shear stress distribution throughout the adhesive. Second, all geometries were modeled with the three adhesive bond thicknesses and as bulk adhesive to determine if the stress state varied depending on adhesive thickness.

The optimal state of stress within the adhesive is one in which the shear stress is of uniform value throughout the entire adhesive section while the axial and transverse normal stresses are minimal. The uniformity of the shear stress in the adhesive is important for measuring both the shear strength and shear modulus. For measuring shear strength, it is desirable to minimize stress concentrations such that the specimen fails cohesively in the adhesive bond under a state of uniform shear stress. Since the adhesive shear strength τ_{ult} is calculated using the maximum applied shear load $P_{\max}$ transmitted in shear through the adhesive bond and the cross-sectional area A of the adhesive bond

$$\tau_{ult} = P_{\max} / A \tag{1}$$

a constant value of shear stress is desired through the adhesive test section. For determining the adhesive shear modulus, G, the average shear strain γ_{ave} recorded in the adhesive test section is used in conjunction with the average adhesive shear stress τ_{ave}, according to the relation

$$G = \Delta_{\tau ave} / \Delta\gamma_{ave} \tag{2}$$

where Δ is the change in the quantity over the desired data range. The average shear stress τ_{ave} is calculated from the applied shear load P_{app} and the cross-sectional area A of the adhesive bond

$$\tau_{ave} = P_{app} / A \tag{3}$$

Since the average shear stress is used in the shear modulus calculation, the average shear strain γ_{ave} must also be used to obtain the correct value for G. Thus, the shear strain within the region of measurement must be equal to the average shear strain, γ_{ave}, across the centerline of the test section.

3.2 DATA PROCESSING.

For each specimen modeled, the three in-plane components of stress (axial, transverse, and shear) were imported into Microsoft Excel® for postprocessing. All stresses were nondimensionalized prior to generating contour plots. Nodal stresses (axial, transverse, and shear components) were divided by the average shear stress along the test section centerline. Thus, for the ideal state of uniform shear stress and no normal stresses, the nondimensionalized shear stresses would be 1.0 and the nondimensionalized axial and transverse stresses would be 0.0 throughout the adhesive test section.

3.3 ORIGINAL IOSIPESCU V-NOTCHED SPECIMEN.

The first finite element analyses were performed using the standard Iosipescu geometry, but with aluminum specimen halves adhesively bonded together to produce the original specimen geometry. As mentioned previously, the main interest is the stress state in the adhesive layer and, therefore, only stress contours within the adhesive are shown. For the bulk adhesive specimen, stress contours are plotted in the entire notch area since the area of interest is less intuitive with this particular configuration.

3.3.1 Shear Stresses for Original Iosipescu V-Notched Specimen.

Nondimensionalized shear stress contour plots for the original V-notched specimen are shown in figure 10. Plots are shown for each of the three adhesive bondline thicknesses as well as the bulk adhesive specimen. All four adhesive configurations show a relatively uniform distribution of shear stress, within ±3 percent of the average, in the center of the adhesive test section. However, near the notch tips along the axial centerline, there are large stress concentrations. Figure 11 shows that the largest shear stress concentrations are found in the thickest adhesive bond and are almost 20 percent greater than the average shear stress value. The shear stress concentrations in the remaining two bondline thicknesses are approximately 15 percent greater than the average shear stress. The smallest shear stress concentrations in the original V-notched specimen are found in the bulk adhesive, where the concentrations are less than 5 percent of the average shear stress.

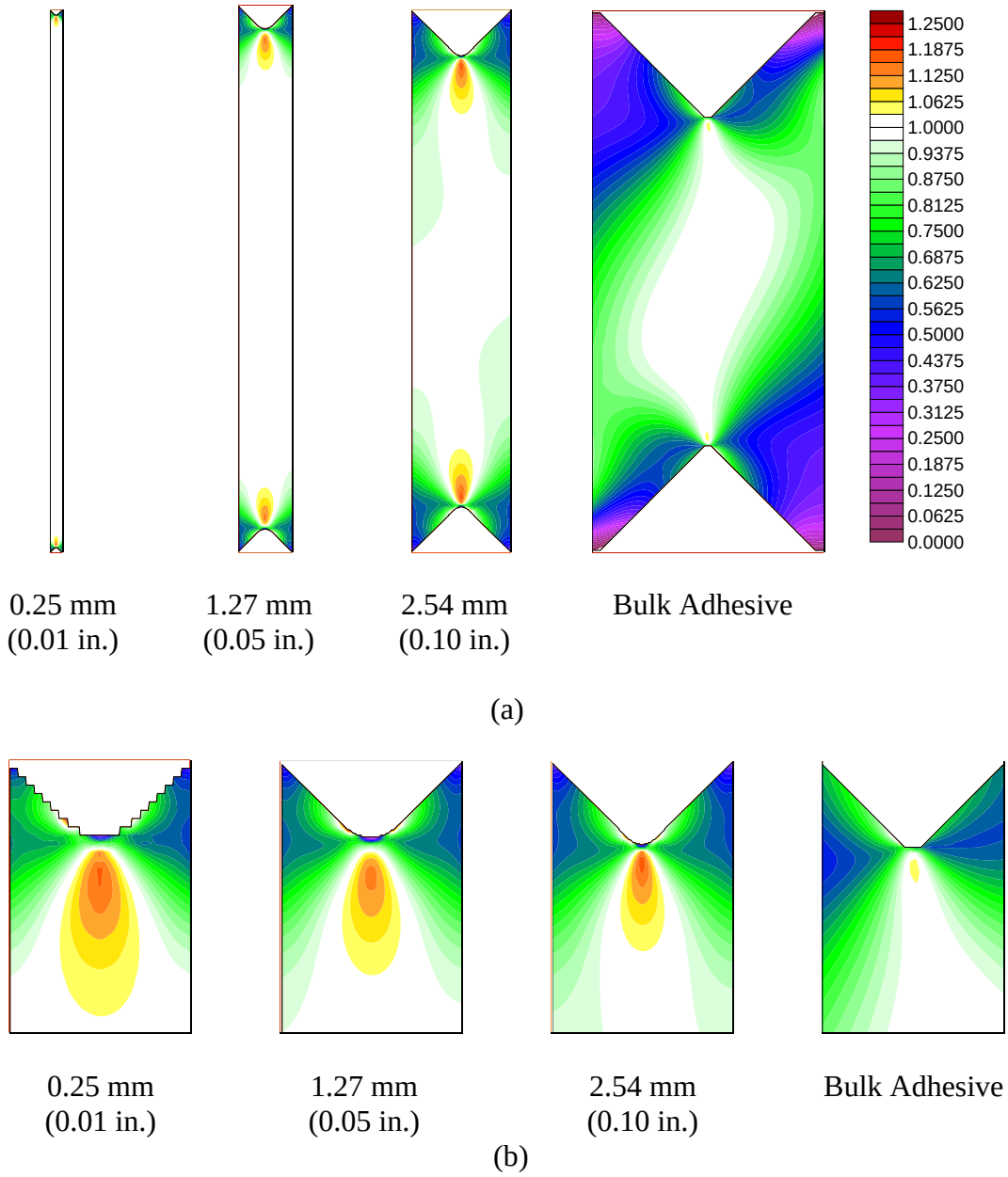

Figure 10. Shear Stress Distributions in (a) Full Adhesive Bond and (b) Around Notch Tip for Original Iosipescu V-Notched Specimens (Normalized)

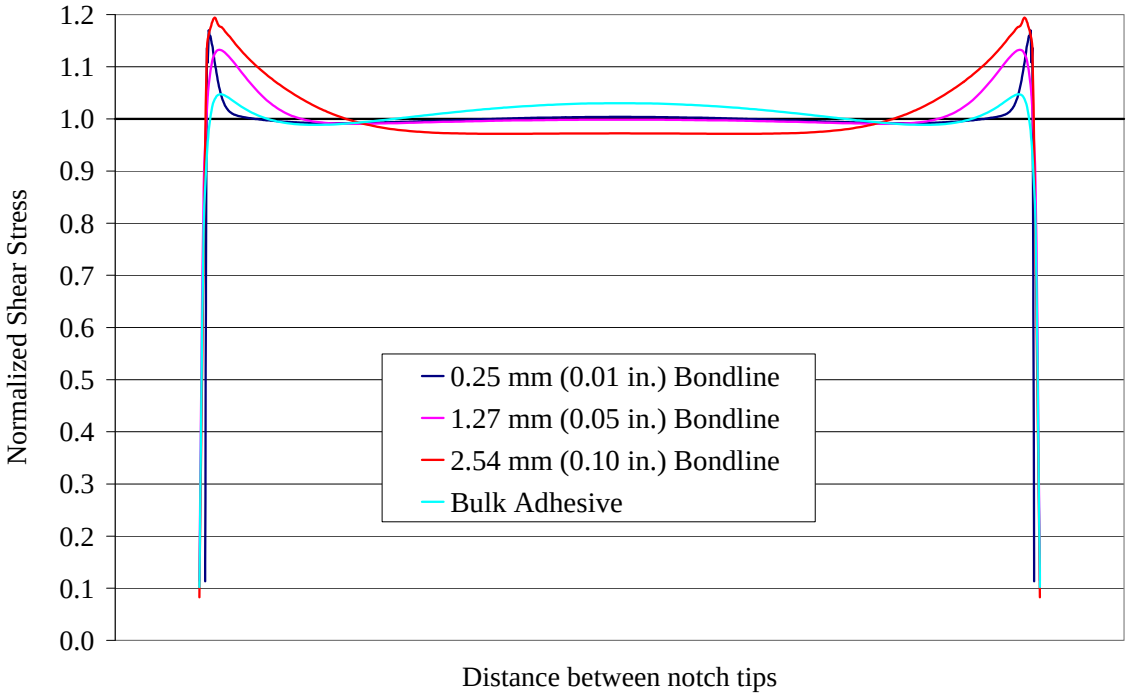

Figure 11. Shear Stress Distributions Along Adhesive Centerline for 90° V-Notched Iosipescu Specimens

3.3.2 Normal Stresses for the Original Iosipescu V-Notched Specimens.

Nondimesionalized contour plots of transverse and axial stresses for all four adhesive configurations are shown in figures 12 and 13, respectively. The transverse normal stresses are negligible throughout most of the center region for all four adhesive thicknesses. The axial normal stresses are also close to zero in the center region for the three bondline thicknesses, but reach values of 25 percent of the average shear stress for the bulk adhesive specimen, indicating a somewhat significant compressive stress in the axial direction along the specimen centerline.

A very significant feature of both the transverse and axial stress contour plots is the presence of large stress concentrations near the notch tips. Unlike the shear stress concentrations, however, the normal stress concentrations are not along the specimen centerline but are to the side of the notch along the notch flank. The concentrations appear at both the top and bottom notches and are asymmetric due to the asymmetric loading of the specimen. Table 3 lists the maximum values of the normal stress components along with the maximum value of shear stress along the test section centerline and at the stress concentration along the notch flank. It is readily apparent that the 90° V-notch minimizes the normal stresses along the axial centerline between the notch tips very well. For the adhesively bonded specimens, the largest normal stress along the centerline occurs in the 0.25-mm (0.01-in.) bond, where the transverse normal stress is only 33 percent of the average shear stress. However, when the total adhesive test section is considered, significant stress concentrations are observed along the notch flank. In these areas, the transverse stresses reach magnitudes of over 190 percent of the average shear stress and the axial stresses reach magnitudes of around 120 percent of the average shear stress. The stress

concentrations along the notch flank in the bulk adhesive are even higher. The tabulated results also show that significant shear stress concentrations exist along the notch flank. In fact, the largest values of all three stress components occur at the notch flank. The presence of these stress concentrations is important since they may lead to an initial failure along the notch flank rather than in the center of the specimen, obscuring the true shear strength of the adhesive.

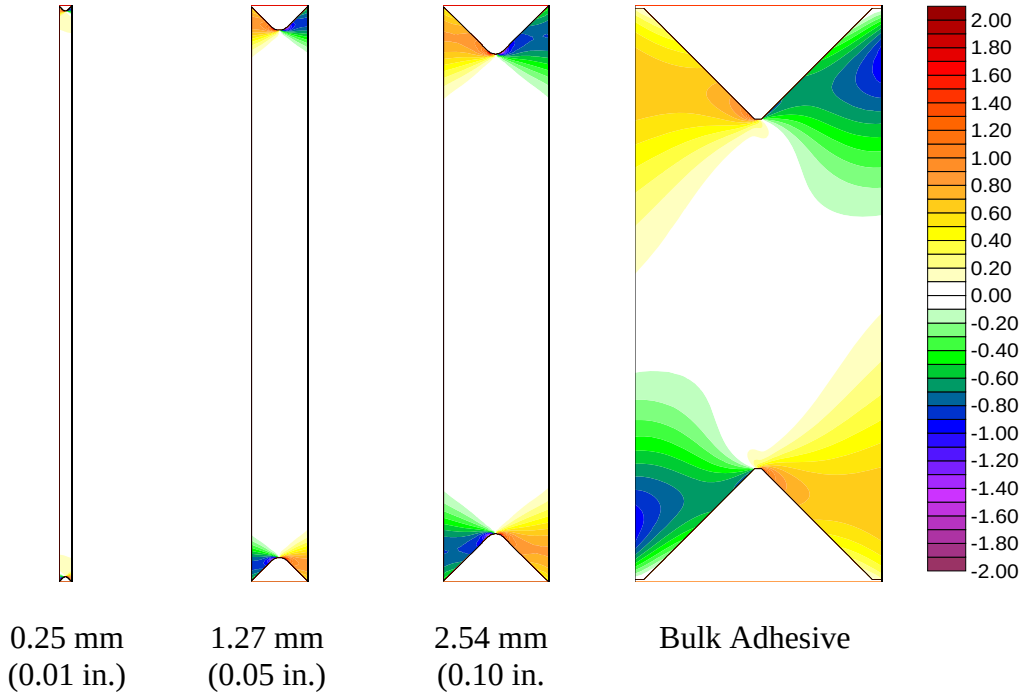

(a)

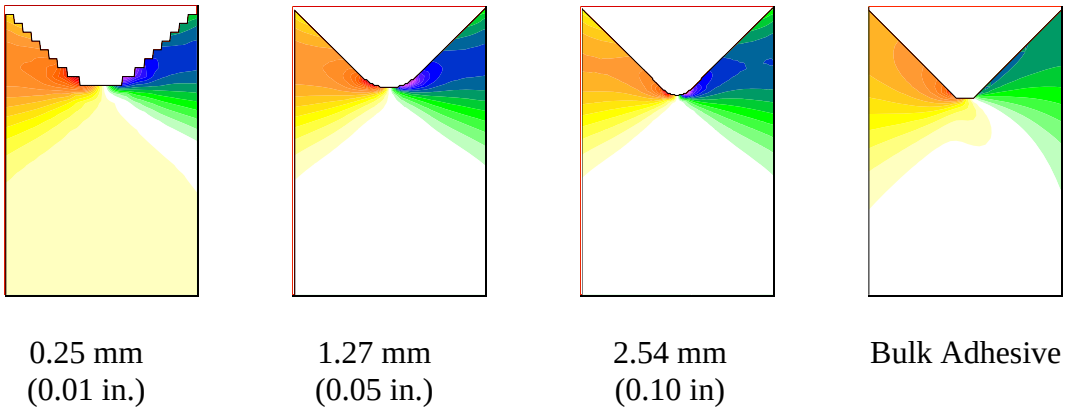

(b)

Figure 12. Transverse Stress Distributions in (a) Full Adhesive Bond and (b) Around Notch Tip for Original Iosipescu V-Notched Specimens (Normalized)

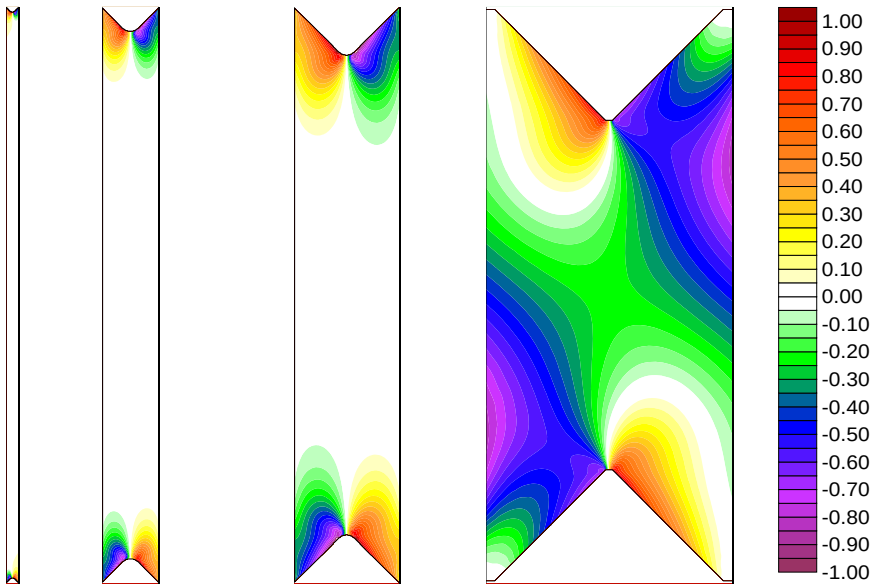

0.25 mm (0.01 in.) | 1.27 mm (0.05 in.) | 2.54 mm (0.10 in.) | Bulk Adhesive

(a)

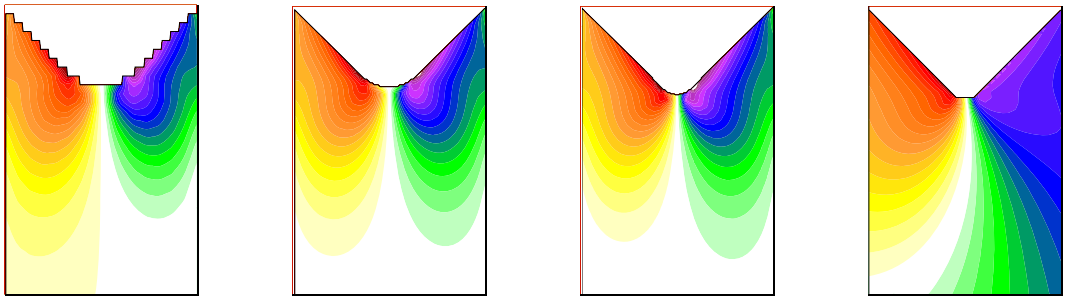

0.25 mm (0.01 in.) | 1.27 mm (0.05 in.) | 2.54 mm (0.10 in.) | Bulk Adhesive

(b)

Figure 13. Axial Stress Distributions in (a) Full Adhesive Bond and (b) Around Notch Tip for Original Iosipescu V-Notched Specimens (Normalized)

Table 3. Maximum Values of Shear and Normal Stress Components for Original Iosipescu V-Notched Specimens

Bond Thickness	Location	τ_{max}/τ_{avg}	$\sigma_{x,max}/\tau_{avg}$	$\sigma_{y,max}/\tau_{avg}$
0.25 mm (0.01 in.)	Along centerline	1.17	0.33	0.06
	Along notch flank	1.31	1.98	1.19
1.27 mm (0.05 in.)	Along centerline	1.13	0.10	0.02
	Along notch flank	1.28	1.92	1.19
2.54 mm (0.10 in.)	Along centerline	1.19	0.07	0.01
	Along notch flank	1.21	1.99	1.28
Bulk Adhesive	Along centerline	1.05	0.82	0.14
	Along notch flank	1.45	2.28	1.32

3.3.3 von Mises Equivalent Stress.

Initial analysis of the original Iosipescu V-notched specimen revealed that the stress state in the adhesive bondline as well as in the bulk adhesive is not pure shear. The presence of the normal stress components, mostly concentrated in small areas near the notch tips but large in magnitudes, indicates a combined stress state. While the purpose of this study was not to establish a failure criterion for adhesive bonds, it is nonetheless instructive to use previously established failure criteria to compare the severity of the combined stress states occurring in the specimens. The stress value chosen to represent the combined stress state is the von Mises or octahedral shear stress.

The von Mises stress is useful for predicting the yielding of ductile materials, such as adhesives. The two-dimensional von Mises stress is related to the shear and normal stress components by the relation

$$\sigma_e = \frac{1}{\sqrt{2}}\sqrt{(\sigma_x - \sigma_y)^2 + \sigma_x^2 + \sigma_y^2 + 6\tau_{xy}^2} \tag{4}$$

where σ_e represents the von Mises stress and the *e* indicates effective or equivalent stress. For the case of pure shear, the equation reduces to

$$\sigma_e = \sqrt{3}\ \tau_{xy} \tag{5}$$

meaning that at the optimum stress state of uniform shear and zero normal stresses, the von Mises stress will differ from the shear stress by a factor of $\sqrt{3}$ or approximately 1.73. Therefore, the von Mises stresses were normalized by dividing by $\sqrt{3}$ times the average shear stress along the centerline of the adhesive test section.

Contour plots of the normalized von Mises stresses are shown in figure 14. The von Mises stress distributions appear similar to the distributions of shear stresses, including the stress concentrations along the axial centerline near the notch tip. The notable differences between the shear and von Mises stress contours are the slightly nonuniform von Mises stresses in the center of the bulk adhesive (due to the axial stress contribution) and the more pronounced stress concentrations along the notch flanks.

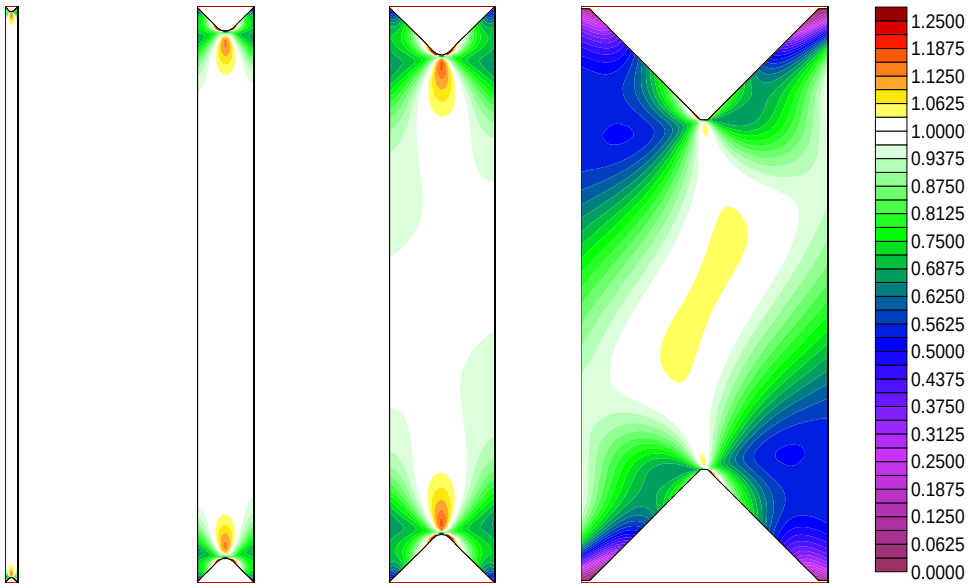

0.254 mm (0/01 in.) 1.27 mm (0.05 in.) 2.54 mm (0.10 in.) Bulk Adhesive

(a)

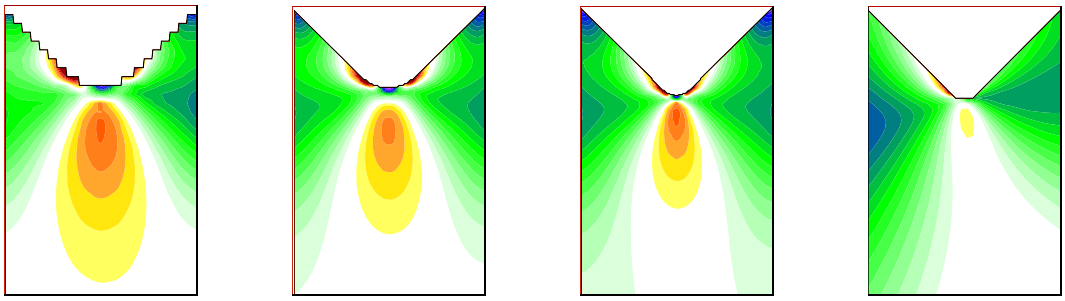

0.254 mm (0.01 in.) 1.27 mm (0.05 in.) 2.54 mm (0.10 in.) Bulk Adhesive

(b)

Figure 14. von Mises Stress Distributions in (a) Full Adhesive Bond and (b) Around Notch Tip for Original Iosipescu V-Notched Specimens (Normalized)

Table 4 lists the maximum values of von Mises stress along both the axial centerline and the notch flanks. Similar to the individual stress components, the stresses along the centerline are fairly uniform with the largest value of von Mises stresses being 1.19 in the thickest bond. However, the stress concentrations at the notch flanks are very large, with the von Mises stress reaching magnitudes of around 150 percent of the average shear stress in all three bondline thicknesses and in the bulk adhesive.

Table 4. Maximum Values of von Mises Stresses for the Original Iosipescu V-Notched Specimen

Bond Thickness	Location	$\sigma_{e,max}/(\sqrt{3}*\tau_{avg})$
0.25 mm (0.01 in.)	Along centerline	1.17
	Along notch flank	1.58
1.27 mm (0.05 in.)	Along centerline	1.13
	Along notch flank	1.60
2.54 mm (0.10 in.)	Along centerline	1.19
	Along notch flank	1.44
Bulk Adhesive	Along centerline	1.05
	Along notch flank	1.49

3.3.4 Conclusions for Original Iosipescu V-Notched Specimen.

The finite element analysis of the original configuration for the Iosipescu V-notched specimen led to several important observations. First, complex states of stress were observed in all three bondline thicknesses as well as the bulk adhesive. These stress states are a combination of all three in-plane stress components and as such requires that the analysis include a description of the von Mises stress. Second, the analysis indicated that the 90° V-notch does not produce an optimal state of stress for evaluating shear strength and shear modulus. The shear stress is not uniform throughout the adhesive test section and there are large concentrations of normal stresses along the notch flanks. Based on the results of this initial geometry, it was decided to investigate several different configurations in an effort to find a specimen with a more optimal stress state.

3.4 IOSIPESCU U-NOTCHED SPECIMEN.

The first modification of the original Iosipescu V-notched specimen was the Iosipescu U-notched specimen. The geometry of the Iosipescu U-notched specimen was very similar to that of the original Iosipescu V-notched specimen except that the sharp angle at the bottom of the V-notch was replaced with a more gradual semicircular, U-shaped notch. It was thought that removing the sharp notch tip would eliminate the stress concentrations at the tip of the V-notch and, more importantly, along the notch flanks.

The U-notched specimens were evaluated with five notch radii: 1.27 mm (0.050 in.), 1.91 mm (0.075 in.), 2.54 mm (0.100 in.), 3.18 mm (0.125 in.), and 3.81 mm (0.150 in.). In each case, the notch depth remained constant at 3.8 mm (0.15 in.). All configurations were evaluated with all three adhesive bondline thicknesses and as a bulk adhesive specimen. As with the original V-notched specimen, only the results for the adhesive test section are presented, as the stress state in the aluminum adherends is not relevant.

3.4.1 Shear Stresses for Iosipescu U-Notched Specimens.

The shear stresses for the adhesively bonded Iosipescu U-notched specimens are shown in figure 15 for the 0.25-mm (0.01-in.) bondline, figure 16 for the 1.27-mm (0.05-in.) bondline, and figure 17 for the 2.54-mm (0.10-in.) bondline. Inspection of these contour plots reveals that by replacing the sharp tip of the V-notch with the rounded U-notch, the shear stress concentrations are removed at the notch tips along the axial centerline as well as along the notch flanks of the adhesive. The shear stresses along the notch flanks are lower than the average shear stress for all three bond thicknesses. However, the shear stresses for the bulk adhesive Iosipescu U-notched specimens shown in figure 18 still exhibit the unwanted shear stress concentrations along the notch flanks. An examination of the shear stresses around the notches of the bonded specimens (figure 19) shows that the shear stress concentrations along the notch flanks do still exist, but are moved outside the adhesive bond into the aluminum adherend. Therefore, with the U-notched design, the shear stress concentrations along the notch flanks are only a problem for the bulk adhesive.

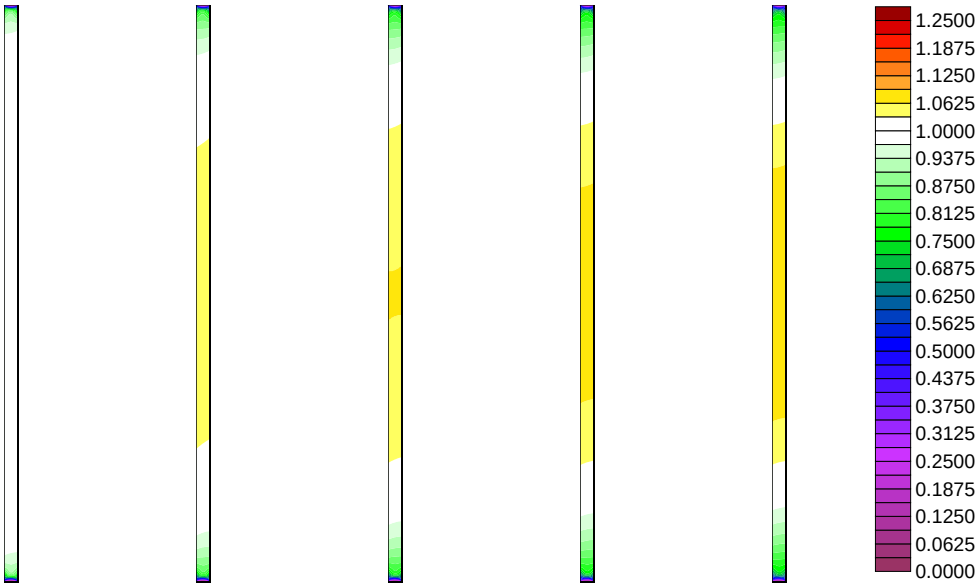

R=1.27 mm (0.050 in.) R=1.91 mm (0.075 in.) R=2.54 mm (0.100 in.) R=3.18 mm (0.125 in.) R=3.81 mm (0.150 in.)

(a)

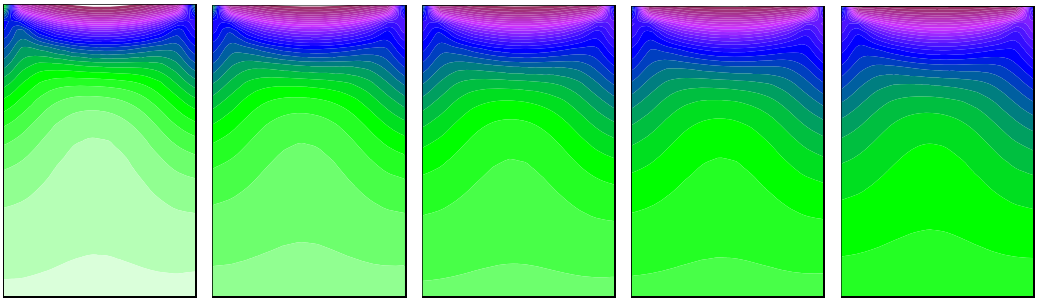

R=1.27 mm (0.050 in.) R=1.91 mm (0.075 in.) R=2.54 mm (0.100 in.) R=3.18 mm (0.125 in.) R=3.81 mm (0.150 in.)

(b)

Figure 15. Shear Stress Distributions in (a) Full Adhesive Bond and (b) Around Notch Tip for Iosipescu U-Notched Specimens With 0.25-mm (0.01-in.) Bondline (Normalized)

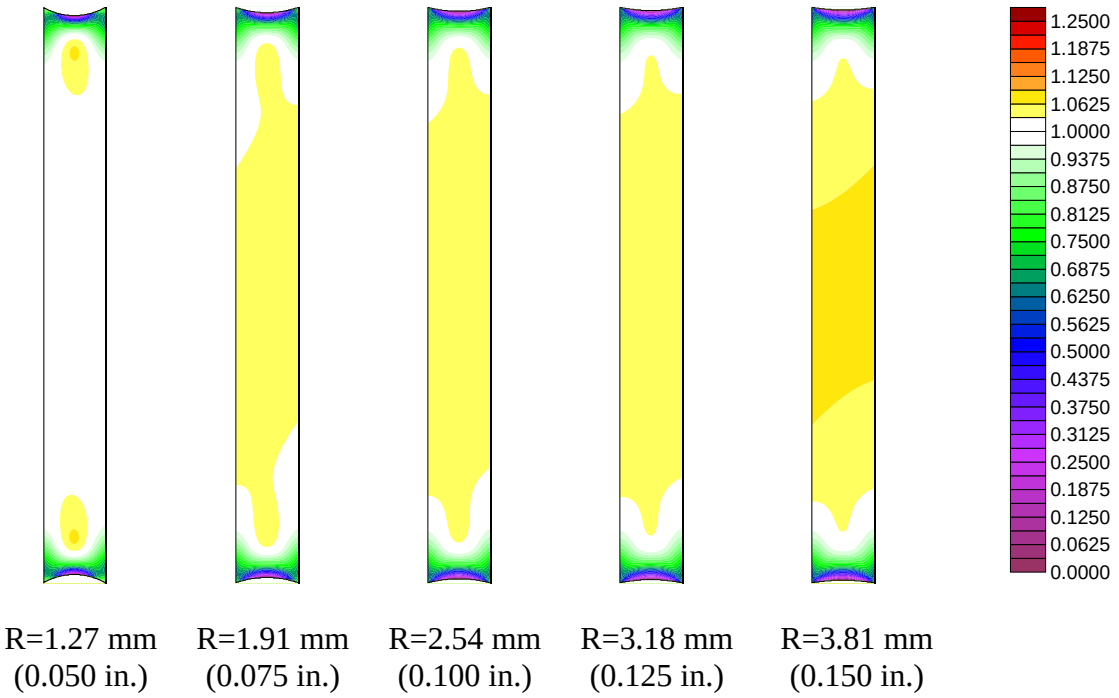

Figure 16. Shear Stresses for Iosipescu U-Notched Specimens With 1.27-mm (0.05-in.) Bondline (Normalized)

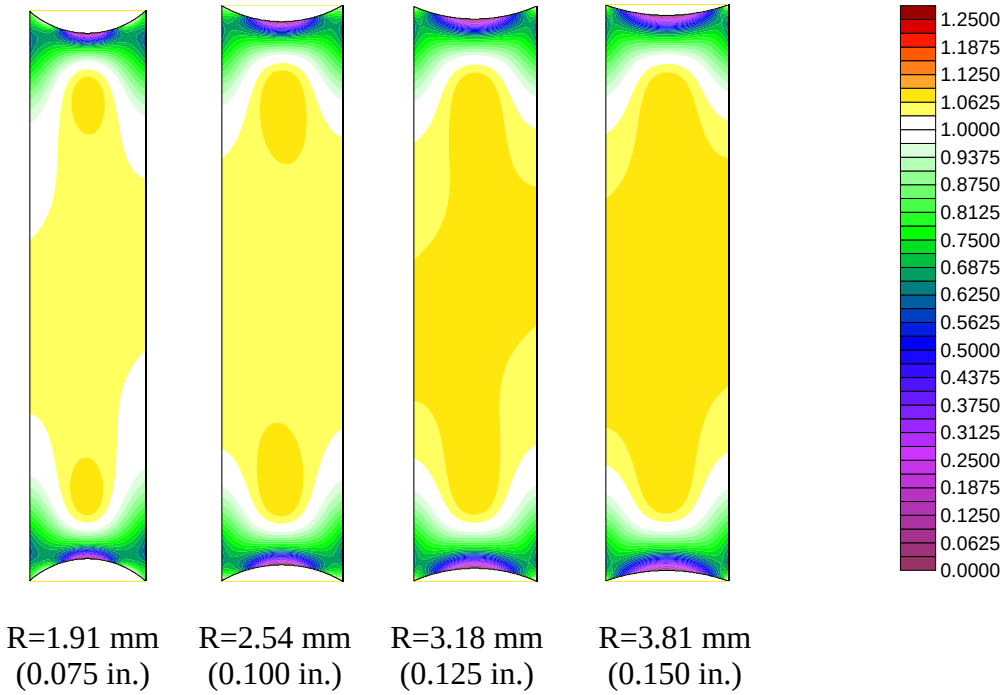

Figure 17. Shear Stresses for Iosipescu U-Notched Specimens With 2.54-mm (0.10-in.) Bondline (Normalized)

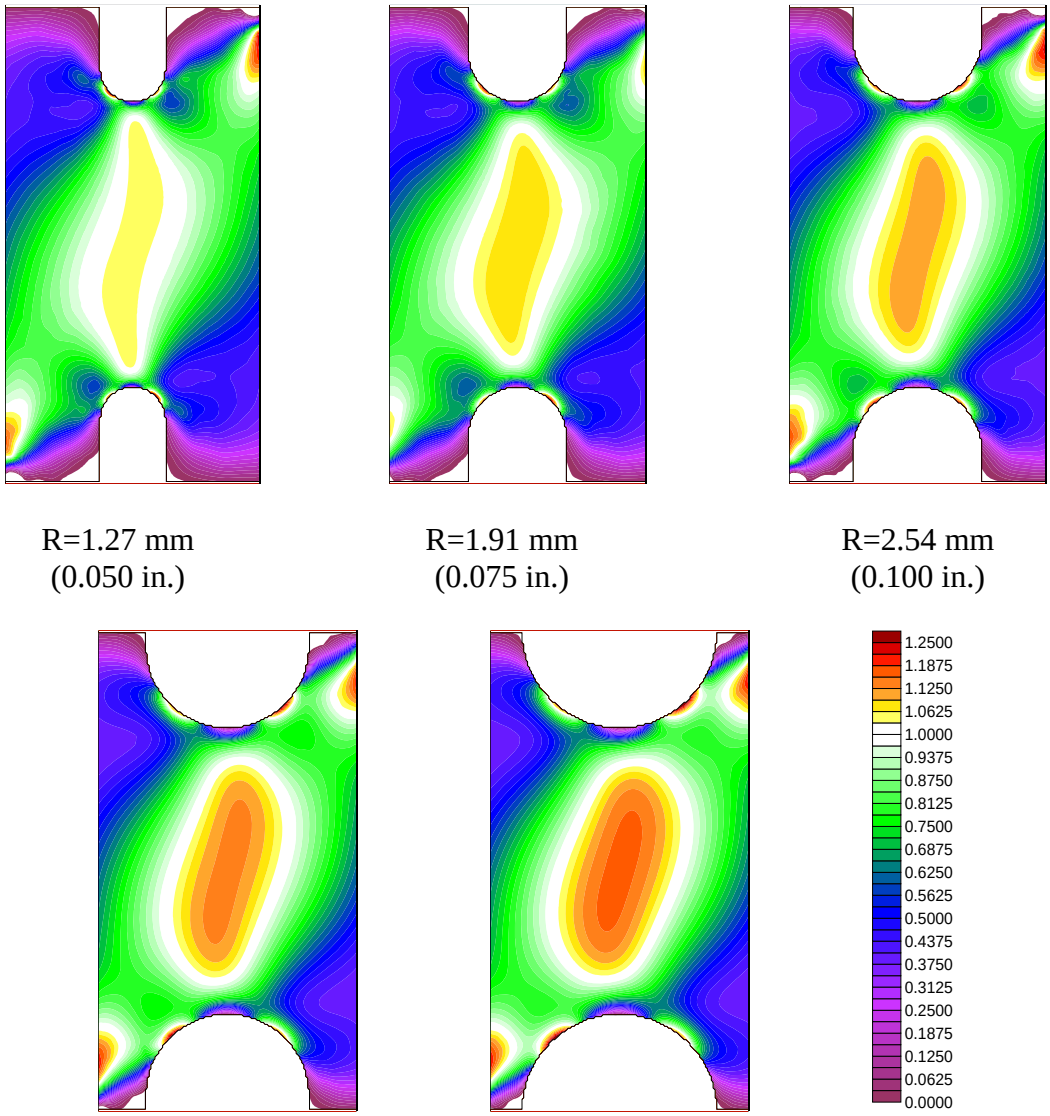

Figure 18. Shear Stresses for Iosipescu U-Notched Bulk Adhesive Specimens (Normalized)

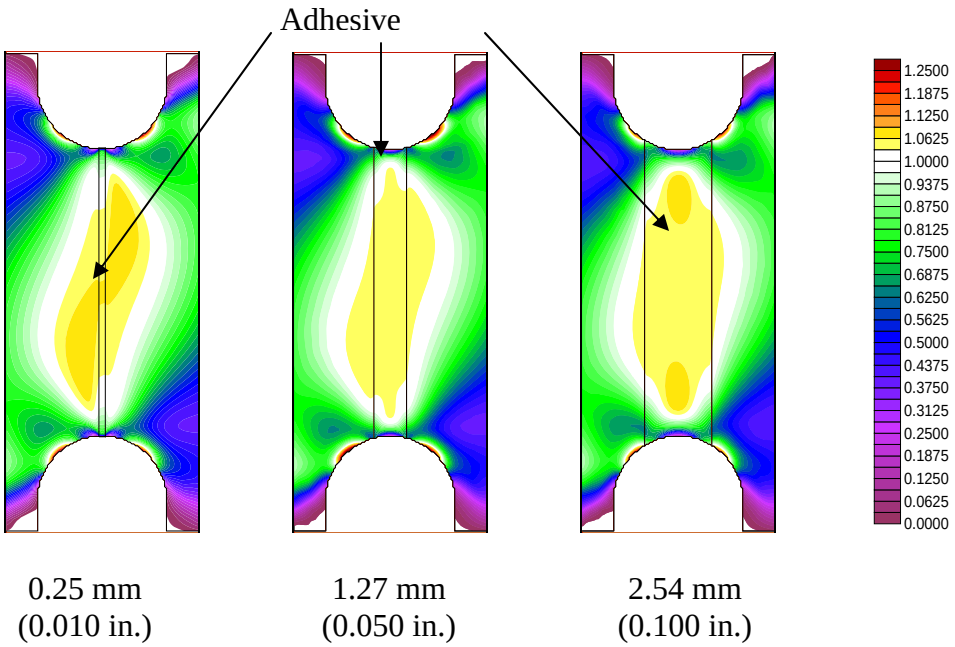

Figure 19. Shear Stresses Around Entire Notch for Adhesively Bonded Iosipescu U-Notched Specimens (Normalized)

Although the U-notch geometry eliminates the shear stress concentrations in the adhesive due to the notch, the shear stress state throughout the adhesive is not entirely uniform. Figures 20, 21, and 22 show the shear stress distribution between the notch tips along the adhesive centerline for the 0.25-mm (0.01-in.), 1.27-mm (0.05-in.), and 2.54-mm (0.10-in.) bonds, respectively. The shear stress distribution for the bulk adhesive is shown in figure 23. As the notch radius increases, the shear stress distribution between the notches becomes more parabolic. For the 0.25-mm (0.01-in.) bond and the bulk adhesive, the most uniform shear distribution is found in the 1.27-mm (0.05-in.) notch radius. For the 1.27-mm (0.05-in.) and 2.54-mm (0.10-in.) bonds, the shear stress is maximum near the notches with the peak magnitude decreasing as the notch radius increases. The most uniform shear distribution in the center of the specimen for these two bonds is found in the 1.27-mm (0.05-in.) notch radius, although this notch radius also creates the largest stress peaks near the notches.

The parabolic shear stress distribution, with the peak shear stress midway between the two notches, is what would be expected from a rectangular beam subjected to a shear loading. In fact, when the radius of curvature of the U-notch is much larger than the thickness of the adhesive bondline, the adhesive has almost no notch at all and it behaves similarly to a beam with a rectangular cross-section. This rectangular adhesive geometry is most evident in the thinnest adhesive bond, but also evident in the other two bondline thicknesses. It is also apparent that the parabolic shear distribution becomes more pronounced as the notch radius increases, due to the cross-section becoming more rectangular.

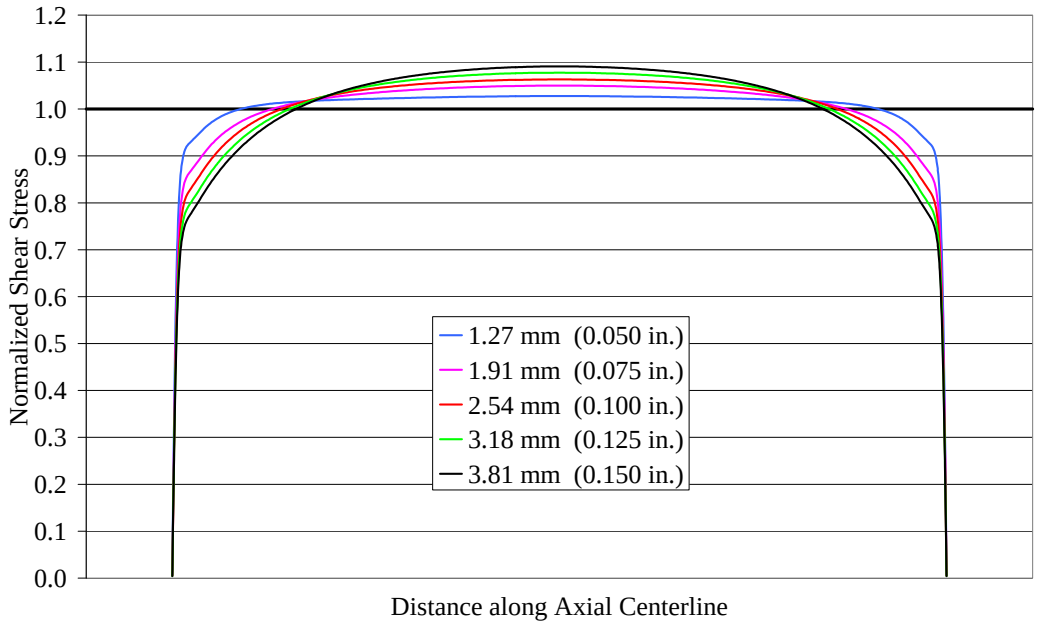

Figure 20. Shear Stress Distribution Along Axial Centerline for Iosipescu U-Notched Specimens With Different Notch Radius Values, 0.25-mm (0.01-in.) Bondline

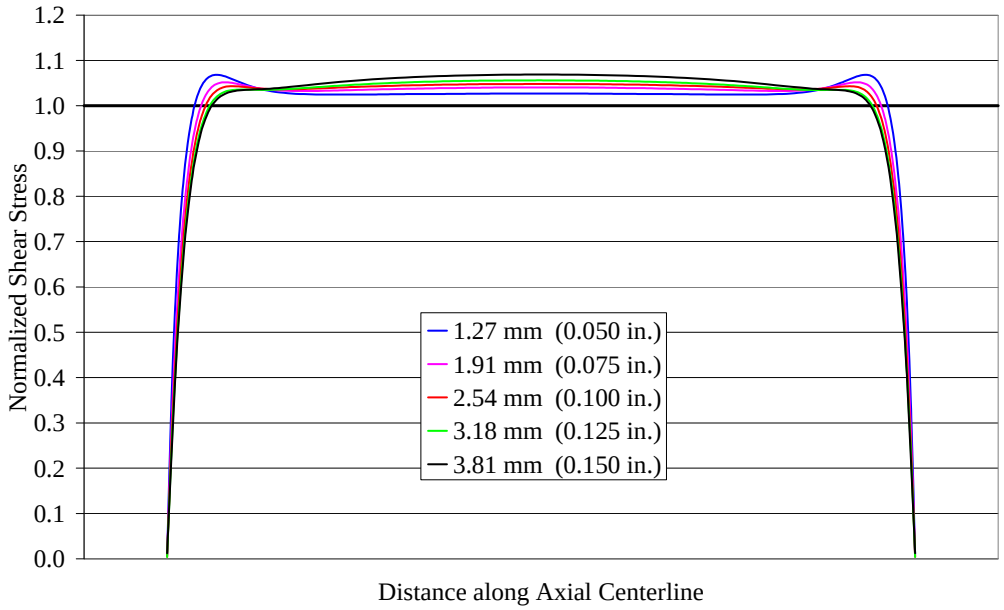

Figure 21. Shear Stress Distribution Along Axial Centerline for Iosipescu U-Notched Specimens With Different Notch Radius Values, 1.27-mm (0.05-in.) Bondline

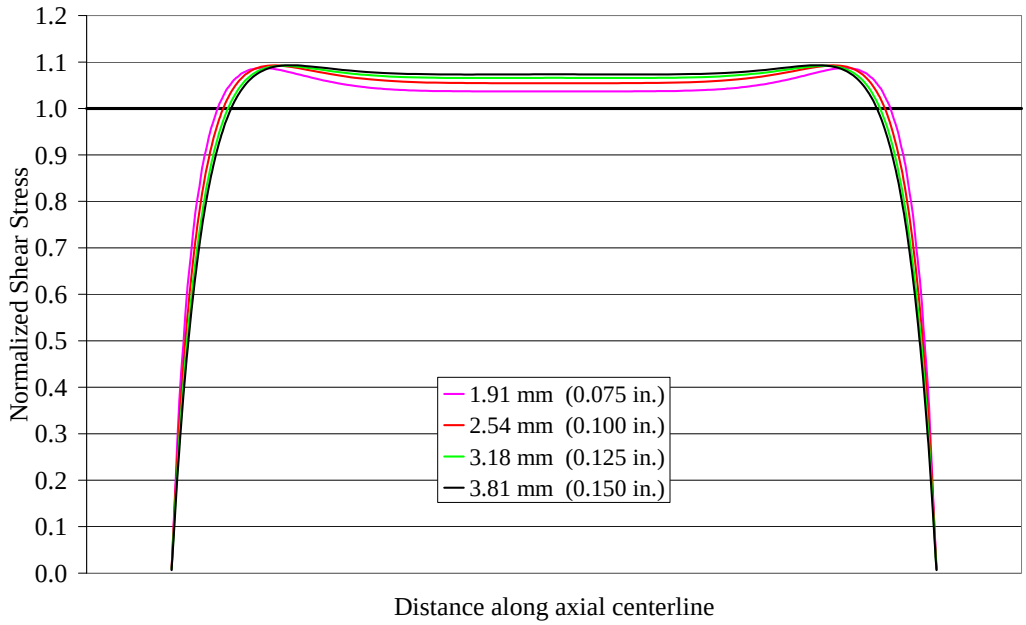

Figure 22. Shear Stress Distribution Along Axial Centerline for Iosipescu U-Notched Specimens With Different Notch Radius Values, 2.54-mm (0.10-in.) Bondline

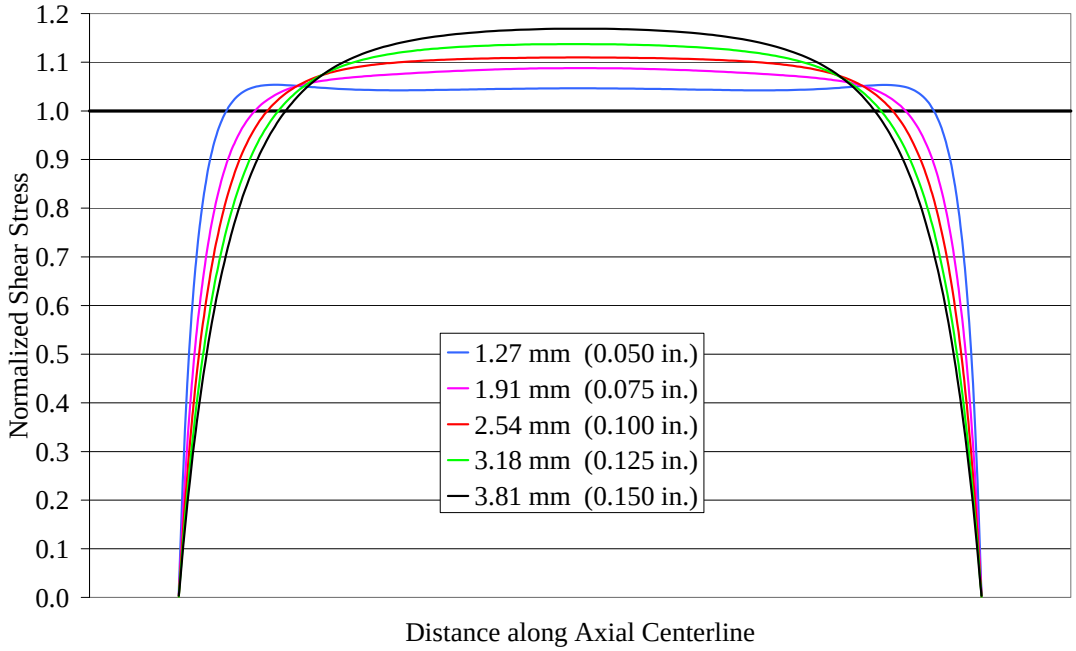

Figure 23. Shear Stress Distribution Along Axial Centerline for Iosipescu U-Notched Bulk Adhesive Specimens With Different Notch Radius Values

3.4.2 Normal Stresses for Iosipescu U-Notched Specimens.

The transverse and axial normal stresses for the bonded Iosipescu U-notched specimens are shown in figures 24 and 25 for the 0.25-mm (0.01-in.) bondline, figures 26 and 27 for the 1.27-mm (0.05-in.) bondline, and figures 28 and 29 for the 2.54-mm (0.10-in.) bondline. All three bondline thicknesses for all notch radii have significant concentrations of both transverse and axial stresses at the top and bottom adhesive adherend interface corners. From the stress contour plots, it appears that the interface stress concentrations for both normal stresses have the greatest magnitudes associated with the smallest notch radius. However, along the adhesive centerline for all three bond thicknesses, the transverse stresses are less than 10 percent of the average shear stress and the axial stresses are less than 5 percent.

Normal stress contour plots for the U-notched bulk adhesive specimens are shown in figures 30 and 31. There are significant concentrations of both transverse and axial stresses along the notch flanks. The overall distributions of both components of normal stress are mostly unaffected by the change in notch radius except that the stress concentrations along the notch flanks steadily decrease as the notch widens. As was the case with the 90° V-notched specimens, the axial stresses are not zero along the centerline as they are in the three bonded geometries, but are fairly uniform with a compressive stress that is about 20 percent of the average shear stress.

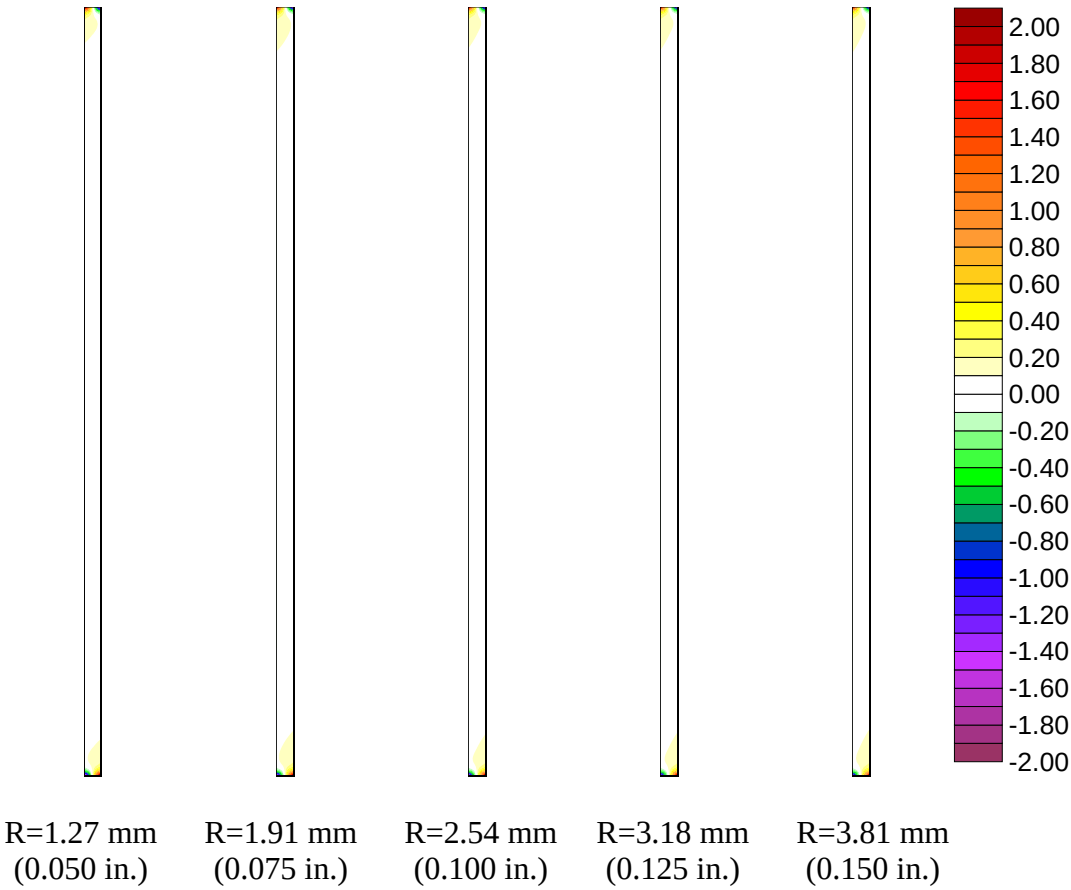

(a)

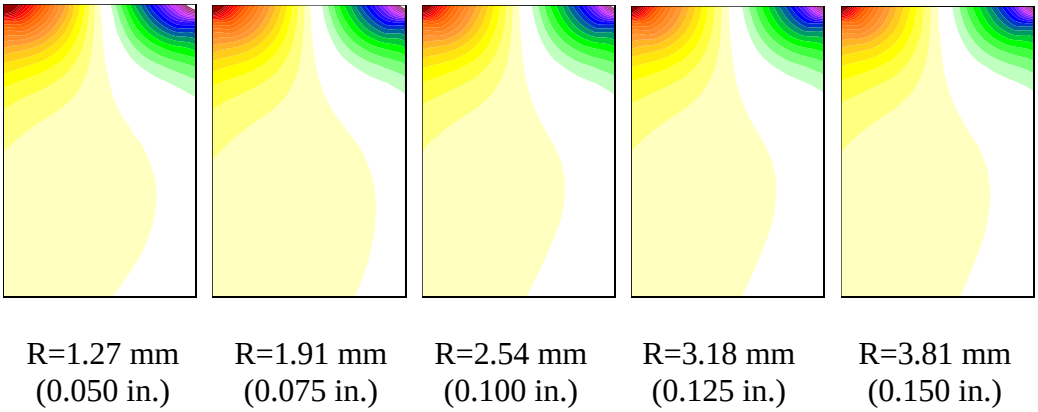

(b)

Figure 24. Transverse Stress Distributions in (a) Full Adhesive Bond and (b) Around Notch Tip for Iosipescu U-Notched Specimens With 0.25-mm (0.01-in.) Bondline (Normalized)

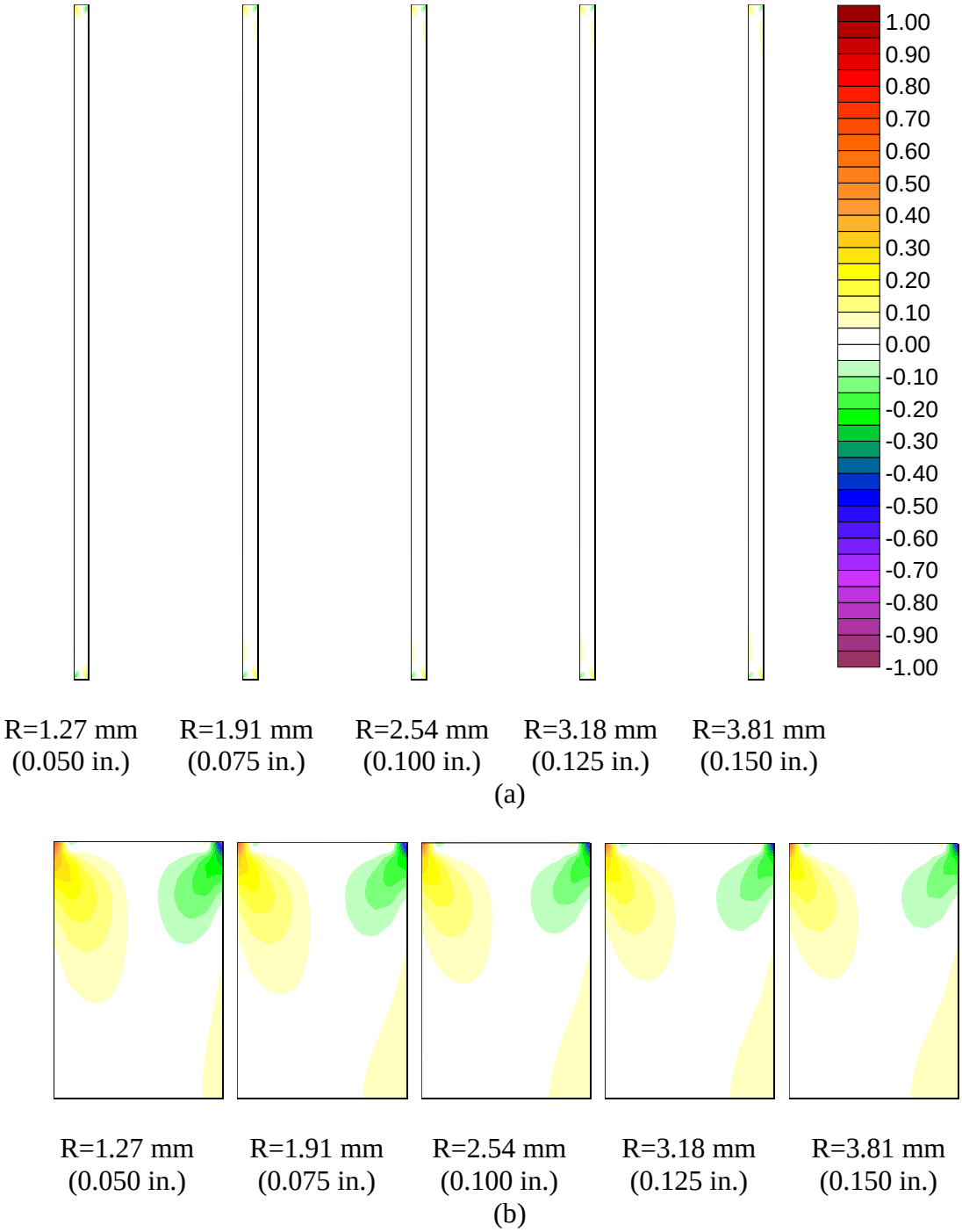

Figure 25. Axial Stress Distributions in (a) Full Adhesive Bondline and (b) Around Notch Tip for Iosipescu U-Notched Specimens With 0.25-mm (0.01-in.) Bondline (Normalized)

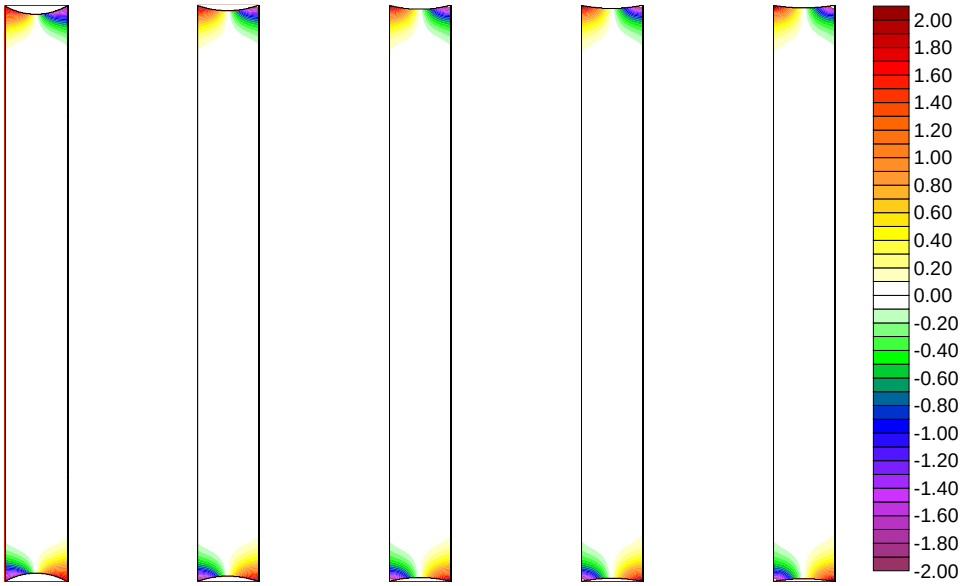

R=1.27 mm (0.050 in.) R=1.91 mm (0.075 in.) R=2.54 mm (0.100 in.) R=3,18 mm (0.125 in.) R=3.81 mm (0.150 in.)

Figure 26. Transverse Stresses for Iosipescu U-Notched Specimens With 1.27-mm (0.05-in.) Bondline (Normalized)

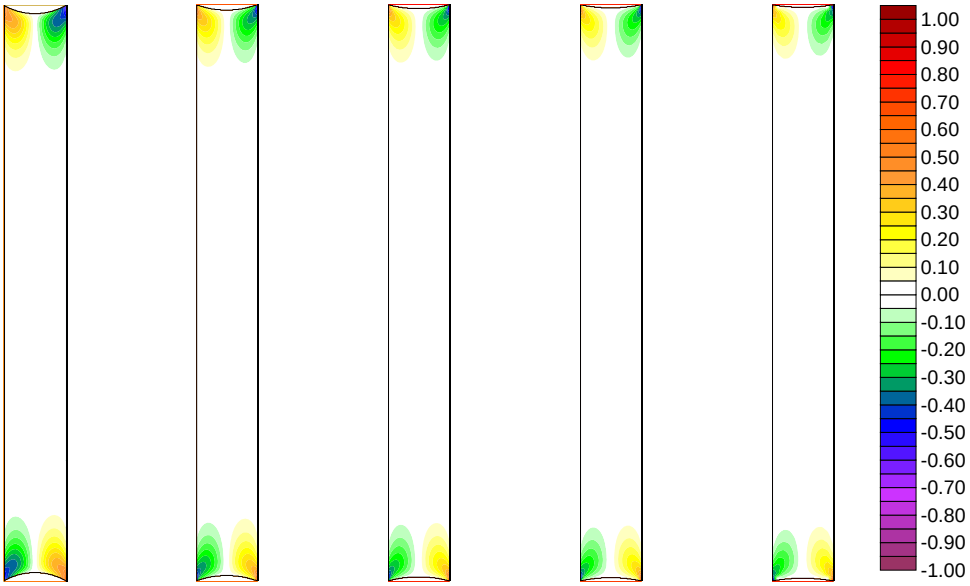

R=1.27 mm (0.050 in.) R=1.91 mm (.075 in.) R=2.54 mm (0.100 in.) R=3.18 mm (0.125 in.) R=3.81 mm (0.150 in.)

Figure 27. Axial Stresses for Iosipescu U-Notched Specimens With 1.27-mm (0.05-in.) Bondline (Normalized)

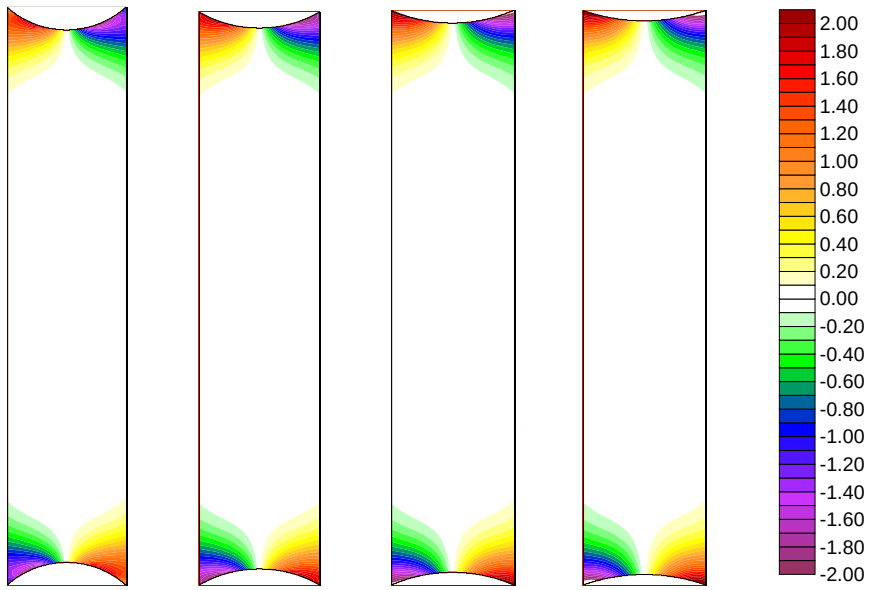

R=1.91 mm (0.075 in.) R=2.54 mm (0.100 in.) R=3.18 mm (0.125 in.) R=3.81 mm (0.150 in.)

Figure 28. Transverse Stresses for Iosipescu U-Notched With 2.54-mm (0.10-in.) Bondline (Normalized)

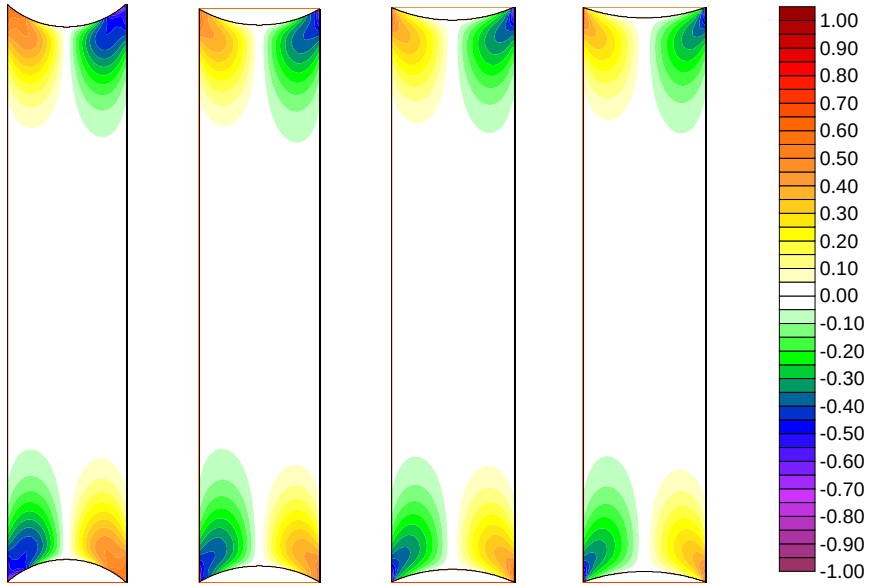

R=1.91 mm (0.075 in.) R=2.54 mm (0.100 in.) R=3.18 mm (0.125 in.) R=3.81 mm (0.150 in.)

Figure 29. Axial Stresses for Iosipescu U-Notched With 2.54-mm (0.10-in.) Bondline (Normalized)

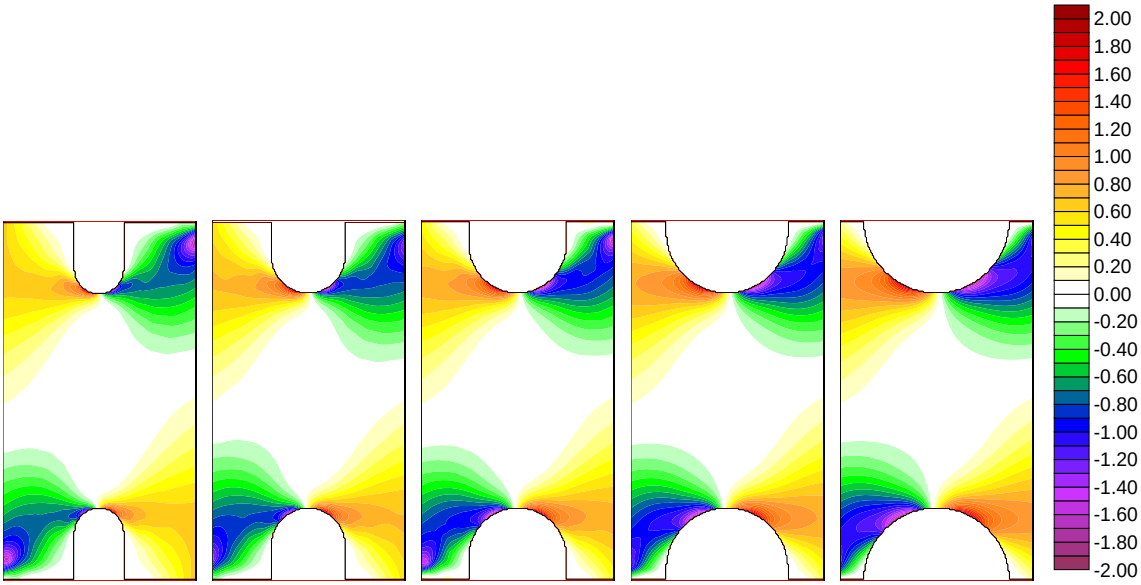

R=1.27 mm (0.050 in.) R=1.91 mm (0.075 in.) R=2.54 mm (0.100) R=3.18 mm (0.125 in.) R=3.81 mm (0.150 in.)

Figure 30. Transverse Stresses for Iosipescu U-Notched Bulk Adhesive (Normalized)

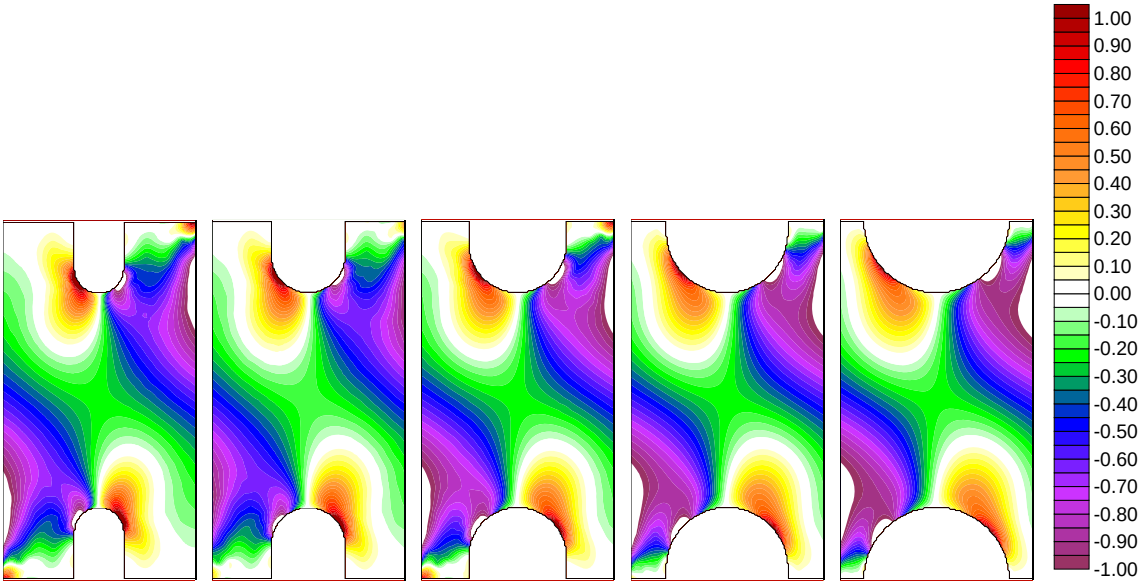

R=1.27 mm (0.050 in.) R=1.91 mm (0.075 in.) R=2.54 mm (0.100 in.) R=3.18 mm (0.125 in.) R=3.81 mm (0.150 in.)

Figure 31. Axial Stresses for Iosipescu U-Notched Bulk Adhesive (Normalized)

3.4.3 Combined Stresses for Iosipescu U-Notched Specimens.

As with the original V-notched Iosipescu specimens, the U-notched Iosipescu specimens have a complex stress state that requires evaluation of the combined stress components. As before, this was accomplished using the von Mises equivalent stress. Combined stresses for the 0.25-mm (0.01-in.) bondline are shown in figure 32, for the 1.27-mm (0.05-in.) bondline in figure 33, and for the 2.54-mm (0.10-in.) bondline in figure 34. Plots of combined stresses in the bulk adhesive specimen are shown in figure 35.

The von Mises stress distribution in the center of the adhesive is almost identical to the shear stress distribution, with the peak stresses between the notches occurring in the center of the adhesive and the distributions becoming more parabolic as the notch radius increases. Thus, the dominant stress component throughout most of the adhesive is the shear stress. However, the combined stress states have large stress concentrations at the interface corners. These concentrations make the stress field nonuniform and show the dependence of the von Mises stress on the normal stresses at these locations.

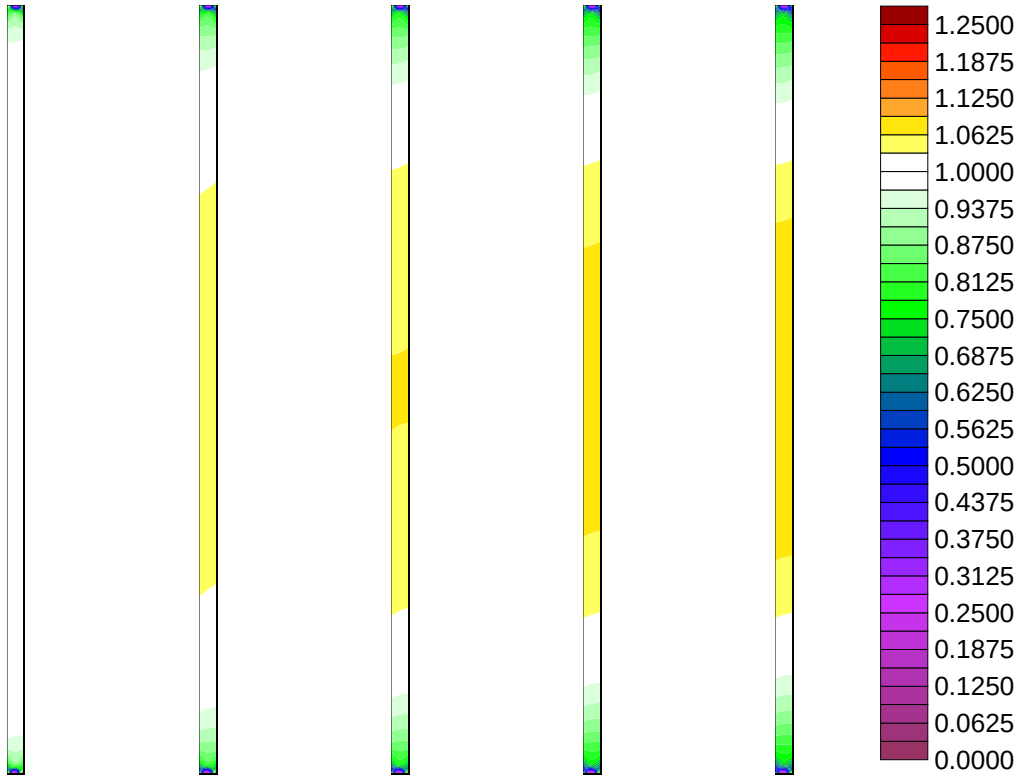

R=1.27 mm (0.050 in.) R=1.91 mm (0.075 in.) R=2.54 mm (0.100 in.) R=3.18 mm (0.125 in.) R=3.81 mm (0.150 in.)

(a)

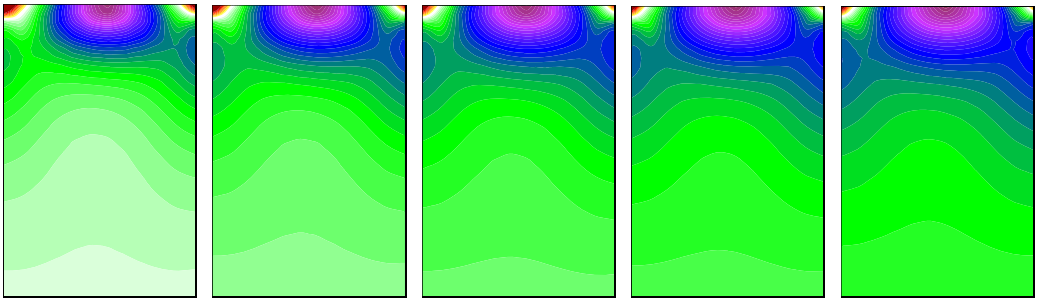

R=1.27 mm (0.050 in.) R=1.91 mm (0.075 in.) R=2.54 mm (0.100 in.) R=3.18 mm (0.125 in.) R=3.81 mm (0.150 in.)

(b)

Figure 32. von Mises Stress Distributions in (a) Full Adhesive Bondline and (b) Around Notch Tip for Iosipescu U-Notched Specimens With 0.25-mm (0.01-in.) Bondline (Normalized)

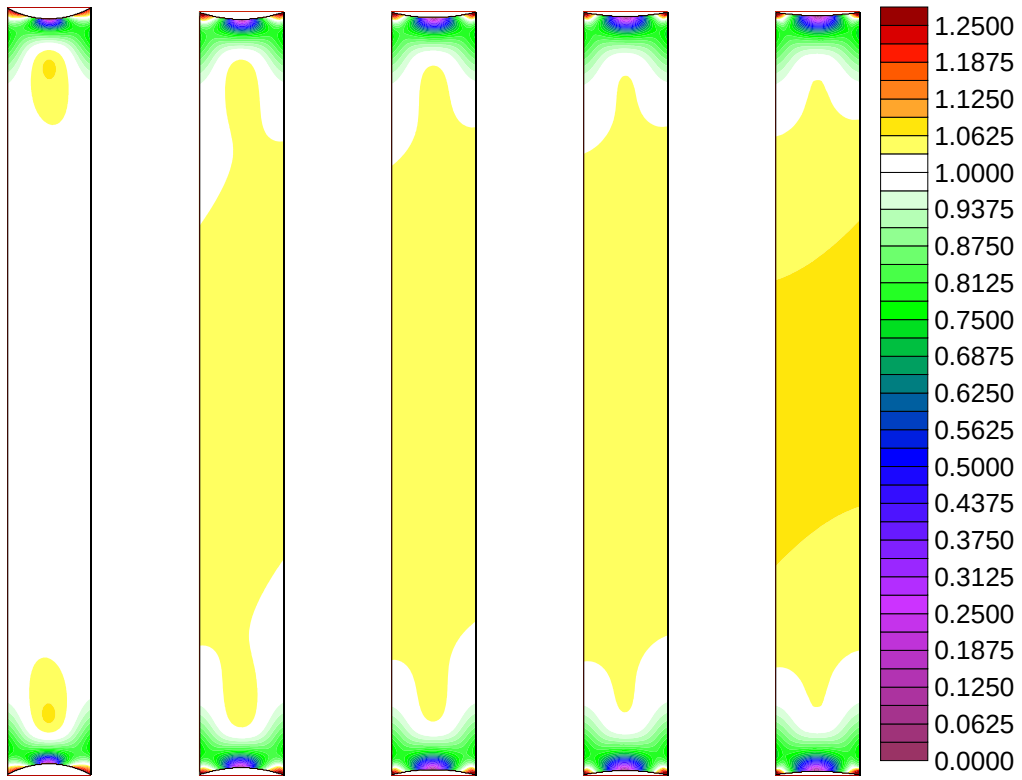

R=1.27 mm (0.050 in.) R=1.91 mm (0.075 in.) R=2.54 mm (0.100 in.) R=3.18 mm (0.125 in.) R=3.81 mm (0.150 in.)

(a)

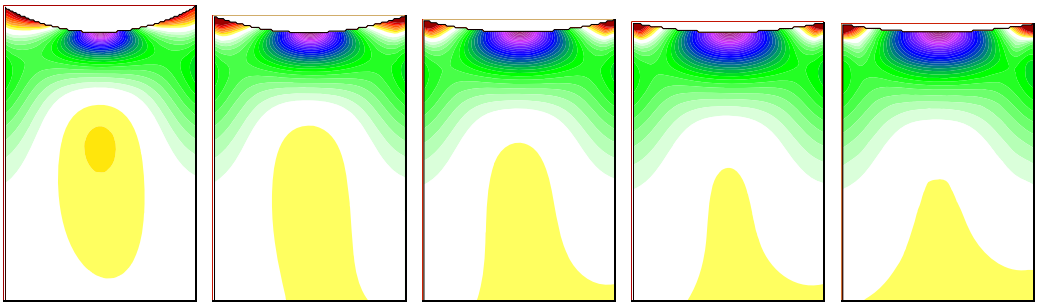

R=1.27 mm (0.050 in.) R=1.91 mm (0.075 in.) R=2.54 mm (0.100 in.) R=3.18 mm (0.125 in.) R=3.81 mm (0.150 in.)

(b)

Figure 33. von Mises Stress Distributions in (a) Full Adhesive Bondline and (b) Around Notch Tip for Iosipescu U-Notched Specimens With 1.27-mm (0.05-in.) Bondline (Normalized)

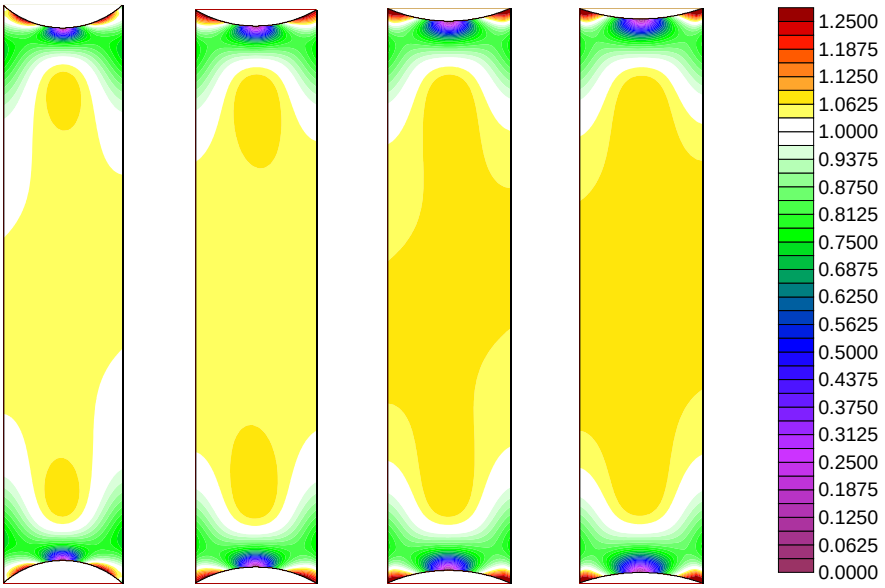

R=1.91 mm (0.075 in.) R=2.54 mm (0.100 in.) R=3.18 mm (0.125 in.) R=3.81 mm (0.150 in.)

Figure 34. von Mises Stresses for Iosipescu U-Notched Specimens With 2.54-mm (0.10-in.) Bondline (Normalized)

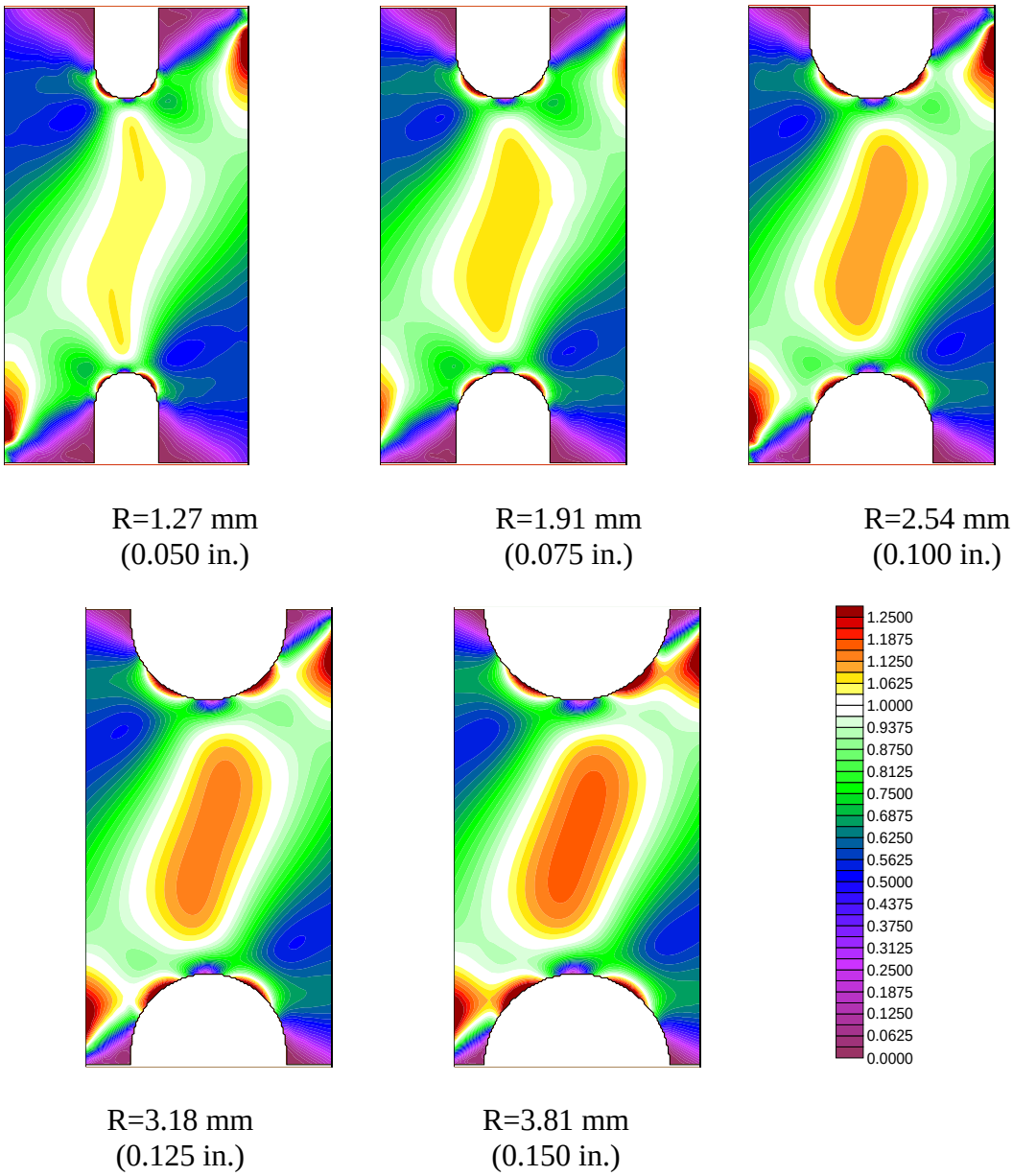

Figure 35. von Mises Stresses for Iosipescu U-Notched Bulk Adhesive Specimens (Normalized)

To evaluate the severity of the interface stress concentrations in the adhesively bonded Iosipescu U-notched specimens and the role of each of the stress components in the concentrations, two additional plots were constructed. The first plot shows the location within the adhesive bond of the maximum value of each of the primary stress components as well as the combined stress maximum value. Although only the top half of the adhesive bondlines are shown, there are asymmetrically located maximum values in the bottom half, since the shear loading is asymmetric. The second plot compares the magnitudes of the maximum stress values (all values are normalized with respect to the average shear stress along the axial centerline).

Plots of maximum stress values for the 0.254-mm (0.01-in.) bondline are shown in figures 36 and 37. The locations of the maximum stress component values appear to be independent of notch radius. However, the magnitudes of the maximum stress component values do depend on notch radius. The maximum shear stress is of lowest magnitude at the smallest notch radius and increases as the radius increases. On the other hand, the two normal stress components as well as the two combined stresses are of highest magnitude at the smallest notch radius and decrease as the radius increases. The largest maximum value of the three in-plane stress components is the transverse stress, which, at the minimum, is about 250 percent of the average shear stress.

For the medium bondline thickness, the maximum stress locations change slightly as the notch radius increases (figure 38). The normal stresses, as well as the combined stress state, have maximums at the interface corners for all notch radii. The maximum shear stress location is very dependent on notch radius, appearing at three different locations starting just below the notch along the centerline with the smallest radius, moving to the interface corners for the midrange radii, and appearing along the interfaces in the center of the specimen for the largest radius. The magnitudes of the stresses do not follow the same trend as in the thinnest bondline. The lowest shear stress peak occurs in the 2.54-mm (0.10-in.) notch radius while the other stress components are minimal in the 1.27-mm (0.05-in.) notch radius. The transverse stress is again the largest in-plane stress component, ranging from 225 percent to almost 350 percent of the average shear depending on notch radius (figure 39).

Plots of maximum stress values for the 2.54-mm (0.10-in.) bondline are shown in figures 40 and 41. The maximum stress locations follow the same trends as in the intermediate bondline thickness. Only the maximum shear stress changes location, moving from between the notches to the interface corner as the notch radius increases. The stress magnitudes are the lowest with the two smallest notch radii and then increase as the radius increases.

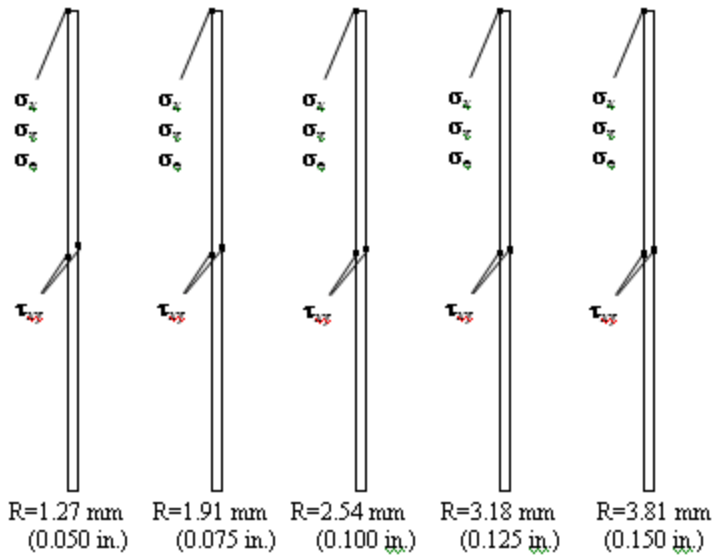

Figure 36. Locations of Maximum Values of Stress Components in Variable Notch Radius Iosipescu U-Notched Specimens With 0.25-mm (0.01-in.) Bondline

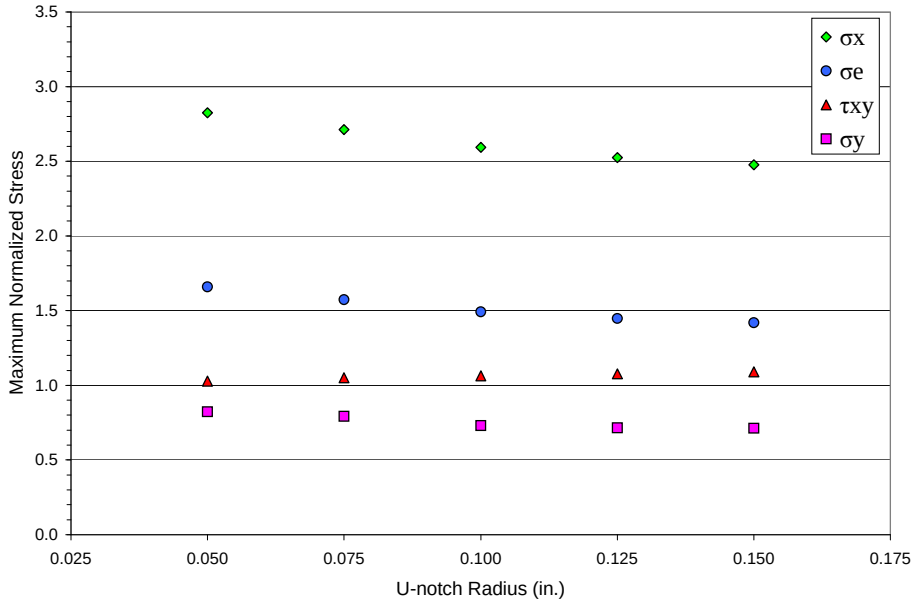

Figure 37. Maximum Values of Stress Components for Variable Notch Radius Iosipescu U-Notched Specimens with 0.25-mm (0.01-in.) Bondline (Normalized)

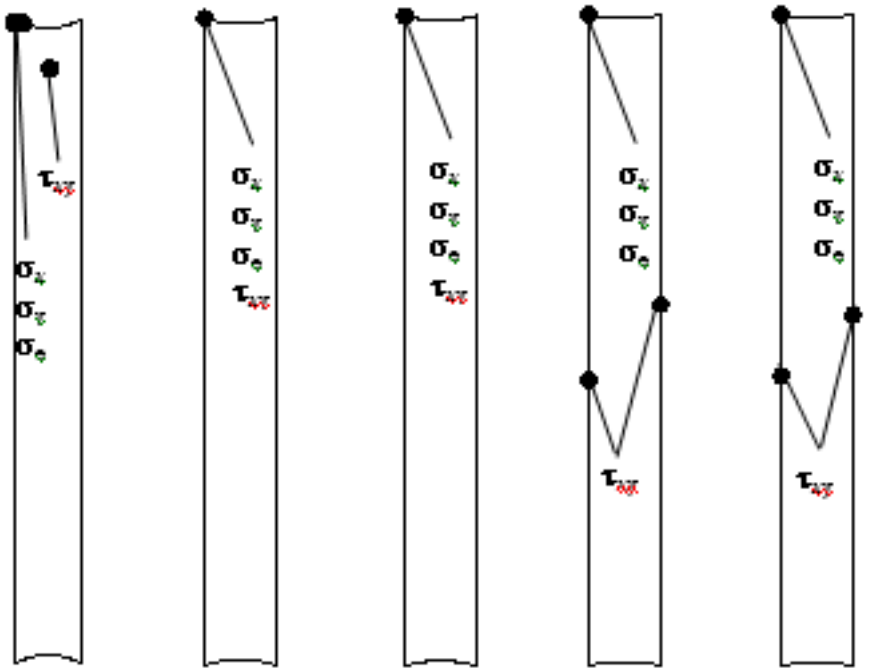

R=1.27 mm (0.050 in.) | R=1.91 mm (0.075 in.) | R=2.54 mm (0.100 in.) | R=3.18 mm (0.125 in.) | R=3.81 mm (0.150 in.)

Figure 38. Locations of Maximum Values of Stress Components in Variable Notch Radius Iosipescu U-Notched Specimens With 1.27-mm (0.05-in.) Bondline

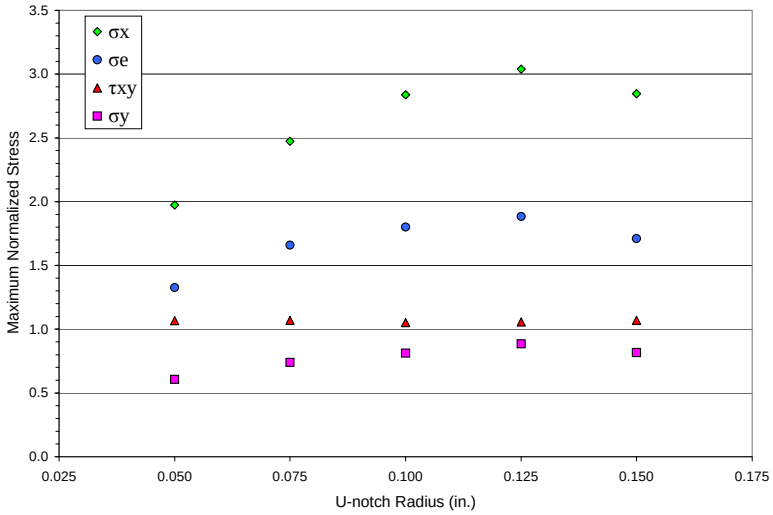

Figure 39. Maximum Values of Stress Components for Variable Notch Width Iosipescu U-Notched Specimens With 1.27-mm (0.05-in.) Bondline (Normalized)

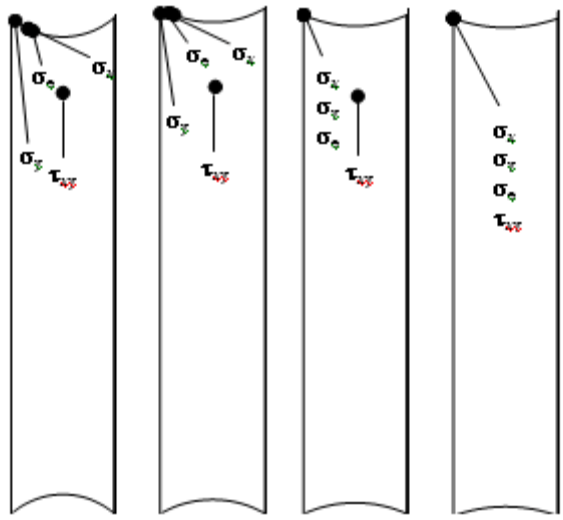

R=1.91 mm (0.075 in.) R=2.54 mm (0.100 in.) R=3.18 mm (0.125 in.) R=3.81 mm (0.150 in.)

Figure 40. Locations of Maximum Values of Stress Components in Variable Notch Radius Iosipescu U-Notched Specimens With 2.54-mm (0.10-in.) Bondline

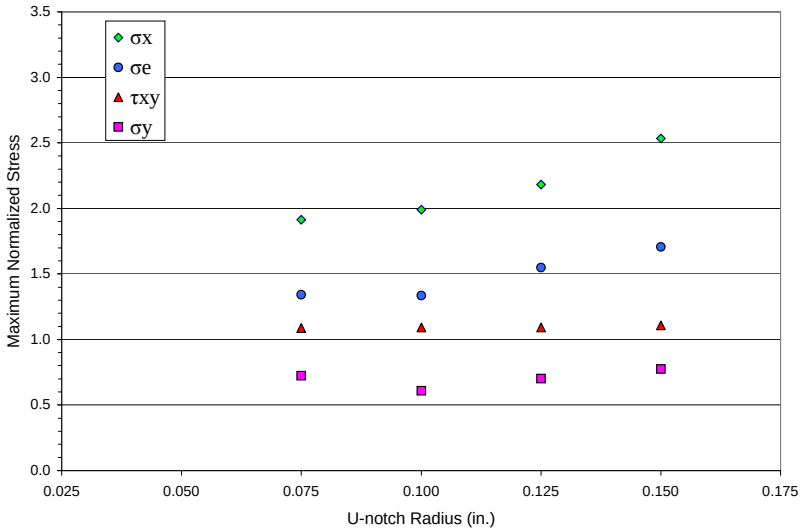

Figure 41. Maximum Normalized Values of Stress Components for Variable Notch Width Iosipescu U-Notched Specimens With 2.54-mm (0.10-in.) Bondline

For the Iosipescu U-notched bulk adhesive specimens, the plot showing the location of maximum stress component values was not created since the region of interest was not as well defined as with the bonded specimens, and the locations of the maximum stress component values were usually located away from the notches. The plot for the maximum magnitudes of each stress component for the Iosipescu U-notched bulk adhesive specimens is shown in

figure 42. The minimum peak normal stress magnitudes are found in the specimen with the 3.18-mm (0.125-in.) notch radius while the minimum peak shear stress magnitude is in the 1.90-mm (0.075-in.) notch radius specimen. Also, the peak magnitudes of both normal stresses in the bulk adhesive specimens are much lower than in all three bonded specimens.

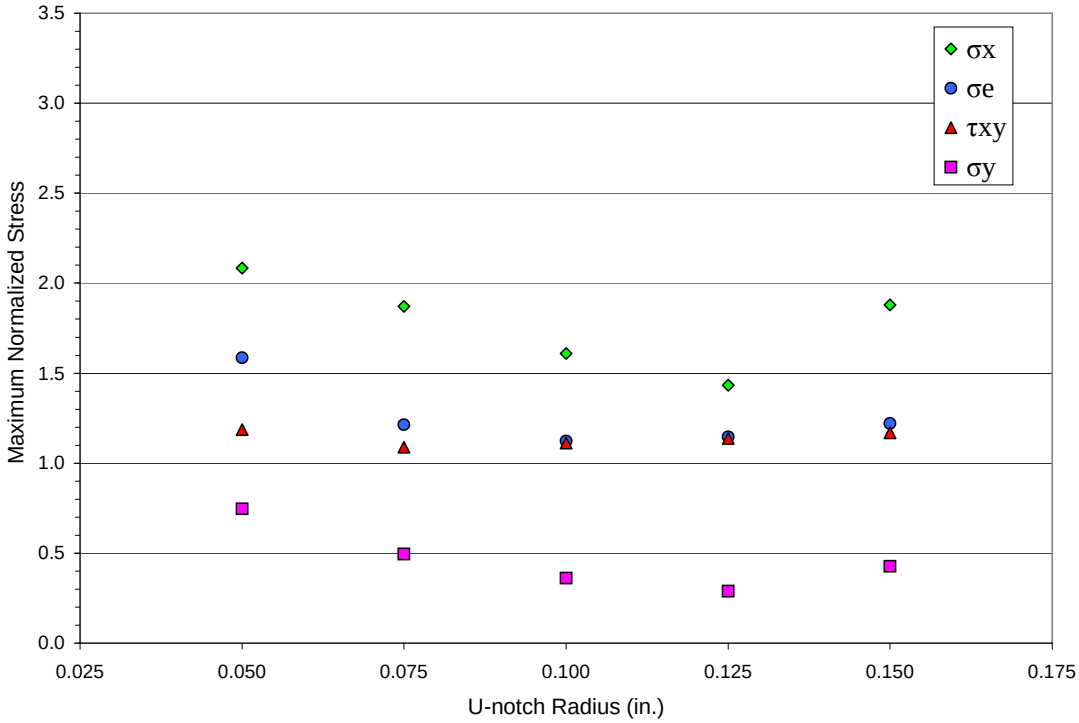

Figure 42. Maximum Normalized Values of Stress Components for Variable Notch Width Iosipescu U-Notched Bulk Adhesive Specimens

3.4.4 Conclusions for Iosipescu U-Notched Specimens.

Replacing the sharp V-notch with the rounded U-notch yielded several changes in the stress state of the adhesive. The most attractive features of the U-notch are that the stress concentrations at the notch tips are significantly reduced and the stress concentrations along the notch flanks are moved out of the adhesive and into the aluminum adherends. The drawbacks to the U-notched specimens are that in all but the smallest notch radius, the notch curvature is so gradual that the adhesive area becomes almost rectangular and the shear stress distribution becomes parabolic instead of the desired uniform distribution. The other drawback to the U-notch is the very large normal stress concentrations at the adhesive adherend interface. These large stresses could initiate failure along the interface and create an adhesive failure rather than the preferred cohesive failure. While the changes in stress distributions due to changes in notch radius follow similar trends for the different bondline thicknesses, there is no one U-notch geometry that is optimal for all bondline thicknesses.

3.5 IOSIPESCU V-NOTCHED SPECIMENS WITH VARIABLE NOTCH ANGLE.

The results of the Iosipescu U-notched specimen analysis showed that varying the notch radius could change the stress state in the adhesive. Therefore, the V-notched specimen was revisited to determine if changing the notch angle would produce a more optimal stress state than in the 90° V-notched specimen. The U-notched geometry significantly reduced the stress concentrations at the notch tip by expanding the notch tip. Therefore, the notch angles investigated were all larger than the original 90° notch angle.

The first notch angle variations studied were 103° and 120°. Based on the success of the 120° notch angle, notch angles of 115° and 125° were added to the investigation. Results are presented for all four notch angle variations as well as for the 90° notch for comparison purposes. Results are presented for all three bondline thicknesses as well as the bulk adhesive specimen. As with the previous sections, only the adhesive bondline results are shown.

3.5.1 Shear Stresses for Variable Notch Angle Iosipescu V-Notch.

The shear stress distributions for the Iosipescu V-notched specimens are shown in figure 43 for the 0.25-mm (0.01-in.) bondline, figure 44 for the 1.27-mm (0.05-in.) bondline, and figure 45 for the 2.54-mm (0.10-in.) bondline. As was expected from comparison with the results of the U-notched specimen, the notch tip shear stress concentration is reduced significantly as the notch angle becomes more obtuse. The shear stress concentrations along the notch flanks also disappear as the notch angle increases. Widening the notch angle also creates a more parabolic shear stress distribution in the adhesive, with the maximum stress along the axial centerline occurring in the specimen center for the larger notch angles.

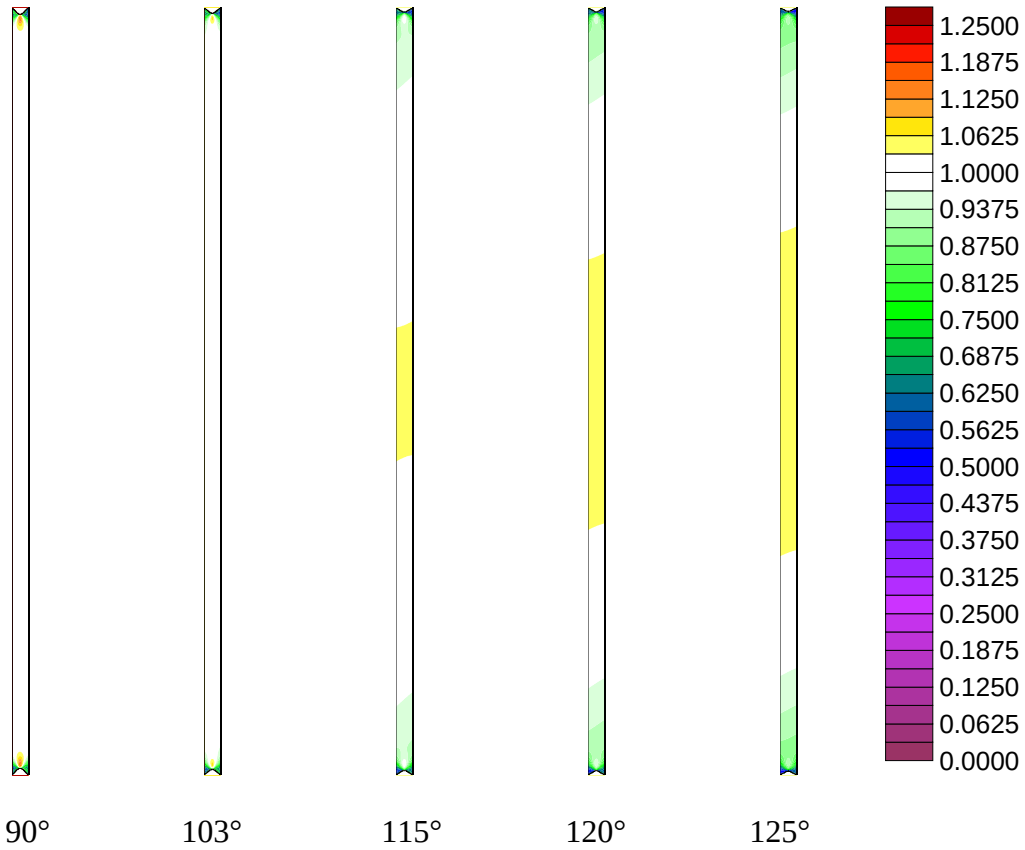

(a)

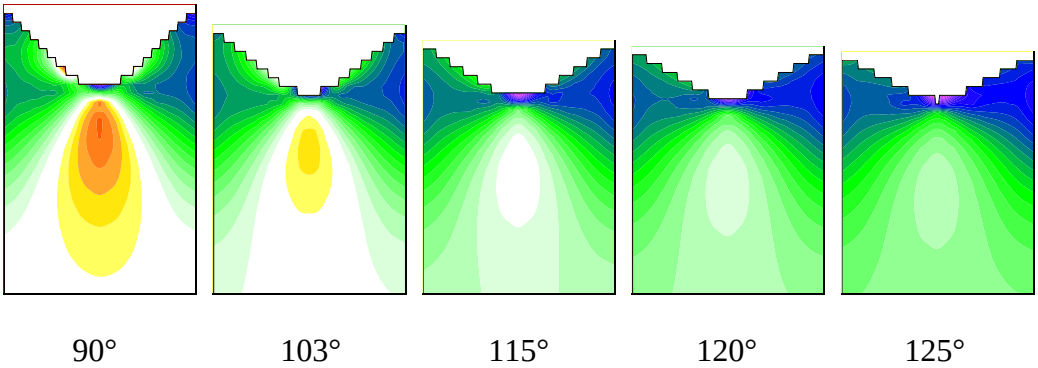

(b)

Figure 43. Shear Stress Distributions in (a) Full Adhesive Bondline and (b) Around Notch Tip for variable Angle Iosipescu V-Notched Specimens With 0.25-mm (0.01-in.) Bondline (Normalized)

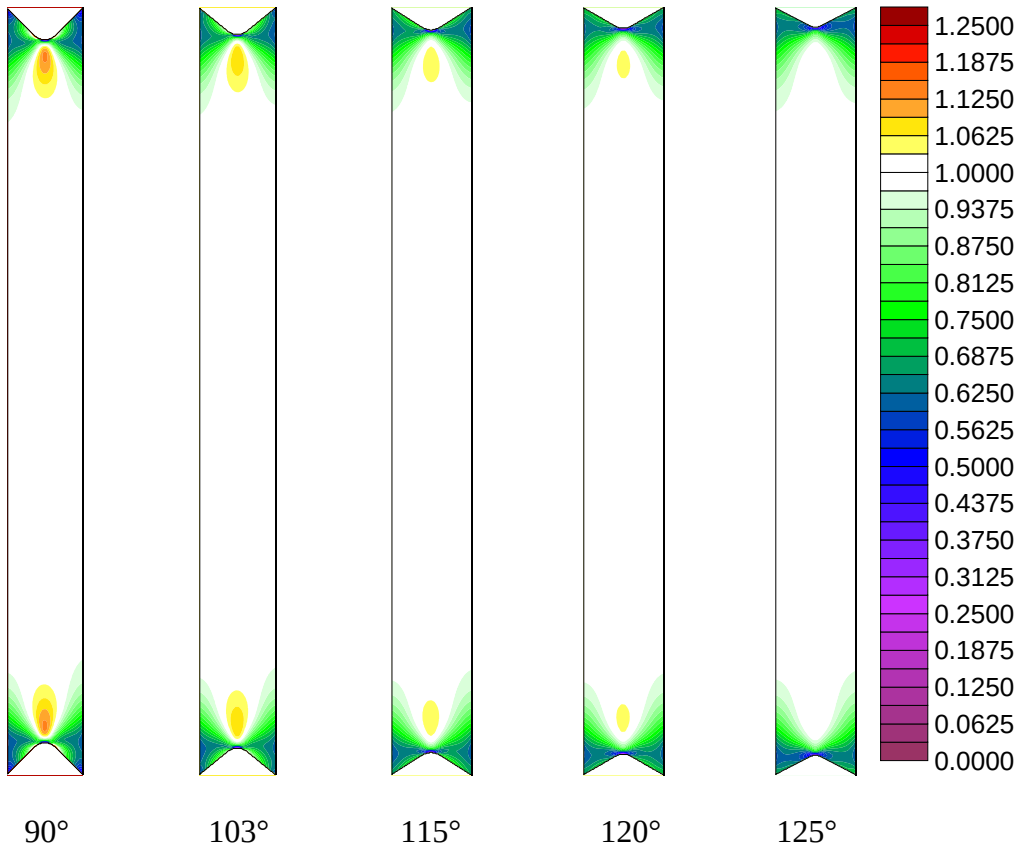

(a)

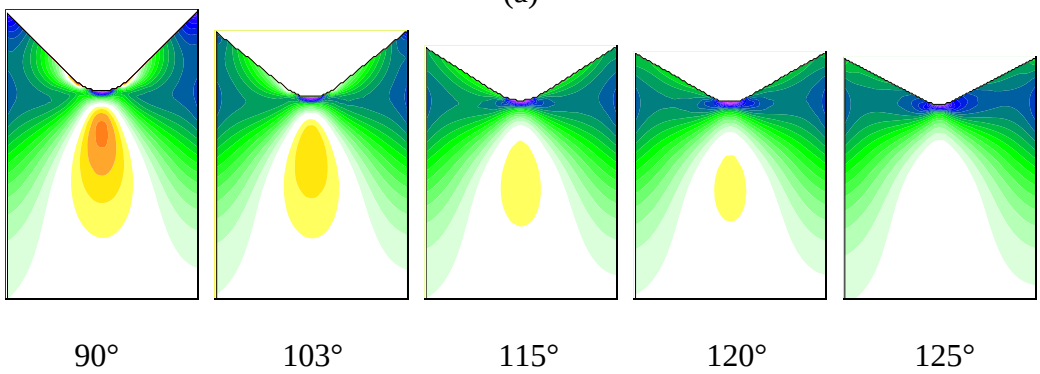

(b)

Figure 44. Shear Stress Distributions in (a) Full Adhesive Bondline and (b) Around Notch Tip for Variable Angle Iosipescu V-Notched Specimens With 1.27-mm (0.05-in.) Bondline (Normalized)

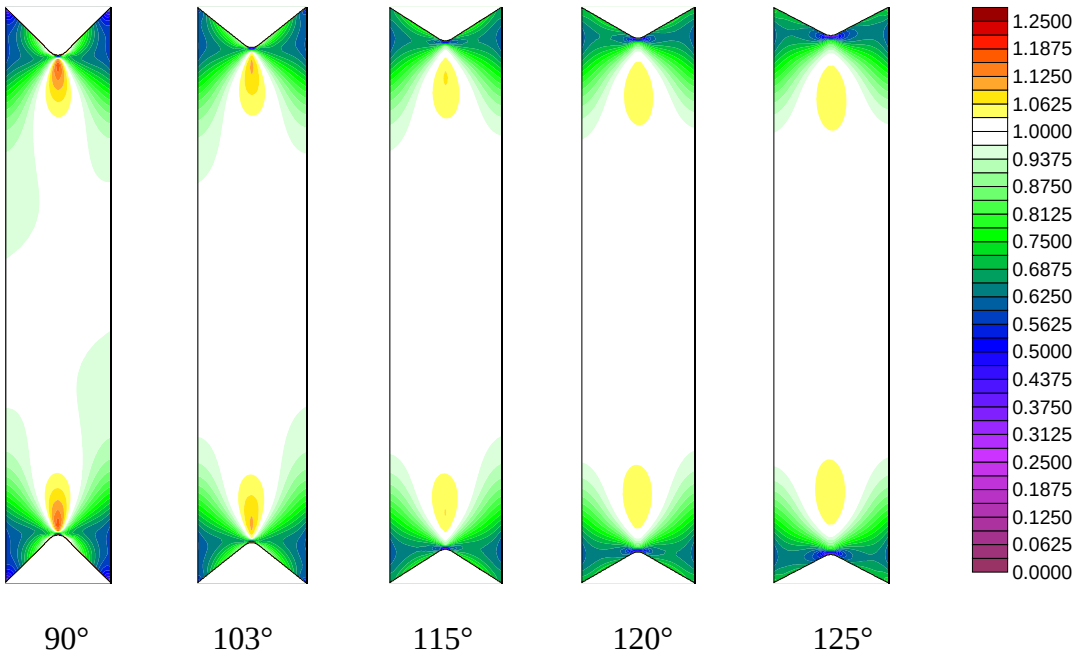

Figure 45. Shear Stress Distributions for Variable Angle Iosipescu V-Notched Specimens With 2.54-mm (0.10-in.) Bondline (Normalized)

The shear stress results for the bulk adhesive are shown in figure 46. The width of each plot is different in order to show the shear stress contours throughout the entire notched section of the specimen. This was done because the region of interest in the bulk adhesive specimens is not as clear as in the bonded specimens where the region of interest is clearly marked by the adherends. The shear stress distribution in the bulk adhesive specimens behaves similarly to the bonded specimens except that the distribution becomes parabolic at smaller notch angles.

The advantage to increasing the notch angle of the V-notched specimens is that at wider angles, the notch tip stress concentrations vanish. However, the tradeoff is that the wider notch angles have a nonuniform parabolic shear stress distribution in the specimen center. To better quantify the change in shear stress as the notch angle changed, plots were constructed showing the normalized shear stress along the axial centerline for each bondline thickness and the bulk adhesive (figures 47 through 50). For all three bonded specimens, the notch tip stress concentrations are not completely eliminated (up to a 125° angle), although for the thinnest bondline the magnitude of the notch tip stress concentration is less than the average shear stress for angles of 115° and greater. For the other two bondline thicknesses, the magnitude of the stress concentration is reduced as the notch angle increases, and eventually the central peak of the parabolic distribution becomes the largest value of shear stress. The most optimal shear stress state, based on reducing the notch tip shear stress concentration while maintaining a uniform distribution in the central region, is found in the 115° notch angle for the 0.25-mm (0.01-in.) bondline, the 125° notch angle for the 1.27-mm (0.05-in.) bondline, and the 120° notch angle for the 2.54-mm (0.10-in.) bondline. For the bulk adhesive, the most optimal state of shear stress occurs with the 90° notch angle. Even though the 90° notch angle has the notch tip shear

stress concentrations, it has the lowest overall shear stress magnitudes as the wider notch angles have significant parabolic distributions.

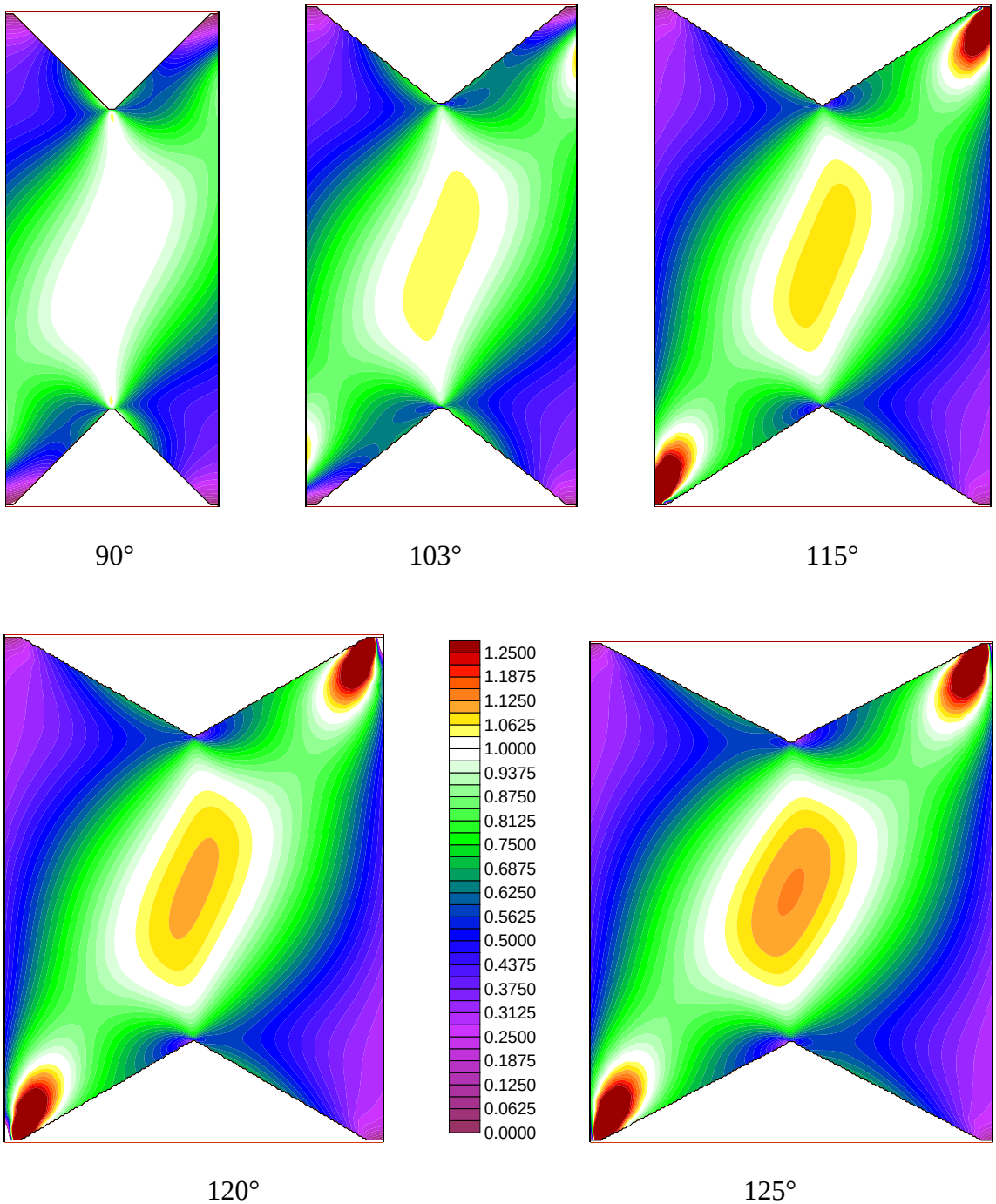

Figure 46. Shear Stress Distributions for Bulk Adhesive Variable Angle Iosipescu V-Notched Specimens (Normalized)

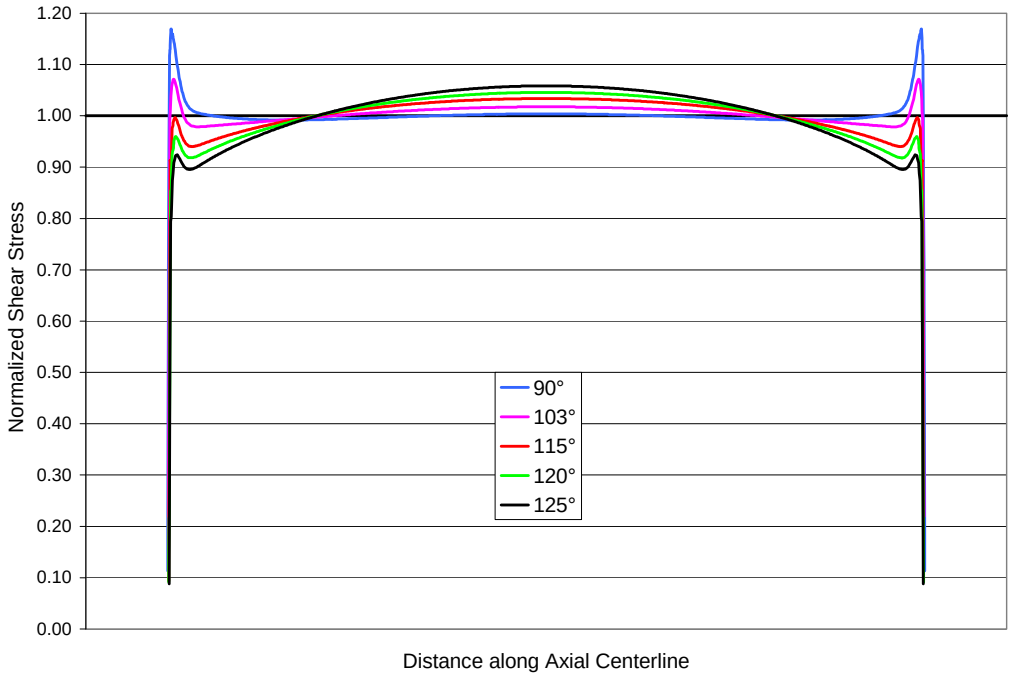

Figure 47. Shear Stress Distribution Along Axial Centerline as a Function of Notch Angle for Iosipescu V-Notched Specimens With 0.254-mm (0.01-in.) Bondline

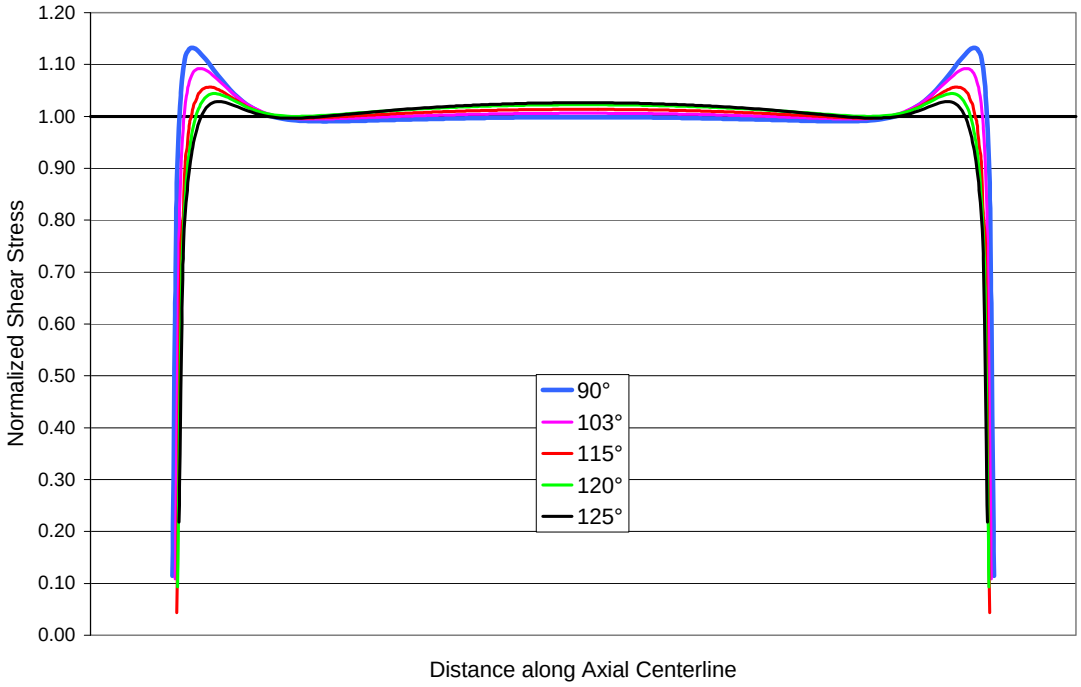

Figure 48. Shear Stress Distribution Along Axial Centerline as a Function of Notch Angle for Iosipescu V-Notched Specimens With 1.27-mm (0.05-in.) Bondline

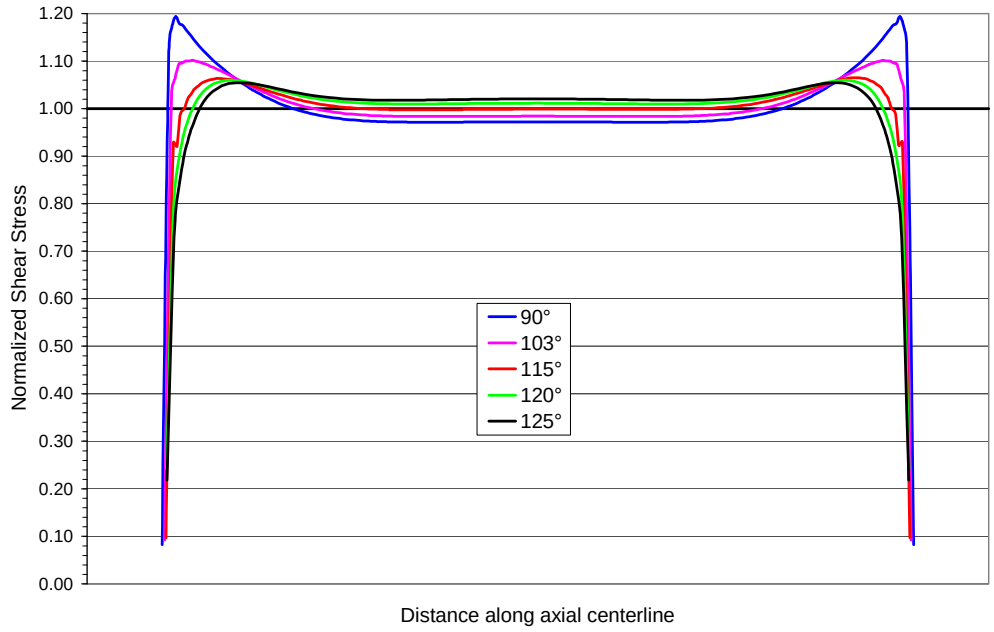

Figure 49. Shear Stress Distribution Along Axial Centerline as a Function of Notch Angle for Iosipescu V-Notched Specimens With 2.54-mm (0.10-in.) Bondline

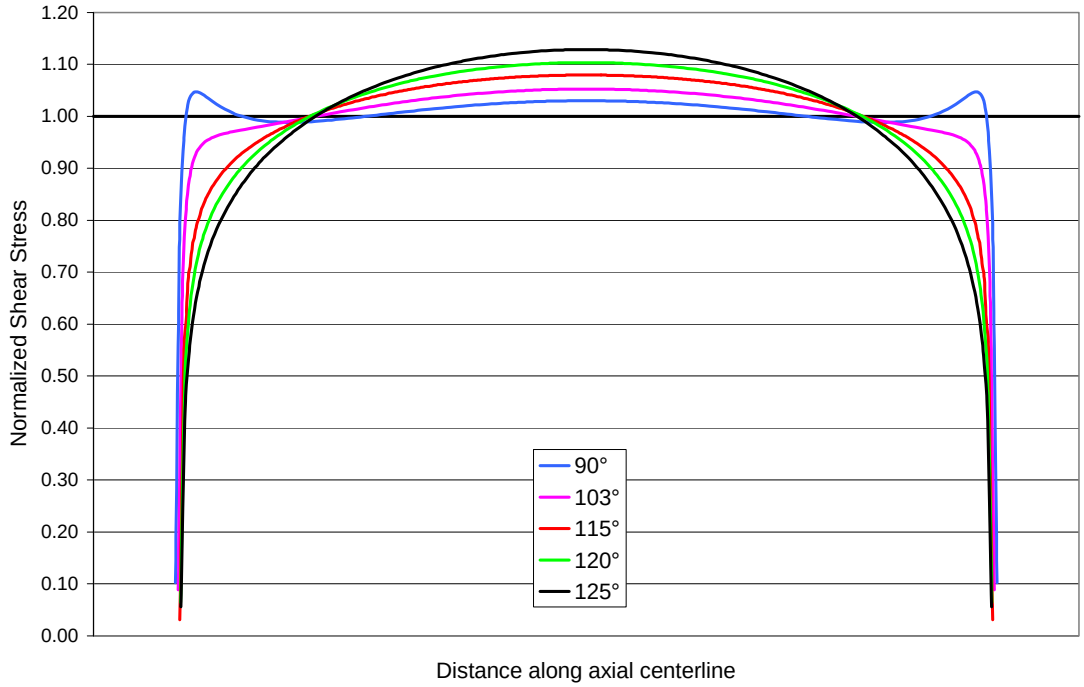

Figure 50. Shear Stress Distribution Along Axial Centerline as a Function of Notch Angle for Bulk Adhesive Iosipescu V-Notched Specimens

3.5.2 Normal Stresses for the Iosipescu V-Notched Specimens.

The transverse and axial normal stress distributions are shown in figures 51 and 52 for the 0.25-mm (0.01-in.) bondline, figures 53 and 54 for the 1.27-mm (0.05-in.) bondline, and figures 55 and 56 for the 2.54-mm (0.10-in.) bondline. The majority of the adhesive section is free of significant normal stresses. As was observed previously in the 90° notch angle specimen, there are large concentrations of both tensile and compressive transverse and axial stresses along the notch flanks. However, the stress concentrations decrease as the notch angle increases. All three bondline thicknesses as well as the bulk adhesive specimens (figures 57 and 58) have very similar distributions of transverse and axial normal stresses.

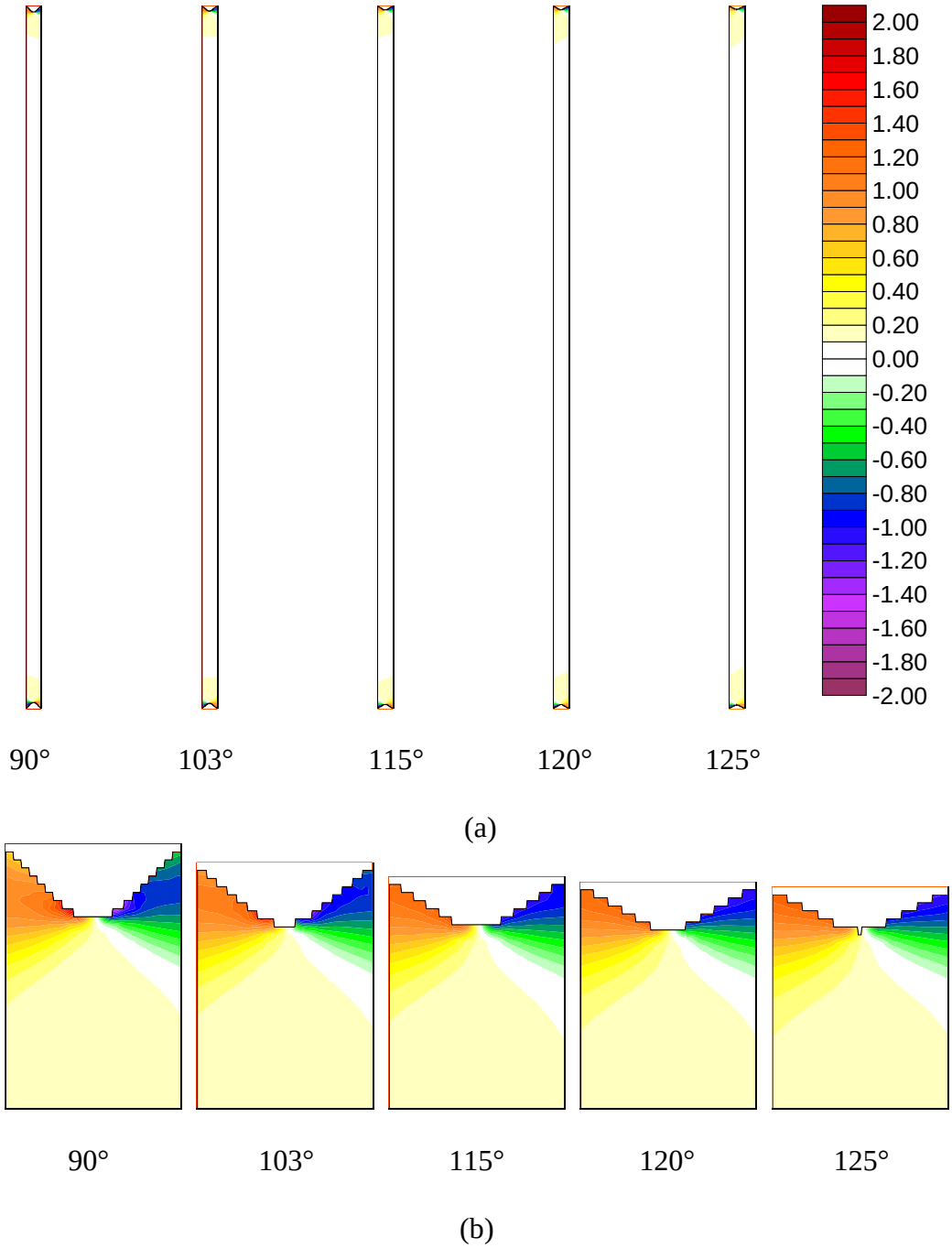

Figure 51. Transverse Stress Distributions in (a) Full Adhesive Bondline and (b) Around Notch Tip for Variable Angle Iosipescu V-Notched Specimens With 0.25-mm (0.01-in.) Bondline (Normalized)

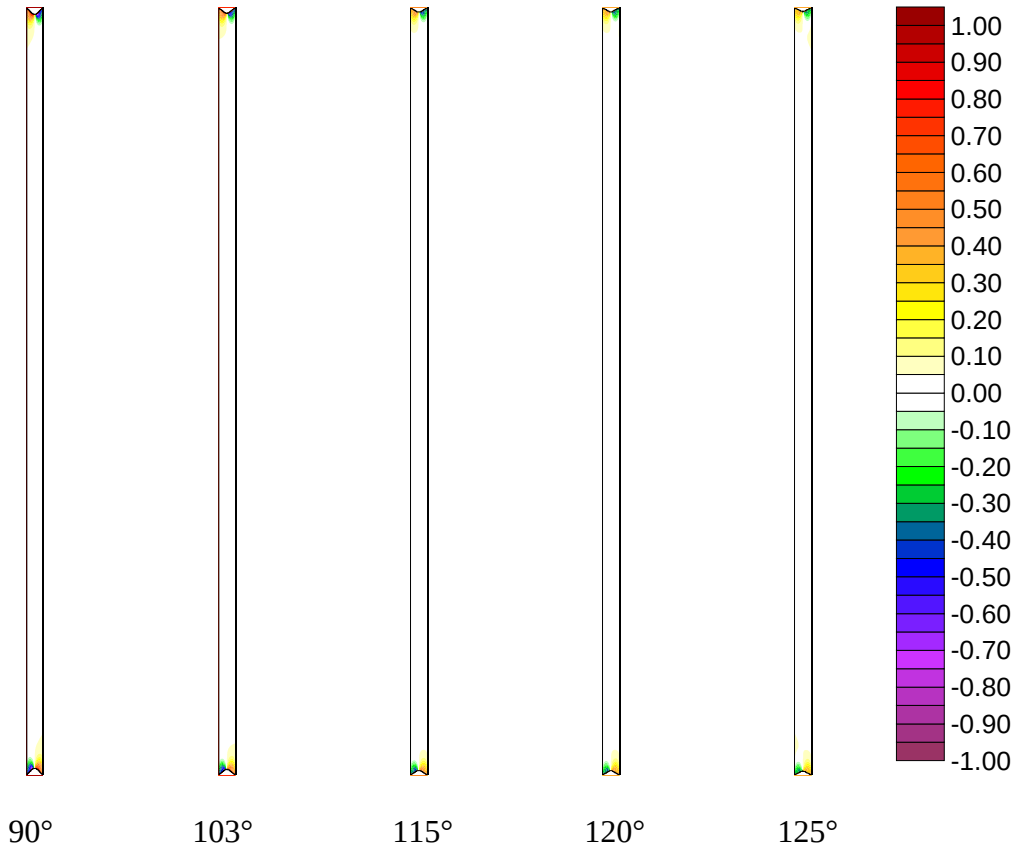

(a)

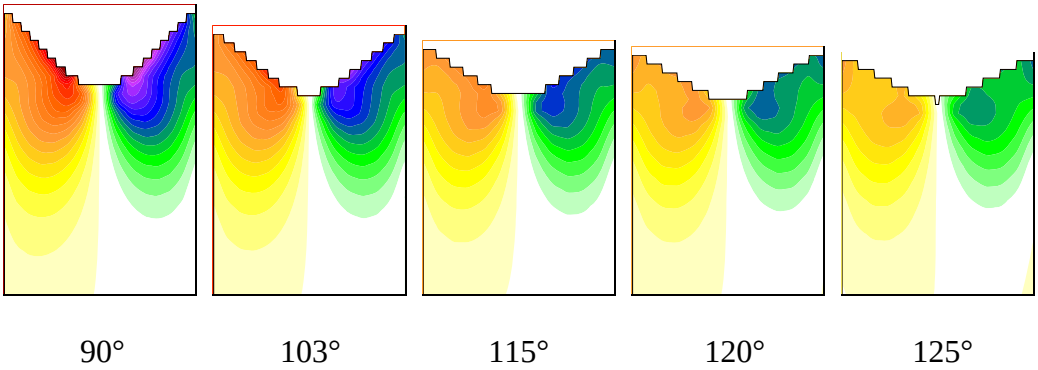

(b)

Figure 52. Axial Stress Distributions in (a) Full Adhesive Bondline and (b) Around Notch Tip for Variable Angle Iosipescu V-Notched Specimens With 0.25-mm (0.01-in) Bondline (Normalized)

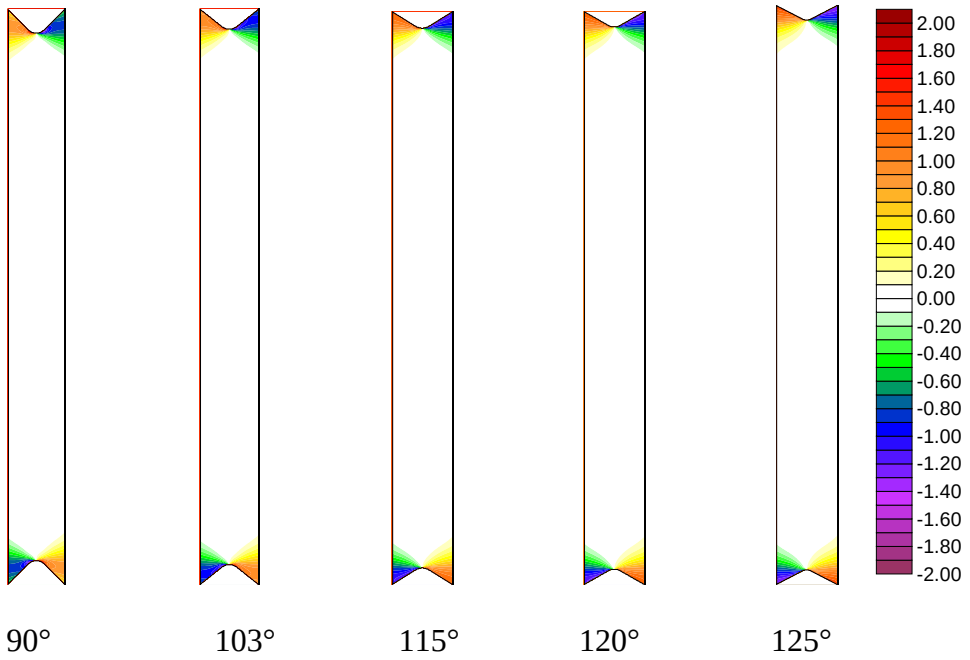

Figure 53. Transverse Stress Distributions for Variable Angle Iosipescu V-Notched Specimens With 1.27-mm (0.05-in.) Bondline (Normalized)

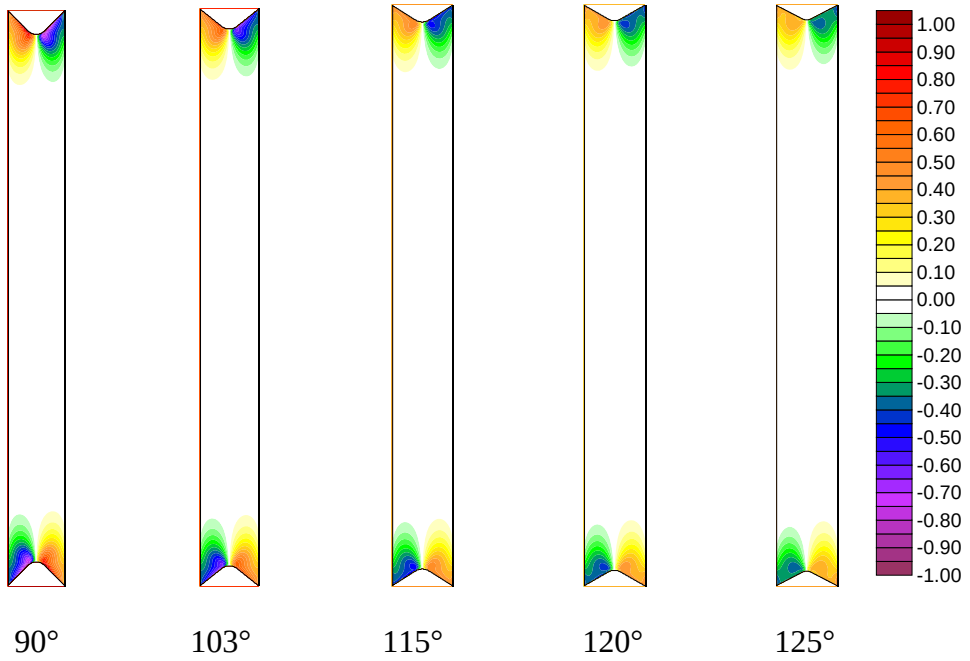

Figure 54. Axial Stress Distributions for Variable Angle Iosipescu V-Notched Specimens With 1.27-mm (0.05-in.) Bondline (Normalized)

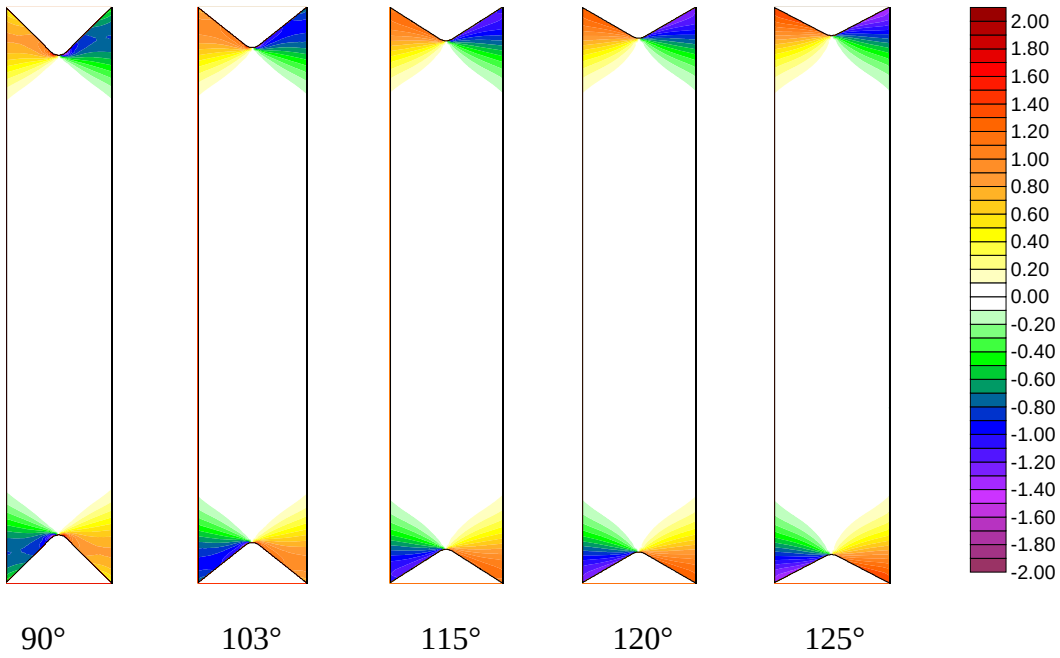

Figure 55. Transverse Stress Distributions for Variable Angle Iosipescu V-Notched Specimens With 2.54-mm (0.10-in.) Bondline (Normalized)

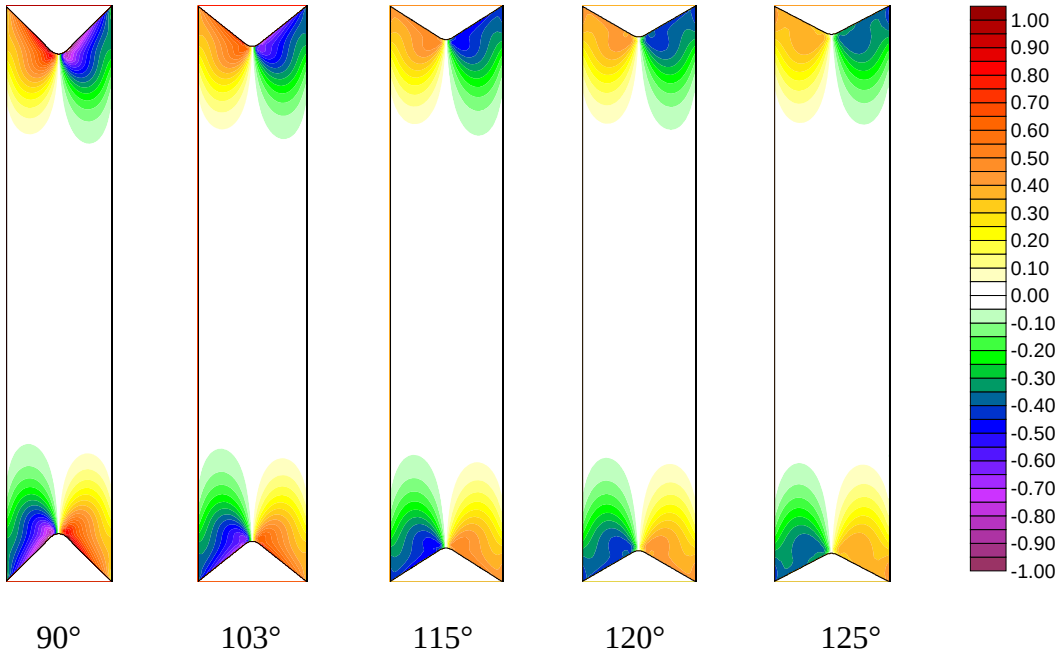

Figure 56. Axial Stress Distributions for Variable Angle Iosipescu V-Notched Specimens With 2.54-mm (0.10-in.) Bondline (Normalized)

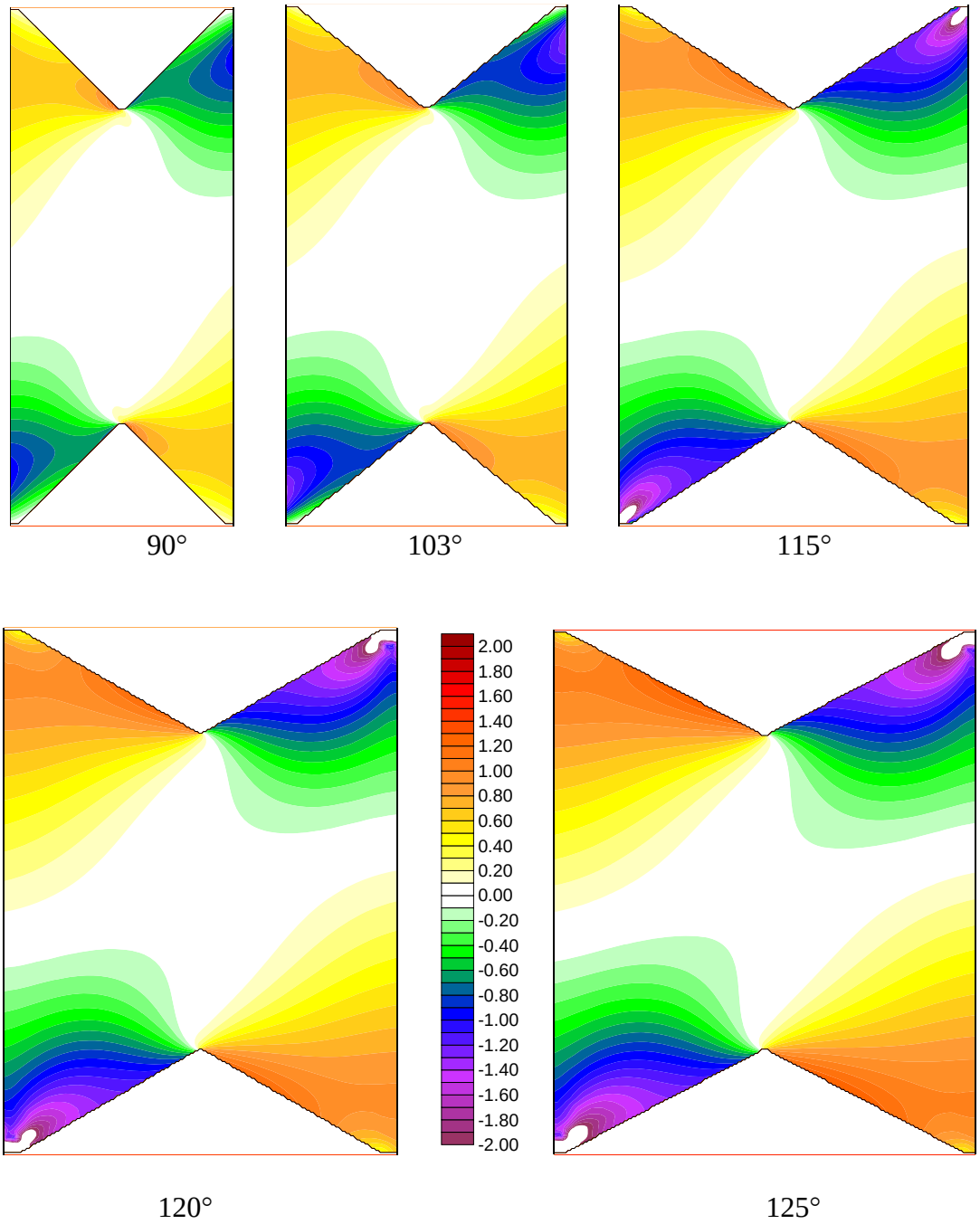

Figure 57. Transverse Stress Distributions for Bulk Adhesive Variable Angle Iosipescu V-Notched Specimens (Normalized)

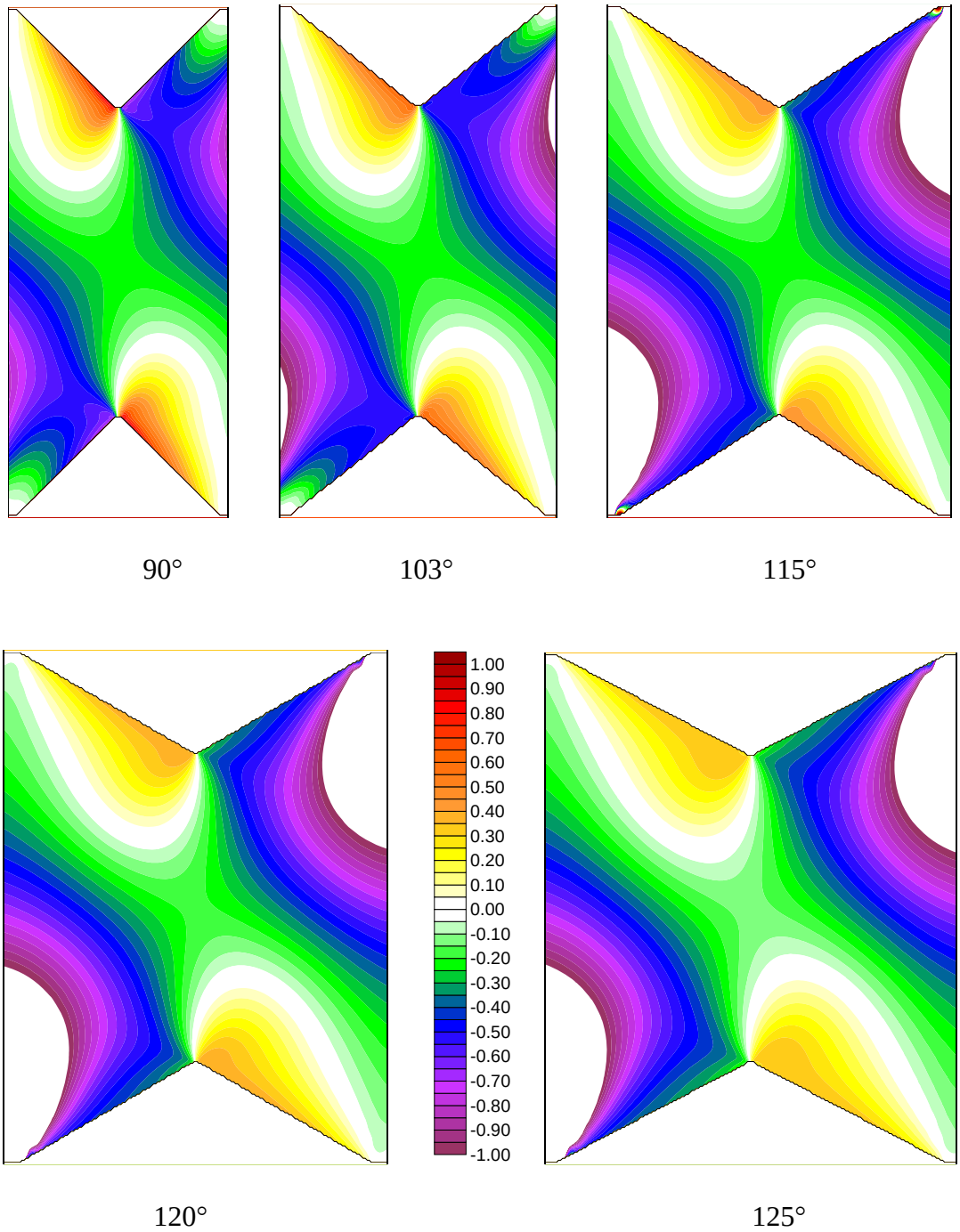

Figure 58. Axial Stress Distributions for Bulk Adhesive Variable Angle Iosipescu V-Notched Specimens (Normalized)

3.5.3 von Mises Stresses for Iosipescu V-Notched Specimens.

The combined stress states of the Iosipescu V-notched specimens are shown in figure 59 for the 0.25-mm (0.01-in.) bondline, figure 60 for the 1.27-mm (0.05-in.) bondline, and in figure 61 for the 2.54-mm (0.10-in.) bondline. The combined stresses for the bulk adhesive are shown in figure 62. For the von Mises stresses, the largest values occur around the notch, both at the notch tip and along the notch flanks, for the 90° notch. For the thin bondline, as the notch angle increases, the largest value of von Mises stress moves to the center of the specimen. For the intermediate and thick bondlines, as the notch angle increases, the maximum von Mises stresses occur near the notch tips; however, there are also large von Mises stresses near the adhesive-adherend interface corners.

As with the U-notch analysis, plots were constructed showing the locations and values of the maximum values of the stress components in the adhesive. These plots are shown in figures 63 and 64 for the 0.25-mm (0.01-in.) bondline, figures 65 and 66 for the 1.27-mm (0.05-in.) bondline, and figures 67 and 68 for the 2.54-mm (0.10-in.) bondline. Inspection of these plots reveals that for all three bondline thicknesses, the magnitudes of the maximum stress values decrease as the notch angle widens, as was previously determined from the contour plots. These plots also show that the maximum values of the stress components reach a minimum at a notch angle of about 120° and then increase as the notch angle continues to increase. Additionally, at a notch angle of 120°, the maximum value of the shear stress and the von Mises stress coincide both in location and in value for all three bondline thicknesses. This is a very important observation, as it identifies a notch geometry in which the primary contribution to the equivalent stress state comes from the shear stress.

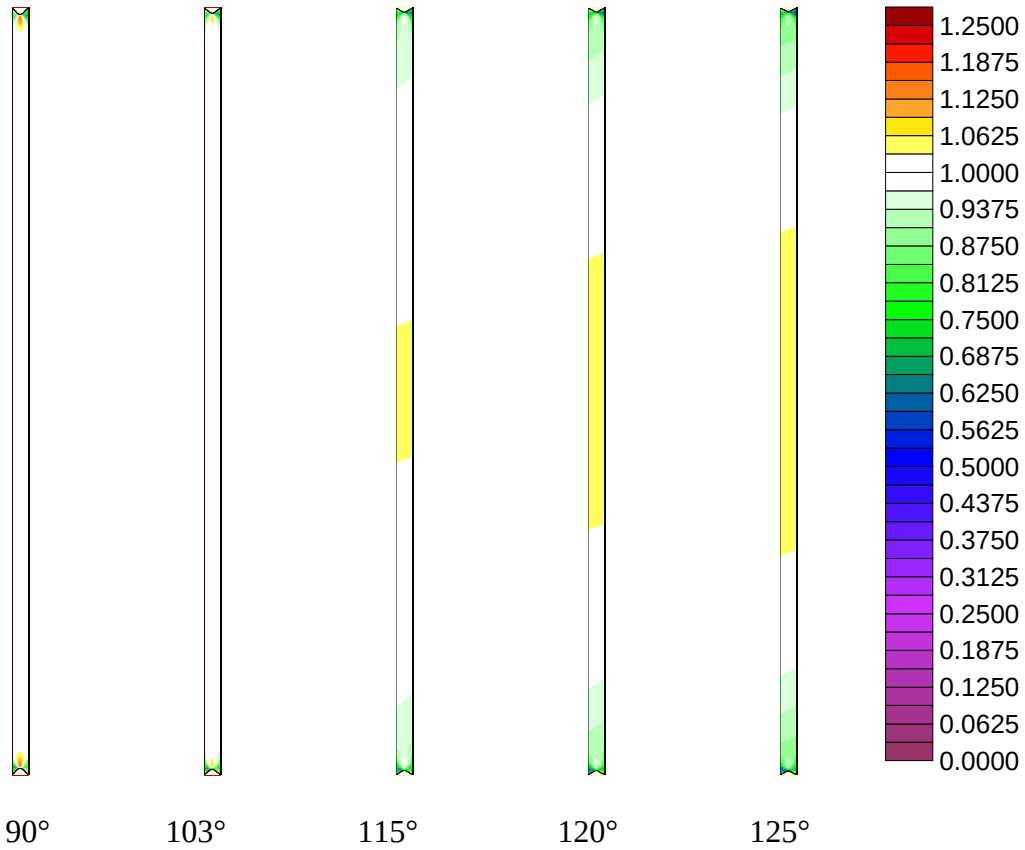

(a)

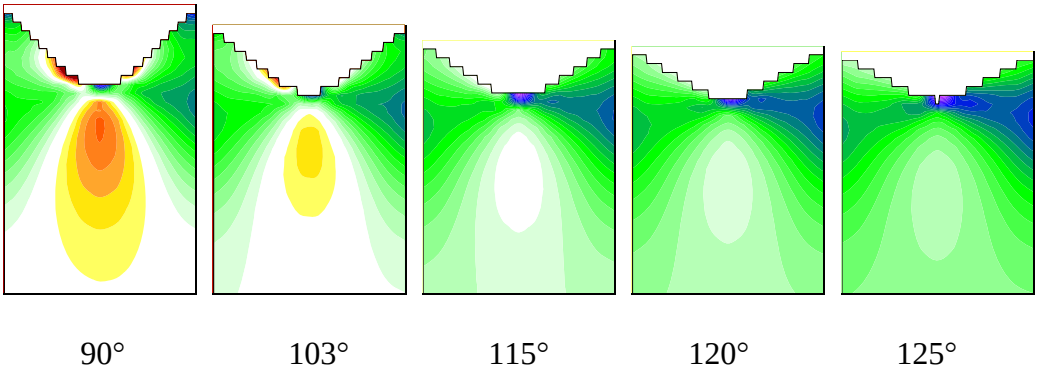

(b)

Figure 59. von Mises Stress Distributions in (a) Full Adhesive Bondline and (b) Around Notch Tip for Variable Angle Iosipescu V-Notched Specimens With 0.25-mm (0.01-in.) Bondline (Normalized)

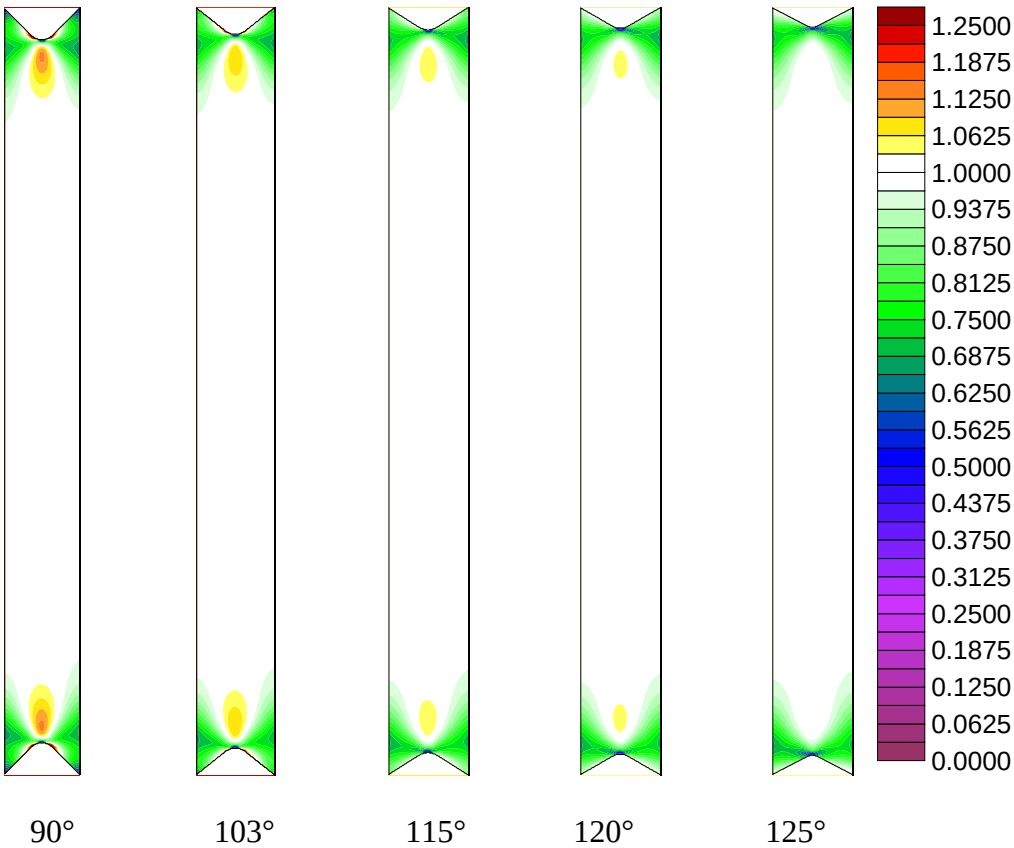

(a)

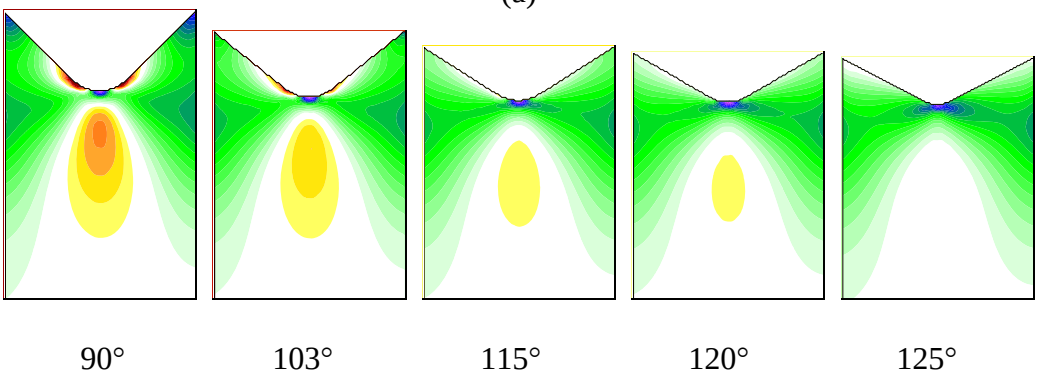

(b)

Figure 60. von Mises Stress Distributions in (a) Full Adhesive Bondline and (b) Around Notch Tip for Variable Angle Iosipescu V-Notch Specimens With 1.27-mm (0.05-in.) Bondline

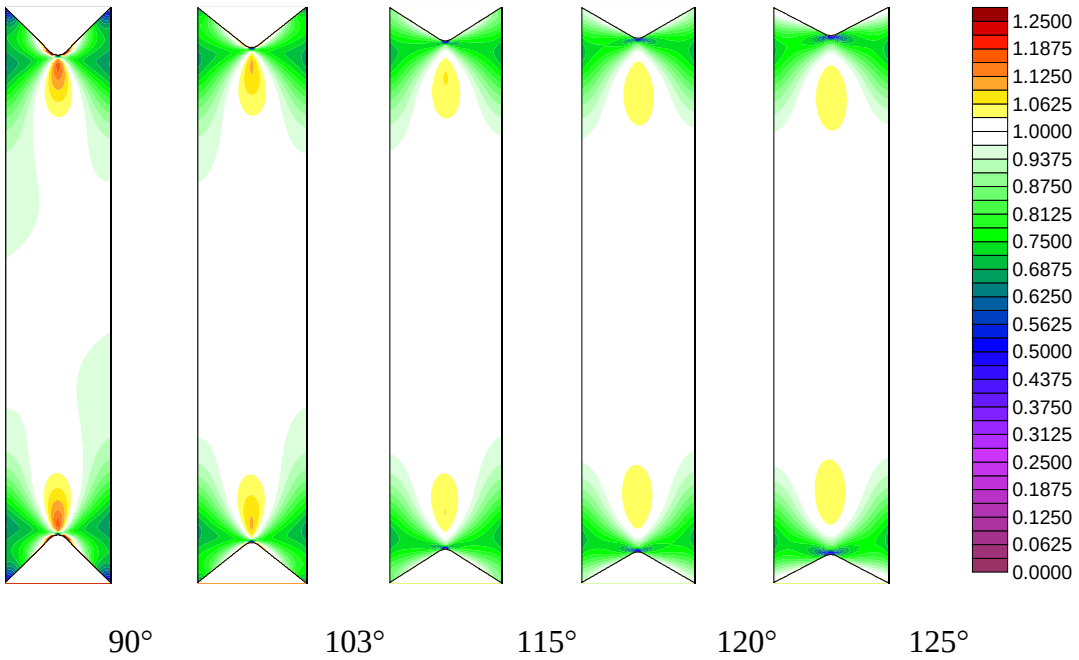

Figure 61. von Mises Stress Distributions for Variable Angle Iosipescu V-Notched Specimens With 2.54-mm (0.10-in.) Bondline (Normalized)

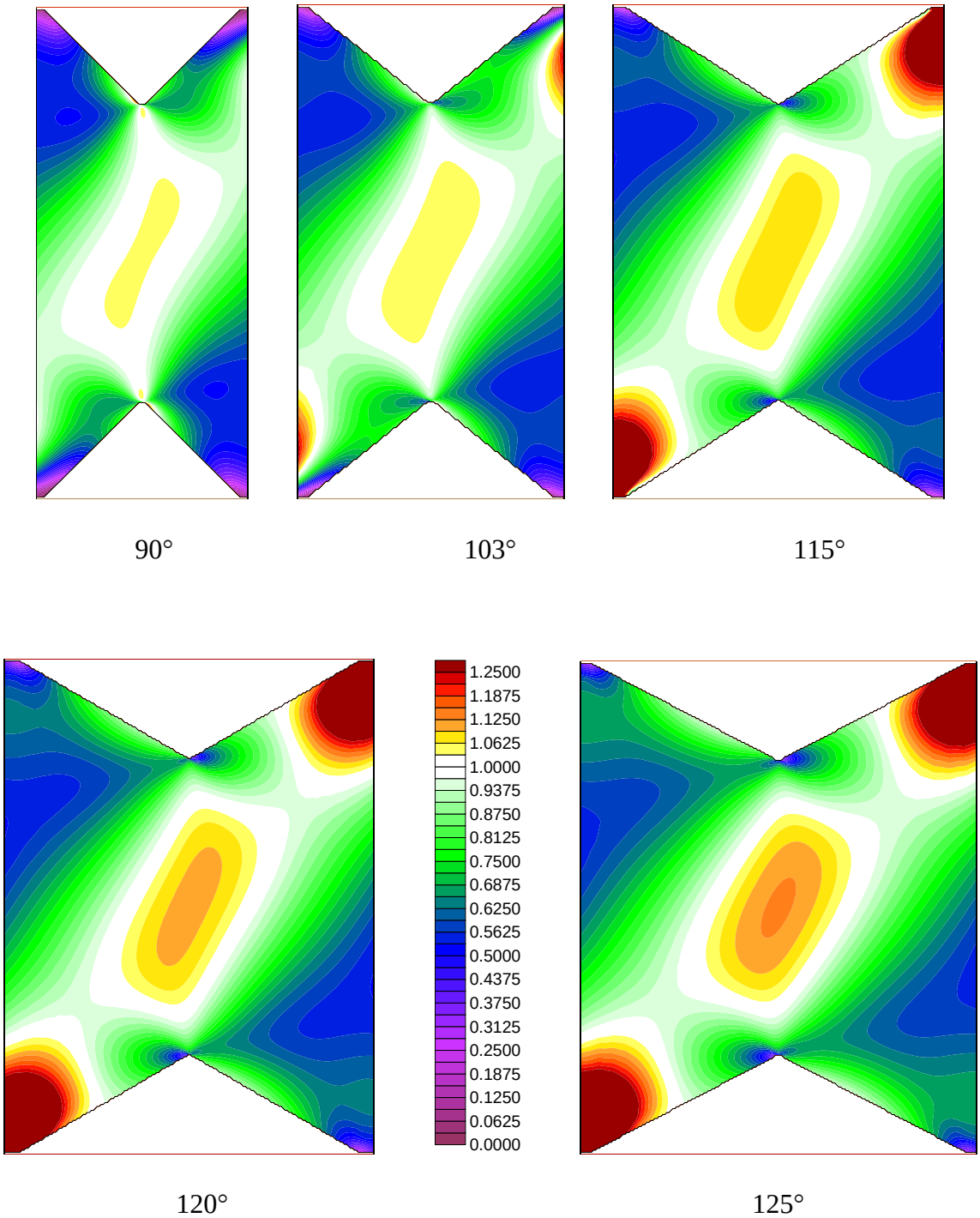

Figure 62. von Mises Stress Distributions for Bulk Adhesive Variable Angle Iosipescu V-Notched Specimens (Normalized)

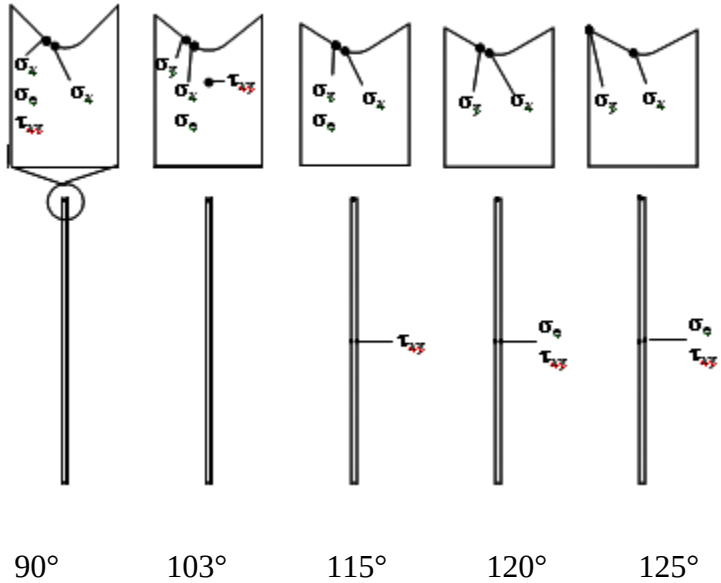

Figure 63. Locations of Maximum Values of Stress Components in Adhesive Bondline for Iosipescu V-Notched Specimens With 0.25-mm (0.01-in.) Bondline

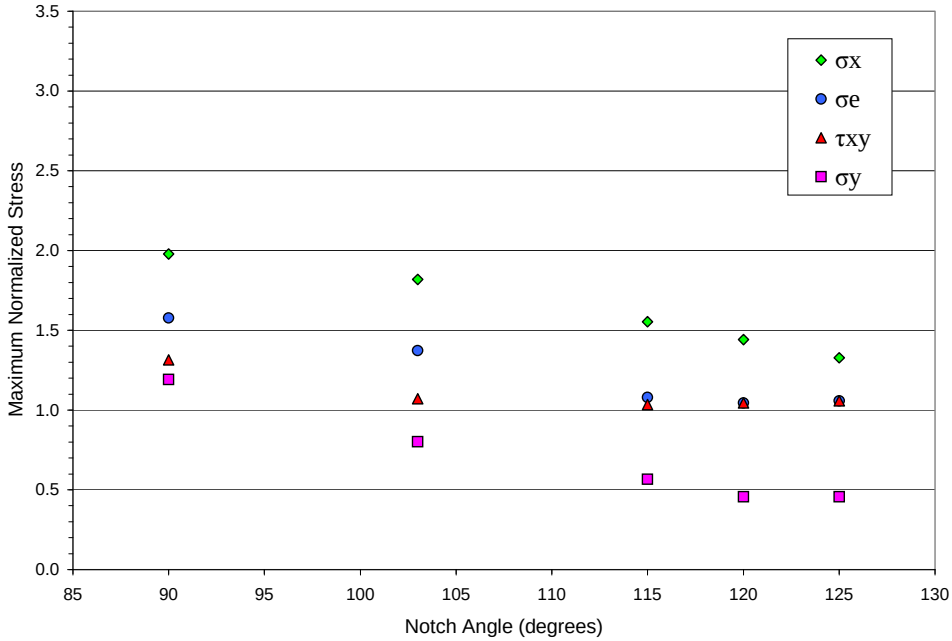

Figure 64. Maximum Normalized Values of Stress Components for Variable Notch Angle Iosipescu V-Notched Specimens With 0.25-mm (0.01-in.) Bondline

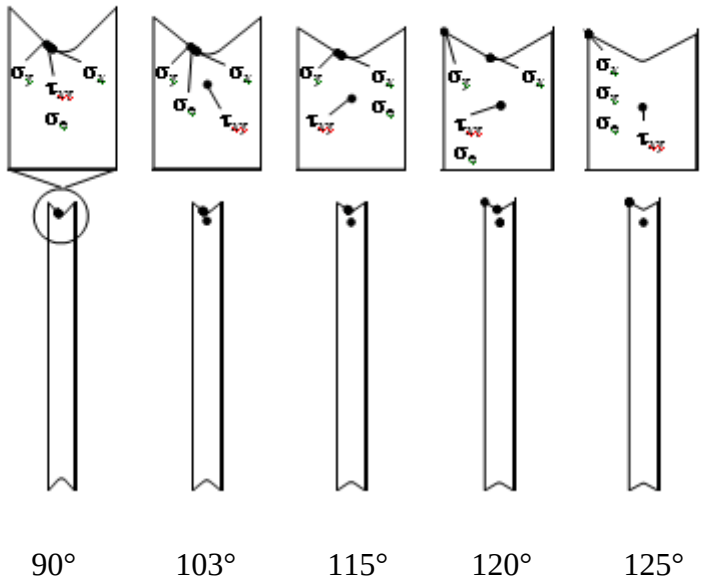

Figure 65. Locations of Maximum Values of Stress Components Adhesive Bondline for Iosipescu V-Notched Specimens With 1.27-mm (0.05-in.) Bondline

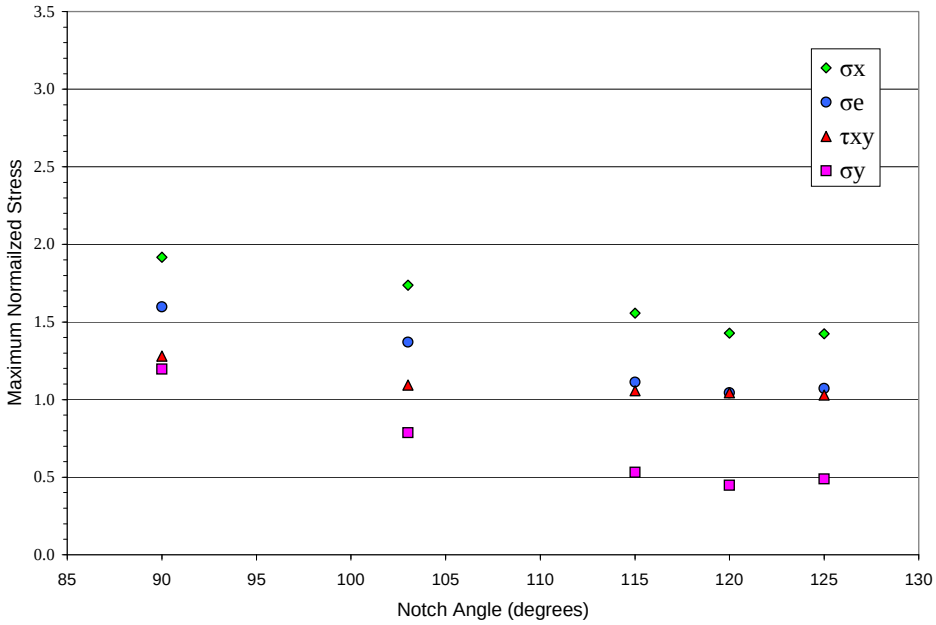

Figure 66. Maximum Normalized Values of Stress Components for Variable Notch Angle Iosipescu V-Notched Specimens With 1.27-mm (0.05-in.) Bondline

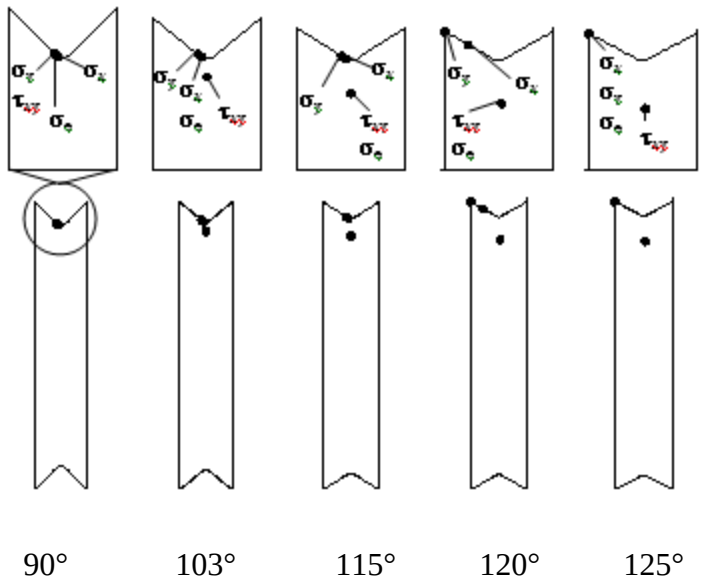

Figure 67. Locations of Maximum Values of Stress Components in Adhesive Bondline for Iosipescu V-Notched Specimens With 2.54-mm (0.10-in.) Bondline

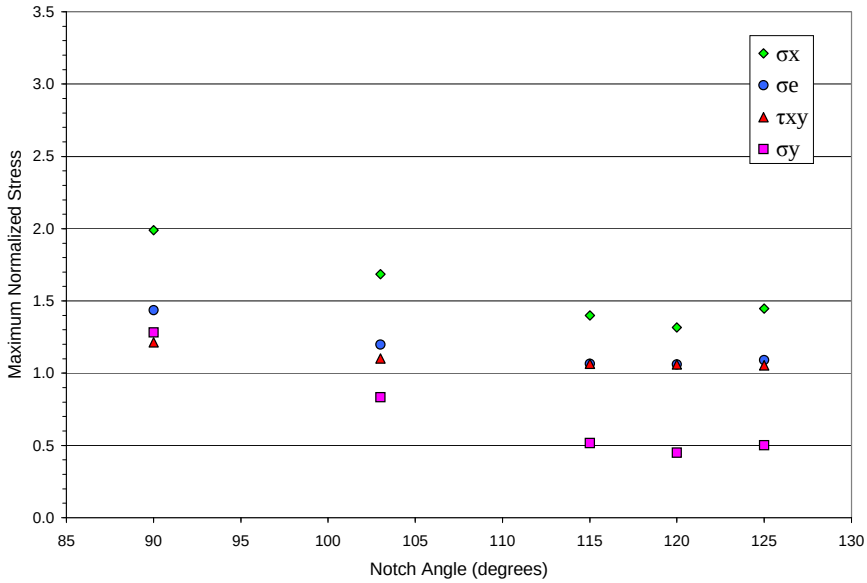

Figure 68. Maximum Normalized Values of Stress Components for Variable Notch Angle Iosipescu V-Notched Specimens With 2.54-mm (0.10-in.) Bondline

The maximum magnitudes of the individual stress components for the bulk adhesive variable notch angle Iosipescu V-notched specimens are shown in figure 69. The maximum magnitudes of the normal stresses steadily decrease as the notch angle increases. The magnitude of the shear stress reaches a minimum at 115° before increasing at greater notch angles.

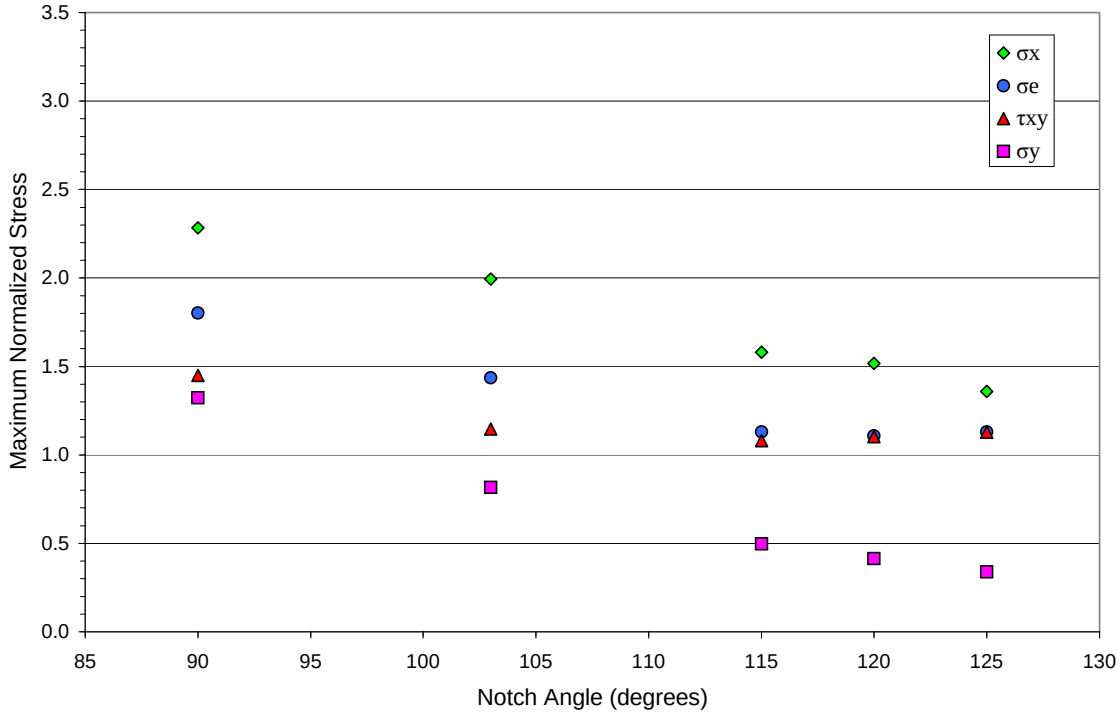

Figure 69. Maximum Normalized Values of Stress Components for Variable Notch Angle Iosipescu V-Notched Bulk Adhesive Specimens

3.5.4 Conclusions for Variable Angled Iosipescu V-Notched Specimens.

The bonded Iosipescu V-notched specimen with a 90° notch angle has an undesirable stress state due to large stress concentrations. However, the stress state within the adhesive bondline can be altered by increasing the notch angle. As the notch angle increases, both the distribution and magnitude of the stress components change. Overall, the most desirable stress state is produced with a notch angle of 120°; for all three bondline thicknesses, the magnitudes of the normal stress concentrations are minimized and the shear stress became the dominant stress component in the von Mises stress. At angles greater than 120°, the normal stress concentrations move to the interface corners and increase in magnitude. Also, at larger angles, the shear stress distribution starts to become parabolic in the specimen center and therefore less uniform. In summary, the advantage of a notch angle of 120° is that it preserves the uniformity of the shear stresses observed in the 90° notch angle while effectively minimizing the stress concentrations at both the notch tips and the notch flanks.

3.6 IOSIPESCU V-NOTCHED SPECIMENS WITH VARIABLE NDR.

The previous sections have identified the optimal Iosipescu specimen as having a V-notch with a notch angle of 120° for bonded configuration. The final geometric feature of the Iosipescu specimen to be studied is the NDR. The NDR is a measure of the notch depth and is the ratio between the notch depth and the overall specimen height. The standard Iosipescu specimen has a notch depth of 3.8 mm (0.15 in.) and an overall height of 19.1 mm (0.75 in.) for an NDR of 0.20. To evaluate the effect of NDR on stress state, the 120° V-notched Iosipescu specimen was analyzed with NDR values of 0.150, 0.175, 0.200, 0.225, and 0.250.

3.6.1 Shear Stress for Variable NDR Specimens.

The shear stresses for the Iosipescu 120° V-notched specimen with variable NDR are shown in figure 70 for the 0.25-mm (0.01-in.) bondline, figure 71 for the 1.27-mm (0.05-in.) bondline, and figure 72 for the 2.54-mm (0.10-in.) bondline. The thin bondline has a parabolic shear stress distribution for all five NDRs, with the 0.150 NDR being the most parabolic and the 0.250 NDR being the most uniform. This trend is also found in the other two bondline thicknesses with the difference of shear stress concentrations appearing at the notch tips for the larger NDRs. The shear stress for the specimen with an NDR of 0.200, while not completely uniform, lies between the two extremes of having a parabolic shear stress distribution for smaller NDRs and notch tip stress concentrations for larger NDRs.

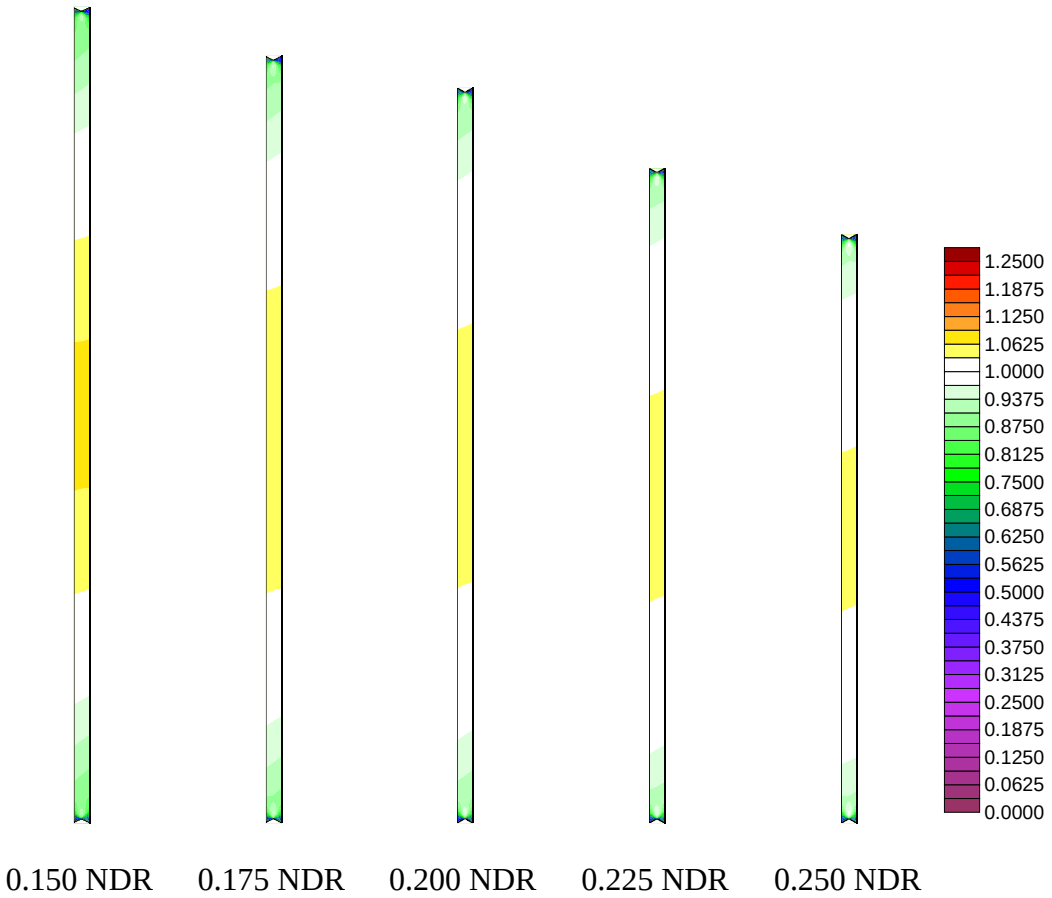

(a)

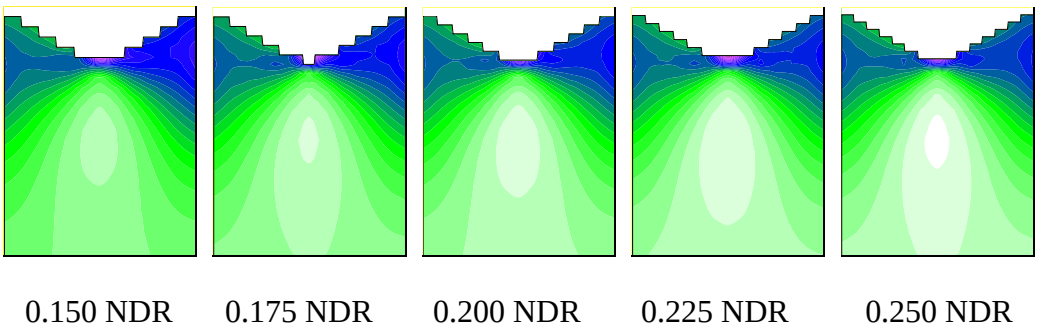

(b)

Figure 70. Shear Stress Distributions in (a) Full Adhesive Bondline and (b) Around Notch Tip for 120° Iosipescu V-Notched Specimens With 0.25-mm (0.01-in.) Bondline (Normalized)

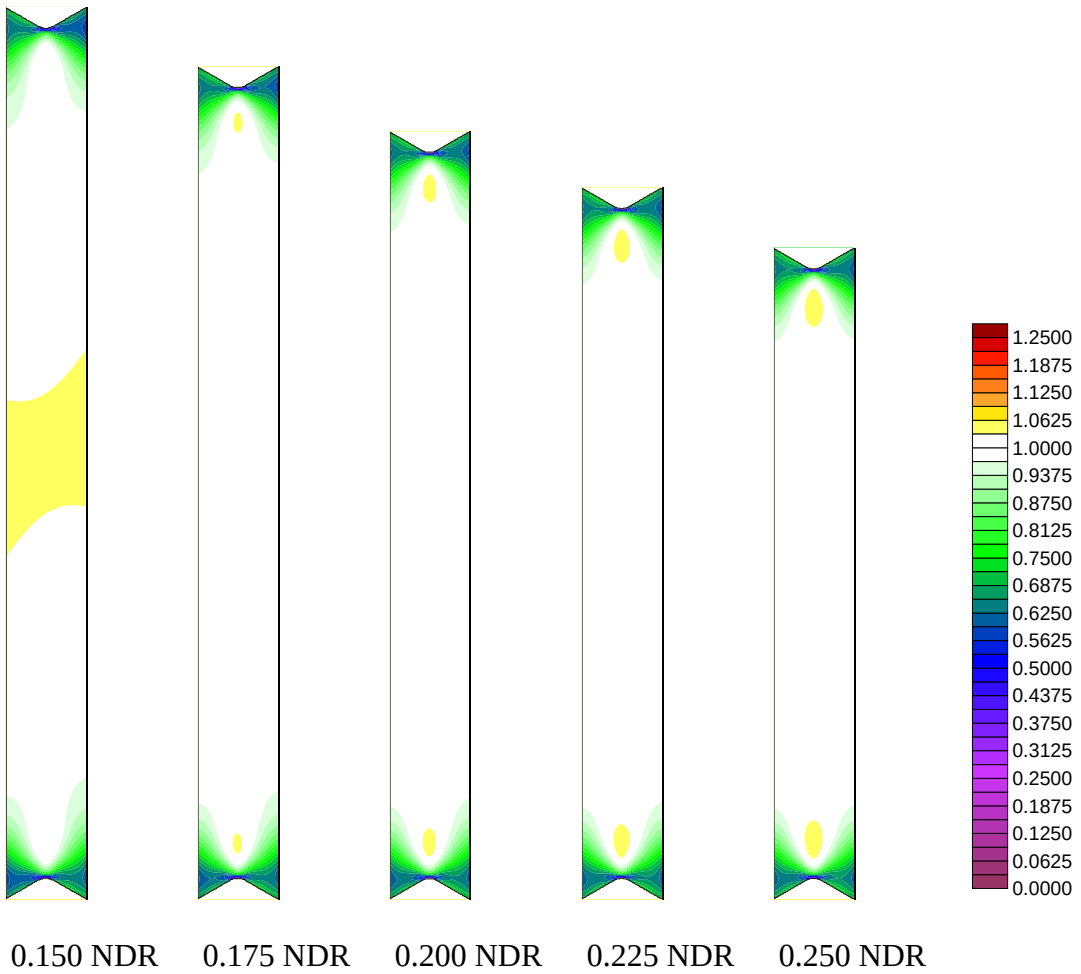

Figure 71. Shear Stress Distributions in Adhesive Bondline for 120° Iosipescu V-Notched Specimens With 1.27-mm (0.05-in.) Bondline (Normalized)

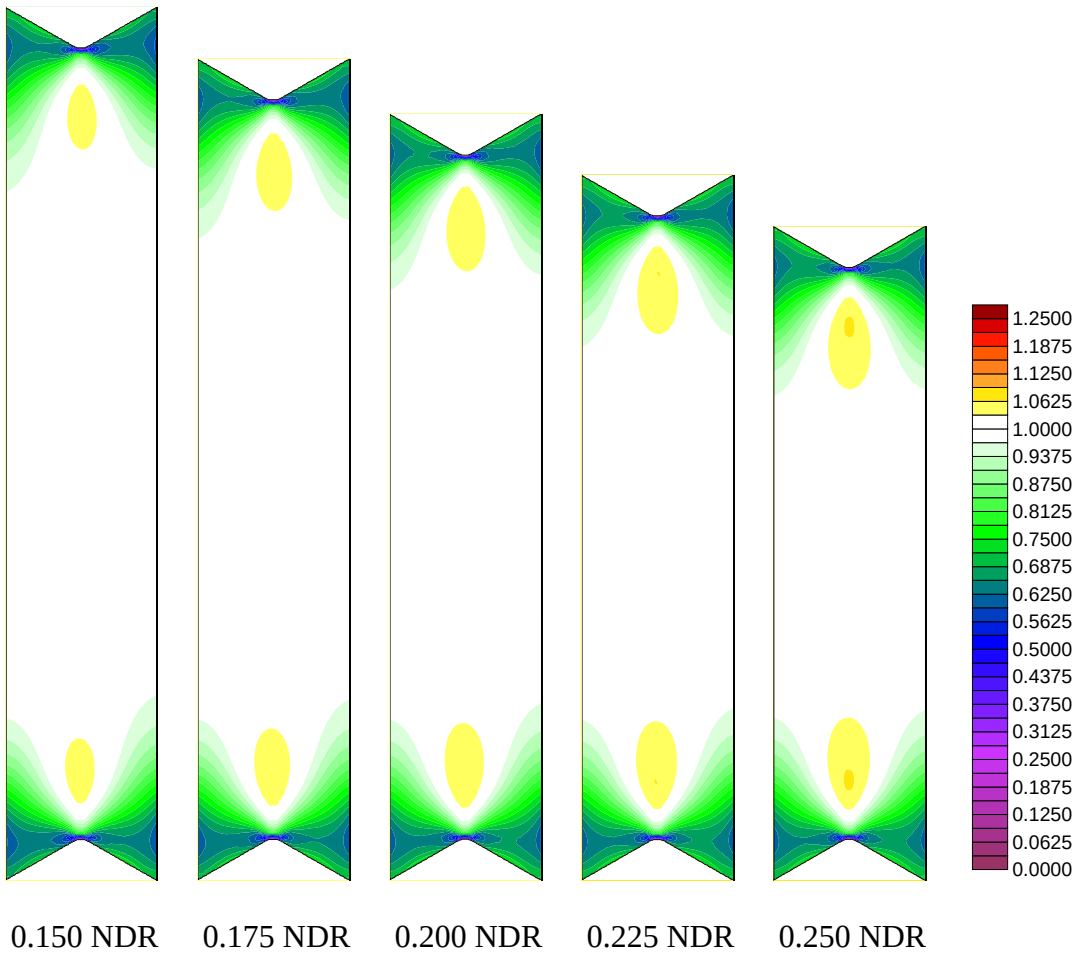

Figure 72. Shear Stress Distributions in Adhesive Bondline for 120° Iosipescu V-Notched Specimens With 2.54-mm (0.10-in.) Bondline (Normalized)

3.6.2 Normal Stresses for Iosipescu V-Notched Specimens With Variable NDR.

Contours of transverse and axial normal stresses for Iosipescu V-notched specimens with variable NDRs and a notch angle of 120° are shown in figures 73 and 74 for the 0.25-mm (0.01-in.) bondline, figure 75 for the 1.27-mm (0.05-in.) bondline, and figure 76 for the 2.54-mm (0.10-in.) bondline. For all three bondline thicknesses, the distribution of normal stresses appears to be independent of notch depth because there is very little if any change in either transverse or axial stresses as the notch depth changes.

3.6.3 Conclusions for Variable NDR Iosipescu V-Notched Specimens.

Since the normal stresses in the Iosipescu V-notched specimen did not change significantly as the NDR changed, it is not instructional to show the von Mises stress distributions. The plots of stress concentration location and magnitude are also omitted since the shear stress distribution was fairly constant as well. Both the von Mises stress contours and stress concentration plots for all NDRs are nearly identical to those already presented in section 3.5.3 for the 120° notch angle specimen with an NDR of 0.2. Since all three stress components did not vary significantly from

baseline values, the original NDR of 0.200 was determined to be a suitable value for all bondline thicknesses.

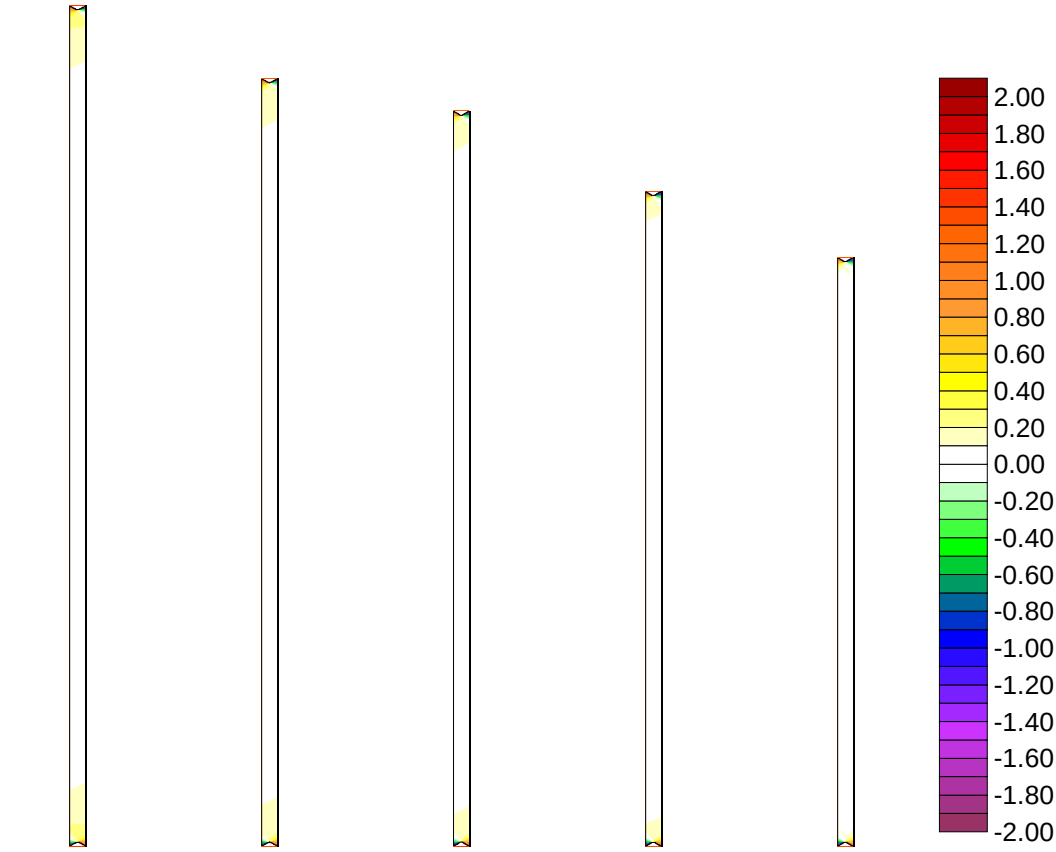

0.150 NDR 0.175 NDR 0.200 NDR 0.225 NDR 0.250 NDR

(a)

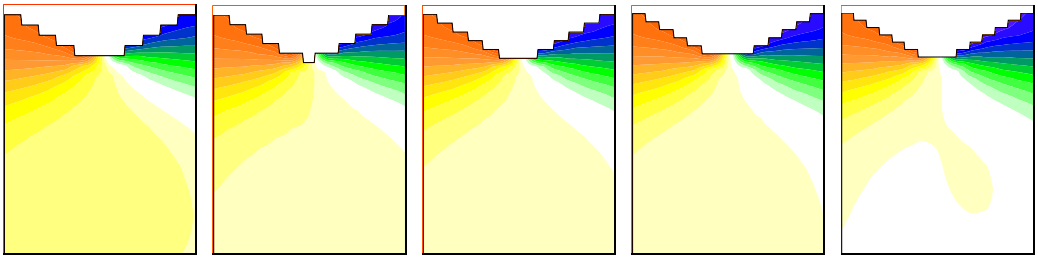

0.150 NDR 0.175 NDR 0.200 NDR 0.225 NDR 0.250 NDR

(b)

Figure 73. Transverse Stress Distributions in (a) Full Adhesive Bondline and (b) Around Notch Tip for 120° Iosipescu V-Notched Specimens With 0.25-mm (0.01-in.) Bondline (Normalized)

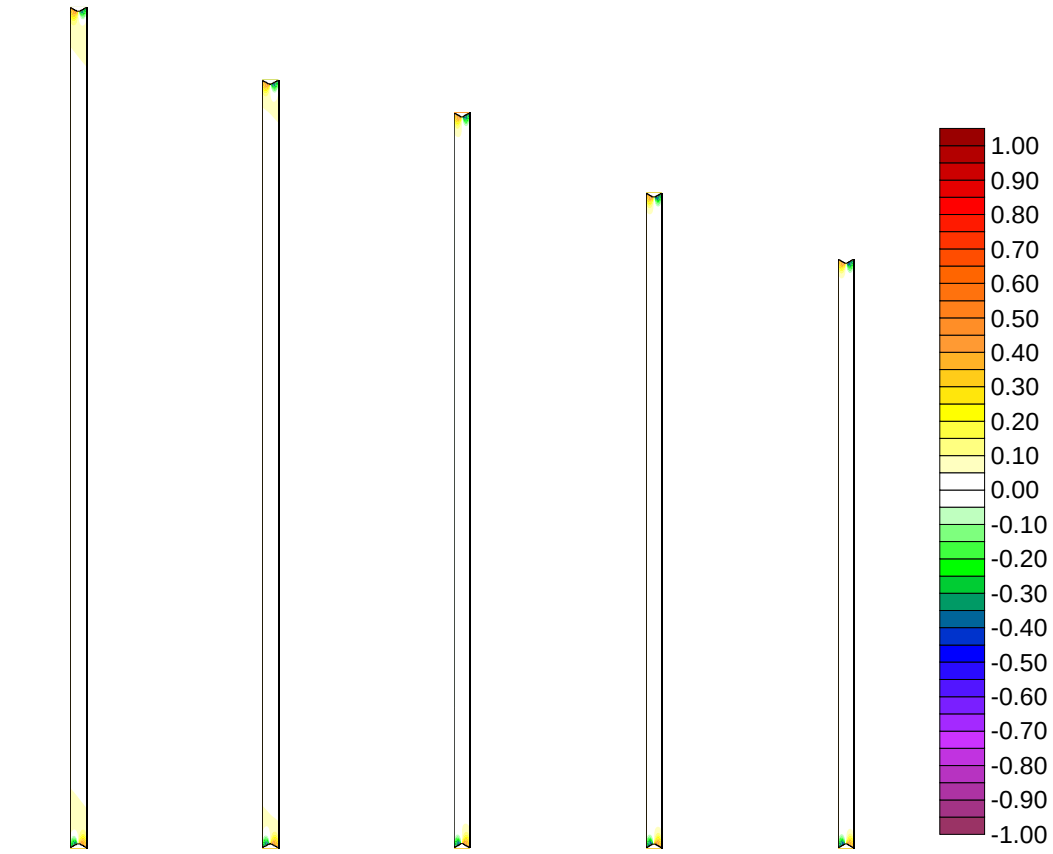

0.150 NDR 0.175 NDR 0.200 NDR 0.225 NR 0.250 NDR

(a)

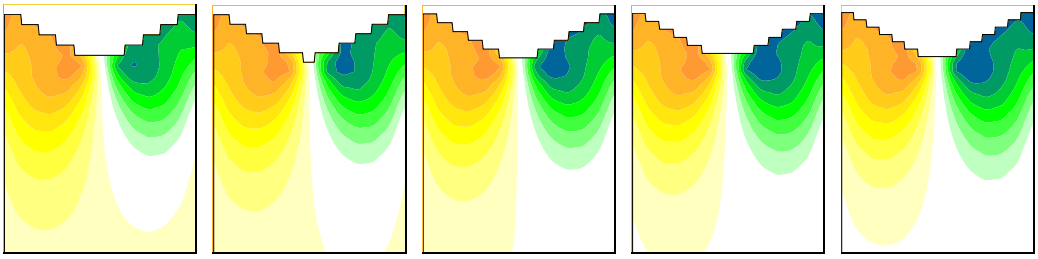

0.150 NDR 0.175 NDR 0.200 NDR 0.225 NDR 0.250 NDR

(b)

Figure 74. Axial Stress Distributions in (a) Full Adhesive Bondline and (b) Around Notch Tip for 120° Iosipescu V-Notched Specimens With 0.25-mm (0.01-in.) Bondline (Normalized)

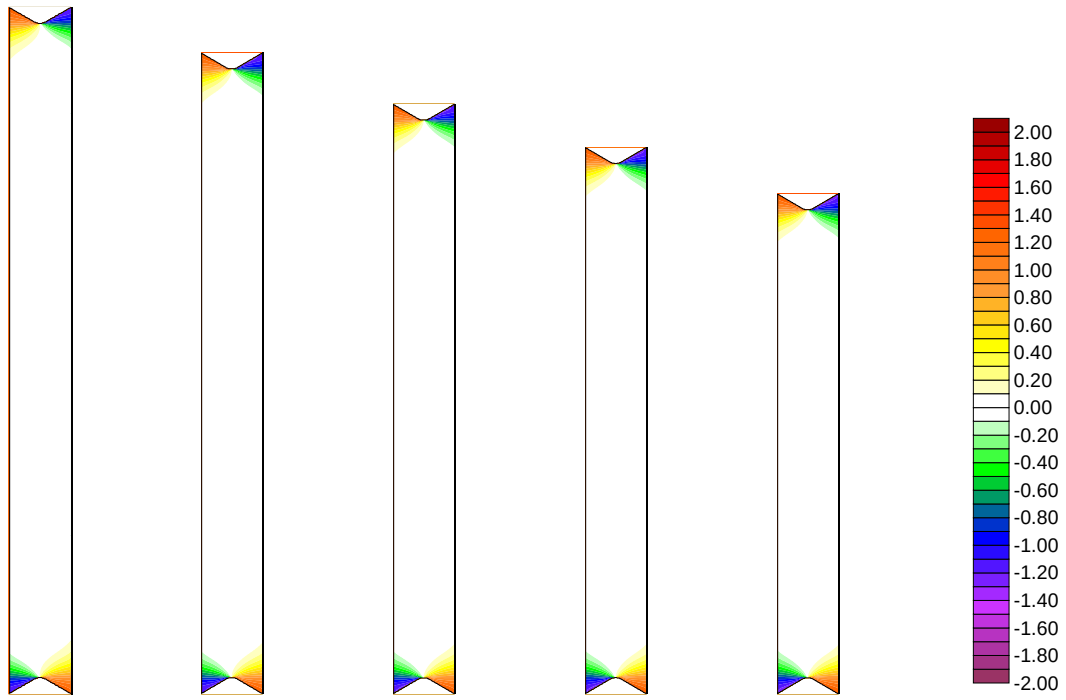

0.150 NDR 0.175 NDR 0.200 NDR 0.225 NDR 0.250 NDR

(a)

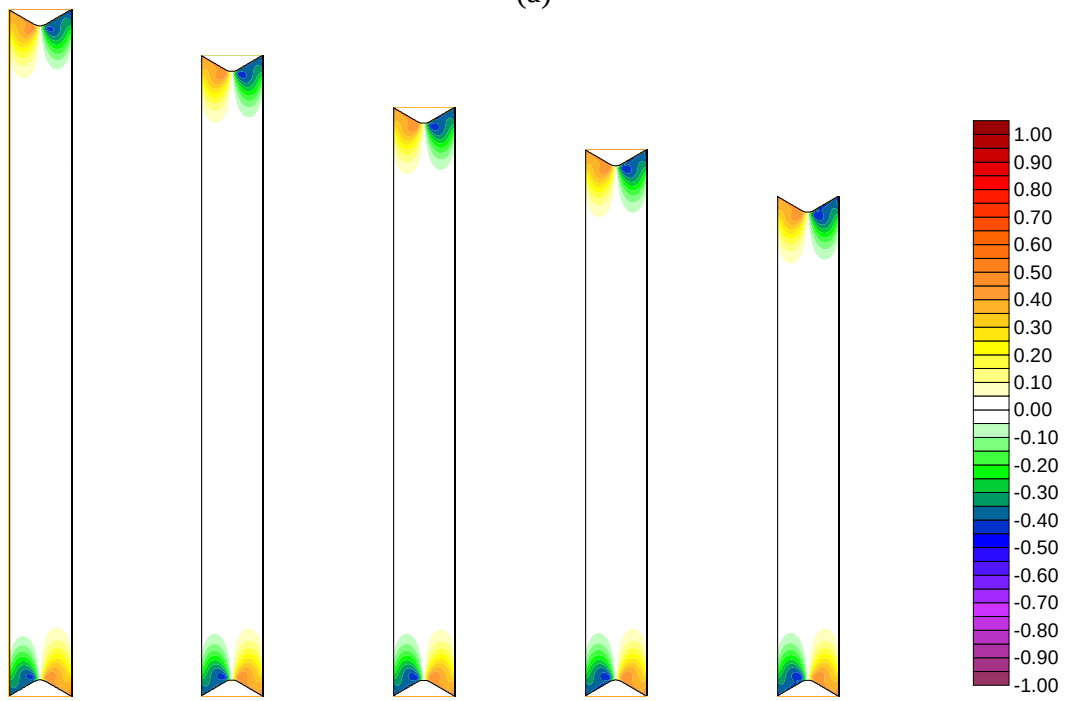

0.150 NDR 0.175 NDR 0.200 NDR 0.225 NDR 0.250 NDR

(b)

Figure 75. (a) Transverse and (b) Axial Stress Distributions in Adhesive Bond for 120° Iosipescu V-Notched Specimens With 1.27-mm (0.05-in.) Bondline (Normalized)

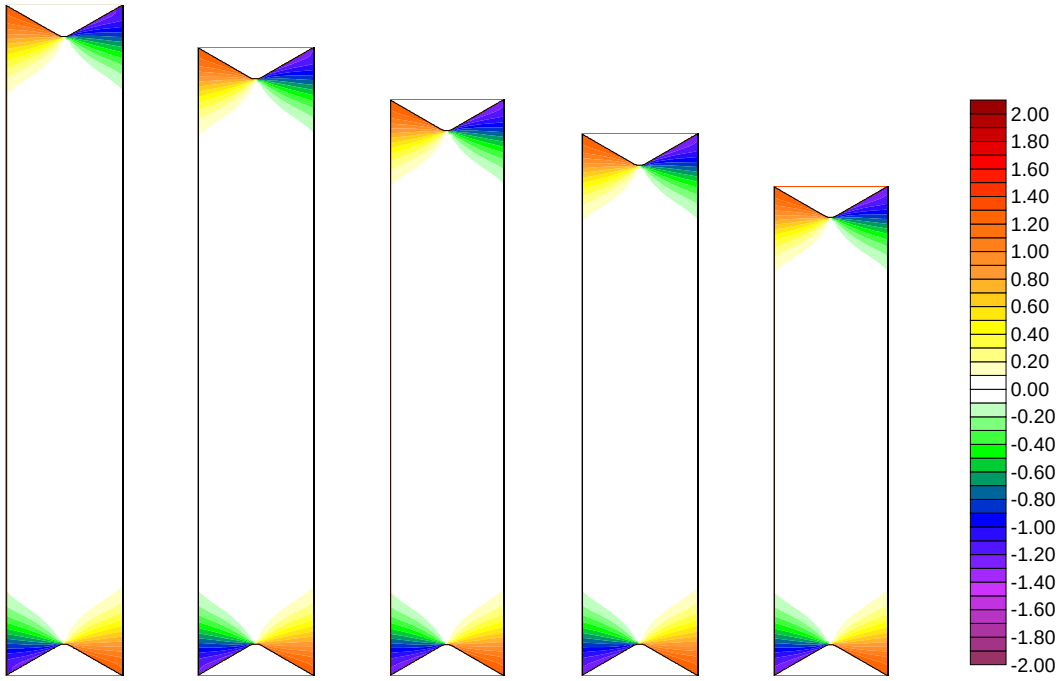

0.150 NDR 0.175 NDR 0.200 NDR 0.225 NDR 0.250 NDR

(a)

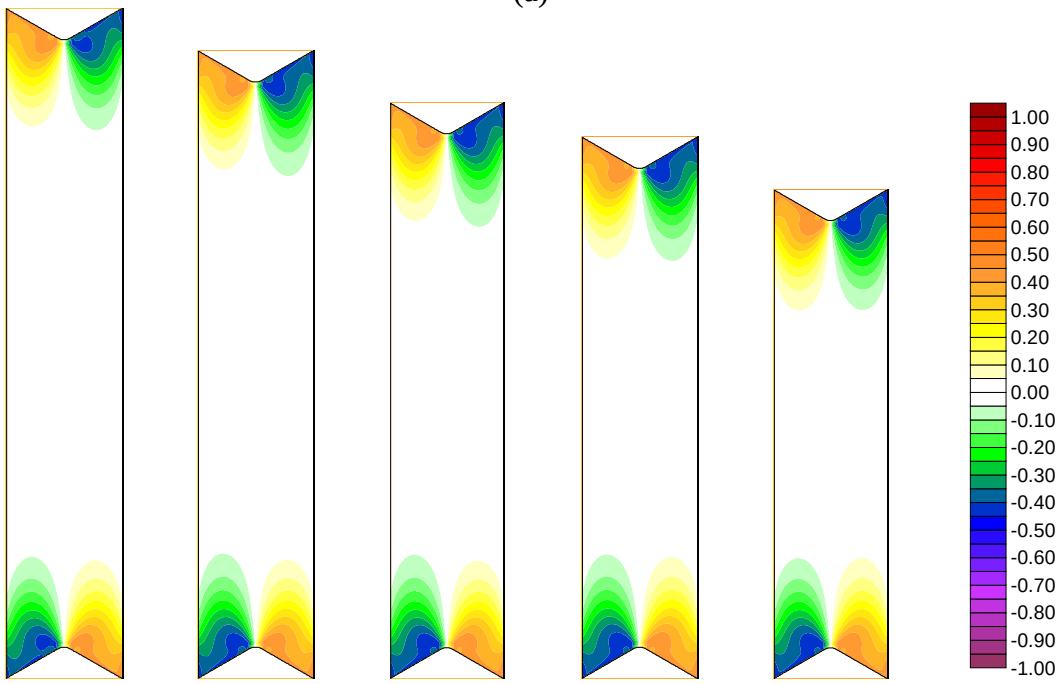

0.150 NDR 0.175 NDR 0.200 NDR 0.225 NDR 0.250 NDR

(b)

Figure 76. (a) Transverse and (b) Axial Stress Distributions in Adhesive Bondline for 120° Iosipescu V-Notched Specimens With 1.27-mm (0.05-in.) Bondline (Normalized)

3.7 CONCLUSIONS FOR IOSIPESCU SPECIMENS.

Based on the results of the above analyses, the final notch geometry chosen for the bonded Iosipescu specimens was a 120° V-notch with an NDR of 0.200. This geometry was chosen for all bonded specimens to allow for consistency in specimen fabrication in the experimental tests portion of the study. However, the optimal notch configuration for the bulk adhesive was determined to be a 90° V-notch with an NDR of 0.200. Note that a notch angle of 120° for the bulk adhesive specimens created a shear stress distribution that was parabolic and nonuniform. Figure 77 shows the distribution of shear stress between the notches for the selected Iosipescu specimen configurations. Note that some differences exist between the shear stress states among the four specimen configurations. These results indicate that as the bondline thickness increases, the shear stress concentrations near the notch tips increases, but the shear stress in the central region decreases. Overall, the magnitude of the peak shear stress increases slightly as the adhesive bondline thickness increases. Figure 77 also shows that the magnitude of the peak shear stress in the bulk adhesive shear specimens is approximately equal to that of intermediate bondline thickness specimens.

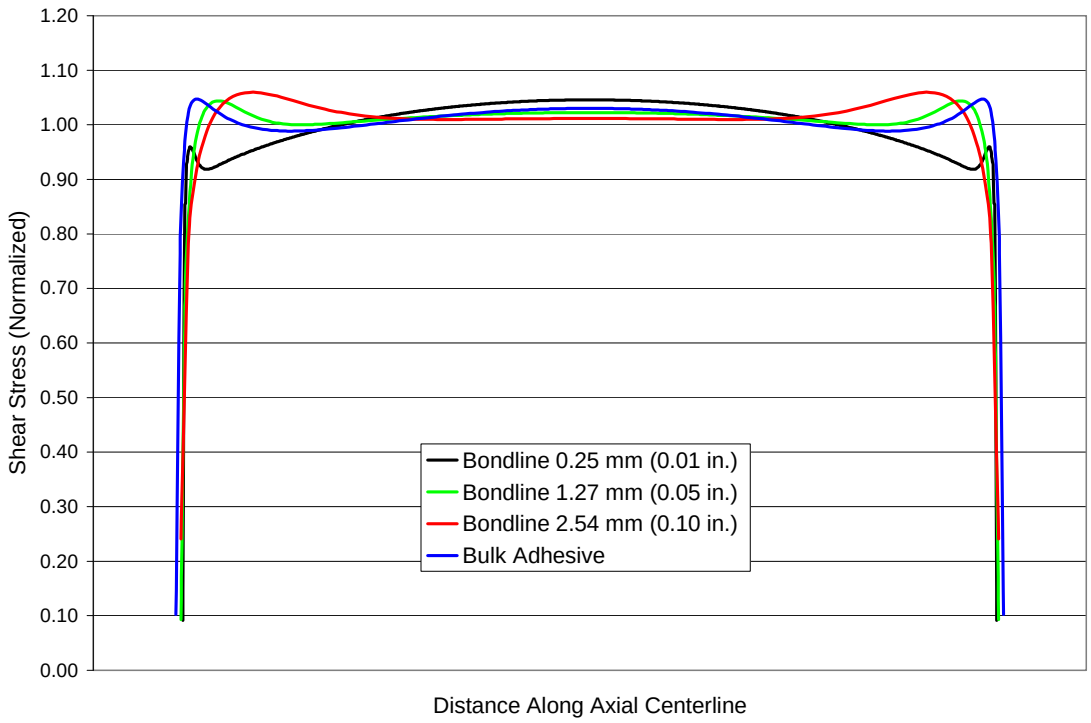

Figure 77. Shear Stress Distributions Along Axial Centerlines for Bonded Iosipescu Specimens With 120° Notch Angle and Bulk Adhesive Iosipescu Specimens With 90° Notch Angle

3.8 THICK ADHEREND LAP JOINT RESULTS.

The lap joint test specimen described in ASTM D 5656 and known as the thick adherend lap joint specimen was modeled to investigate the stress state produced for different bondline thicknesses. As in the previous analyses, each of the three bondline thicknesses were modeled.

3.8.1 Shear Stresses in Thick Adherend Lap Joint.

The thick adherend lap joint test differs from the Iosipescu shear test in that the specimen is loaded in tension rather than in shear. However, despite the different loading methods the goal of acquiring shear response is the same. Additionally, both test methods determine shear strength by assuming that the shear stress state is uniform and by simply dividing the applied shear load by the gage section area.

Figure 78 shows shear stress contours produced in the adhesive test section of the thick adherend lap joint specimen. These results show that the stress state changes significantly as the bondline thickness increases. Additionally, these contour plots show that the state of shear stress is highly nonuniform throughout the adhesive test section.

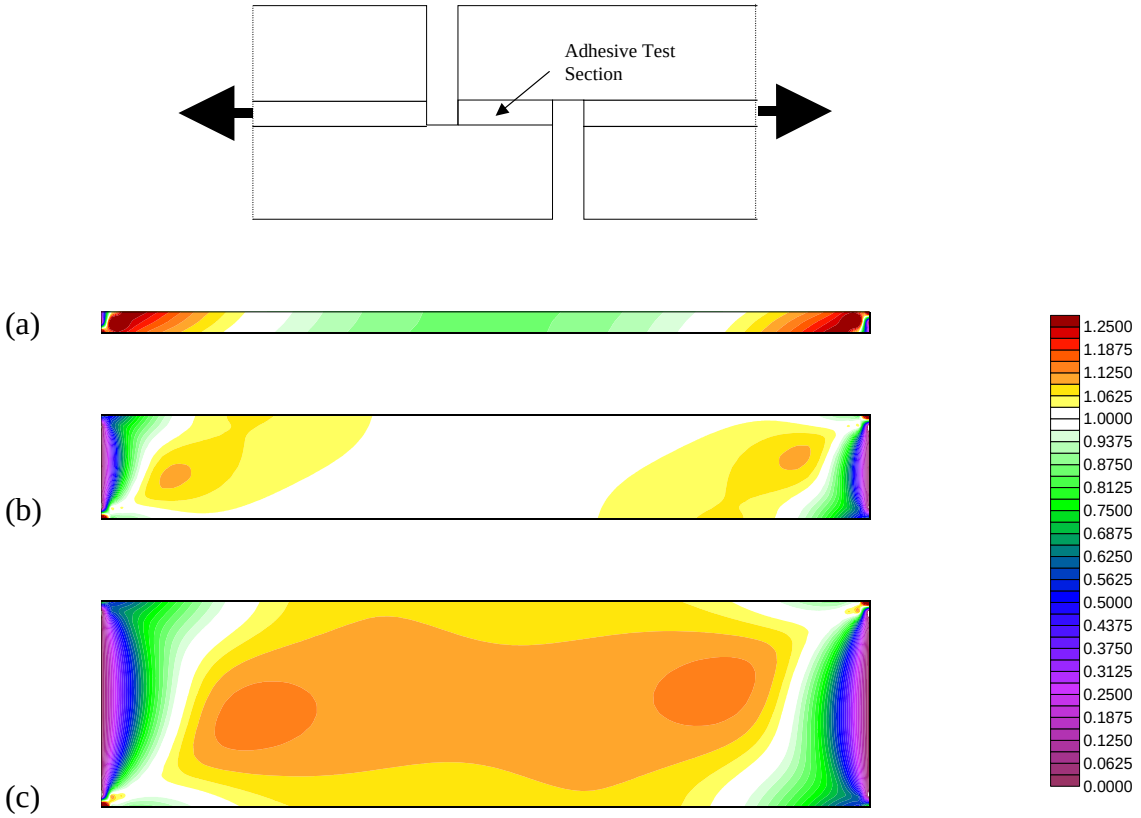

Figure 78. Shear Stresses in the Adhesive Test Section of the Thick Adherend Lap Joint for Bondline Thicknesses (a) 0.25 mm (0.01 in.), (b) 1.27 mm (0.05 in.), and (c) 2.54 mm (0.10 in.) (Normalized)

The variation of shear stress along the midplane of the adhesive test section is shown in figure 79 for all three bondline thicknesses. The intermediate bondline thickness is shown to have the most uniform shear stress distribution along this line. The thinnest bondline has large stress concentrations at the bond ends and all three bondline thicknesses have shear stresses that exceed the average shear stress by at least 10 percent.

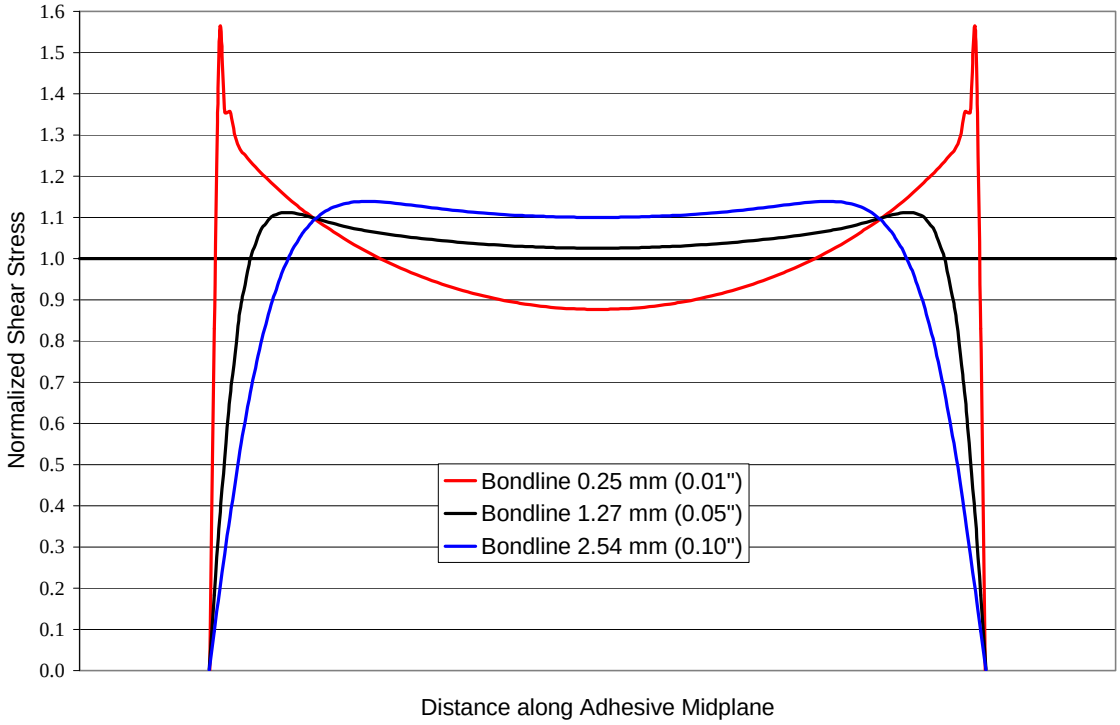

Figure 79. Variation of Shear Stresses Along Adhesive Midplane for Three Bondline Thicknesses

3.8.2 Normal Stresses in Thick Adherend Lap Joint.

A disadvantage of lap joints is the unavoidable and sometimes large peel (normal) stresses. One way to minimize these stresses is to increase the thickness of the adherends, which provides higher bending rigidity. Even with thick adherends, however, the peel stresses are still significant. Figure 80 shows that increasing the bondline thickness reduces the transverse stresses in the center of the test section. However, the thicker bondline also produces higher axial stresses throughout the central region. Overall, the intermediate bondline thickness shows the least amount of influence from normal stresses throughout most of the adhesive test section. Note, however, that all three bondline thicknesses have large normal stress concentrations at the interface corners.

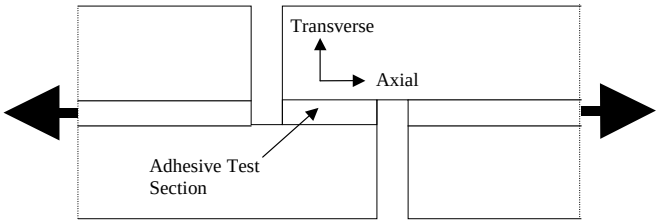

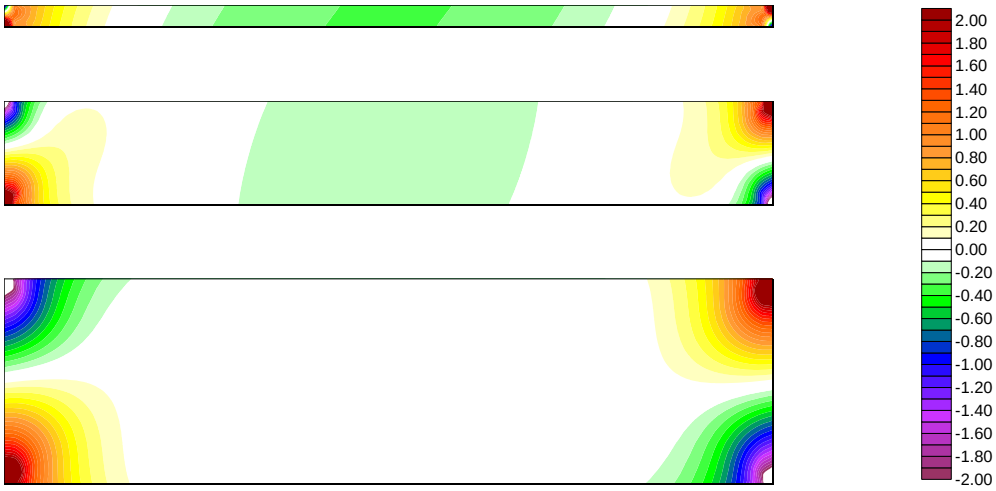

(a)

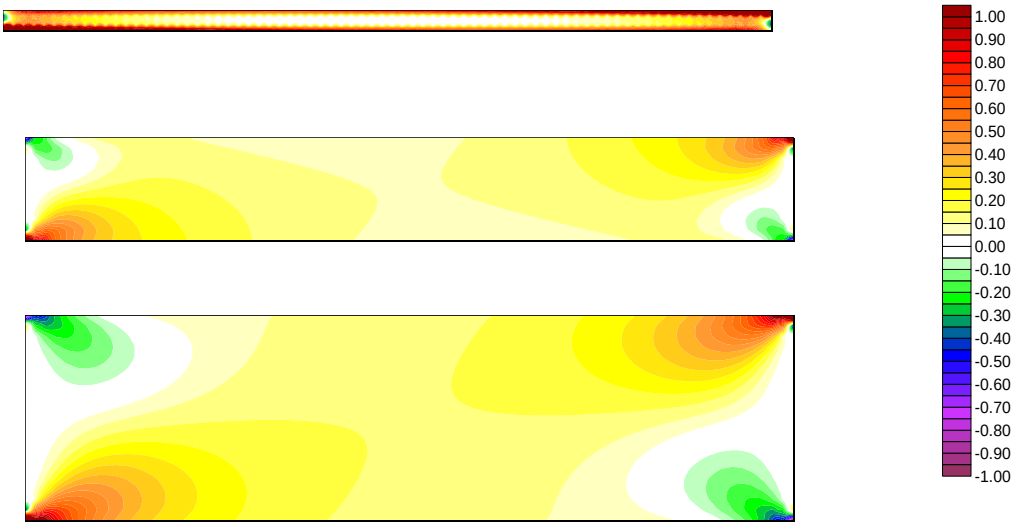

(b)

Figure 80. Transverse (a) and Axial (b) Stresses in the Adhesive Test Section of the Thick Adherend Lap Joint for Bondline Thicknesses 0.25 mm (0.01 in.), 1.27 mm (0.05 in.), and 2.54 mm (0.10 in.), Respectively (Normalized)

3.9 BUTT TENSILE RESULTS.

The adhesive butt joint was analyzed to determine the effect of bondline thickness on an adhesive bond subjected to a tensile loading. Since the butt joint is used primarily to evaluate adhesive tensile properties, the optimum stress state in the butt joint is a state of uniform tension, where the axial tensile stress, σ_y, is defined as the ratio of applied load, P, to cross-sectional area, A, or

$$\sigma_y = P/A \tag{6}$$

The stresses of primary concern in the butt tensile tests are the axial normal stresses, or normal stresses, in the direction of applied load. Figure 81 shows how the axial stresses vary with bondline thickness. The axial stresses have been normalized with respect to the average axial tensile stress as

$$\sigma = \frac{\sigma_y}{P/A} \tag{7}$$

Figure 81 shows that the axial normal stress distribution in the thin bondline is relatively uniform, except around the edges where the stress drops to about 80% of the average value. As the bondline thickness increases, however, the stress state becomes less uniform as the edge nonuniformity extends further into the adhesive, and the stresses in the center of the bondline become larger than the average axial stress. These central axial stresses exceed the average axial stress by approximately 10 percent and 20 percent for the intermediate and thick bondlines, respectively.

The stress state in the butt tensile joint is not a state of simple axial tension. There are significant stresses in the transverse directions due to constraints produced by the aluminum adherends on the Poisson contraction of the adhesive. However, the axial tension results are sufficient to show that the stress state in the adhesive is dependent on bondline thickness, and thus, the transverse stress components are not presented.

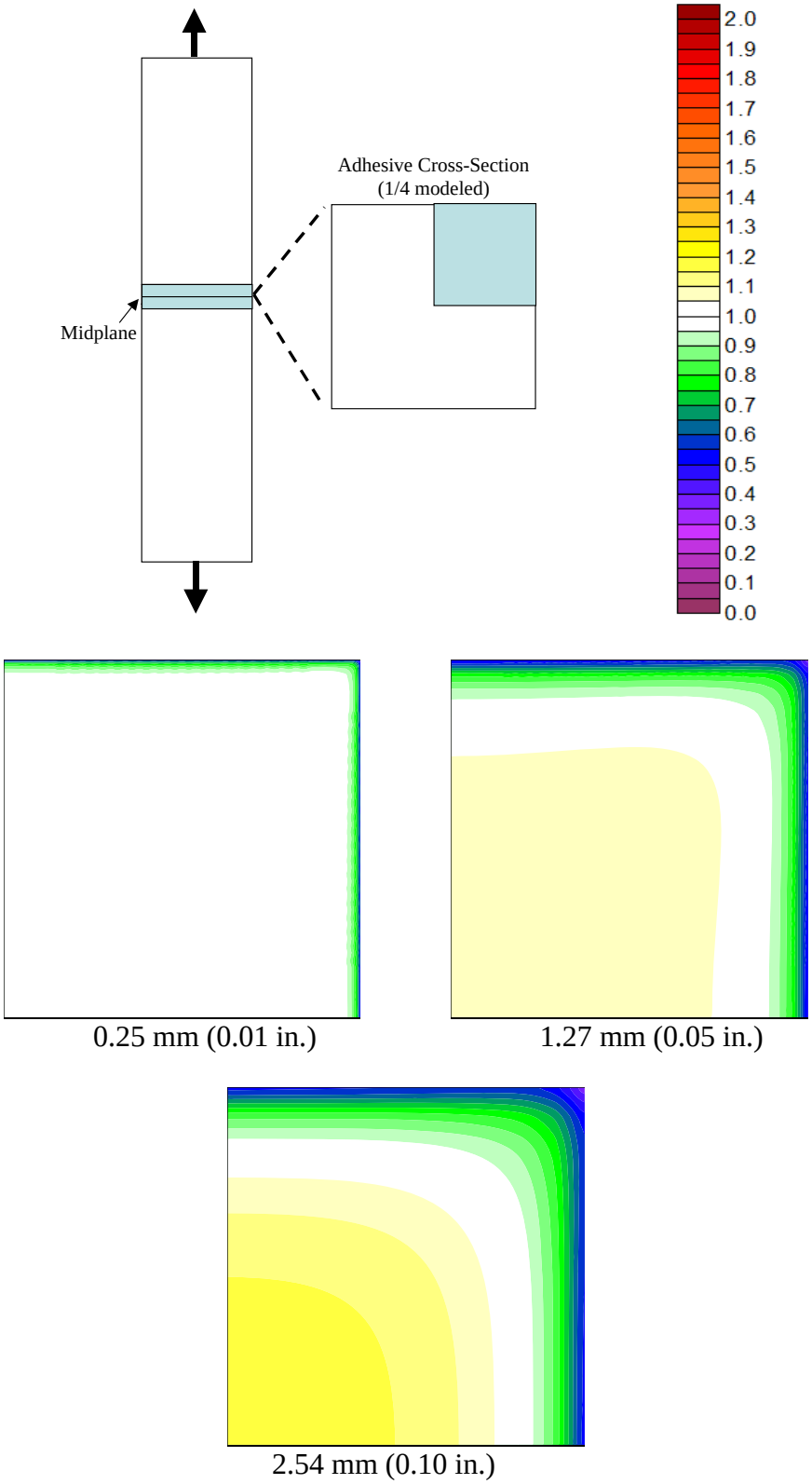

Figure 81. Axial Normal Stresses in Butt Tensile Adhesive Bondlines

4. SPECIMEN FABRICATION AND TEST METHODOLOGIES.

4.1 INTRODUCTION.

Both shear and tensile tests were performed using commercially available paste adhesives. For both types of tests, bulk adhesive specimens as well as bonded aluminum specimens were tested. The majority of the shear tests were performed using ASTM D 5379 [7] Iosipescu shear specimens with the notch angle widened from the standard 90° to 120°. Limited shear tests were also performed according to the ASTM D 5656 thick adherend metal lap shear test [5]. Tensile tests were performed using standard dumbbell-shaped test specimens according to ASTM D 638 [24] for the bulk adhesive and with bar-shaped butt-joined aluminum specimens according to ASTM D 2094 [25] and ASTM D 2095 [26] for the bonded specimens.

4.2 ADHESIVES TESTED.

Tests were performed using three aerospace-grade structural paste adhesives from Loctite Hysol Corporation. The primary adhesive used in all tests was Loctite EA 9394, selected due to the extensive nature of past material characterization. The other two adhesives selected for secondary tests were Loctite EA 9360 and Loctite EA 9392. All three adhesives used in the study were two-part epoxy systems consisting of the resin and hardener.

4.3 BULK ADHESIVE SPECIMEN FABRICATION.

All three adhesives were tested in bulk form to obtain the mechanical properties for finite element analysis and for comparison with the in situ properties. To mix the large quantities of adhesive necessary for the bulk adhesive specimens without introducing air bubbles or voids, the two adhesive components were degassed during mixing. Degassing was accomplished by mixing the two components with a motorized stirrer inside a glass bell jar that was under vacuum. The bell jar setup is shown in figure 82.

After the adhesive was mixed and degassed, it was transferred into aluminum molds for casting into square sheets. The removable top and bottom of the mold were pressed together during curing to form an adhesive sheet of uniform thickness of 4.76 mm (0.1875 in.). The mold was pre-treated with polytetraflouroethylene (PTFE) release agent and had a 3° draft angle on the sides to help in extracting the cured adhesive from the cavity. The adhesive was cured at room temperature for a minimum of 7 days before further fabrication.

Once the adhesive was fully cured, it was cut into the desired shapes. First, the square sheets were rough cut with a band saw. Next, they were machined with a Bridgeport CNC end mill to the dimensions specified in ASTM D 638 [25], as shown in figure 83.

Figure 82. Vacuum Bell Jar for Adhesive Mixing and Degassing

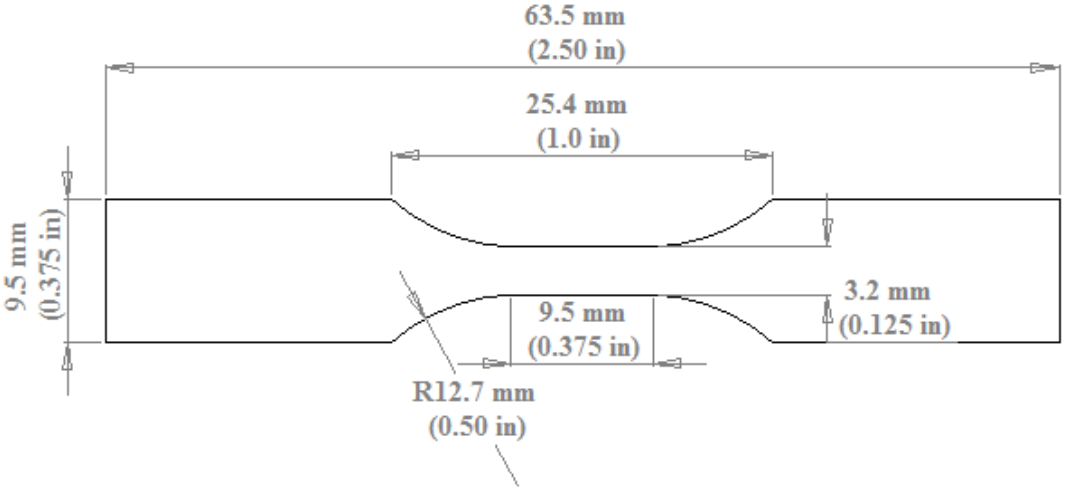

Figure 83. Dimensions for Bulk Adhesive Tensile Specimens

The adhesive sheets used for the Iosipescu specimens were cut into 76-mm by 19-mm (3.0-in. by 0.75-in.) rectangles. The opposing V-notches were later cut into the Iosipescu specimens with a surface grinder using a grinding wheel shaped to a 90° angle. Additionally, Iosipescu specimens with a notch angle of 120° were also fabricated with the primary adhesive for comparison with the bonded Iosipescu specimens that also had a 120° notch angle. This different notch angle was also cut using a surface grinder, but with a grinding wheel shaped to a 120° angle. Figure 84 shows the uncut bulk adhesive casting along with finished Iosipescu specimens cut with 120° and 90° notch angles, respectively.

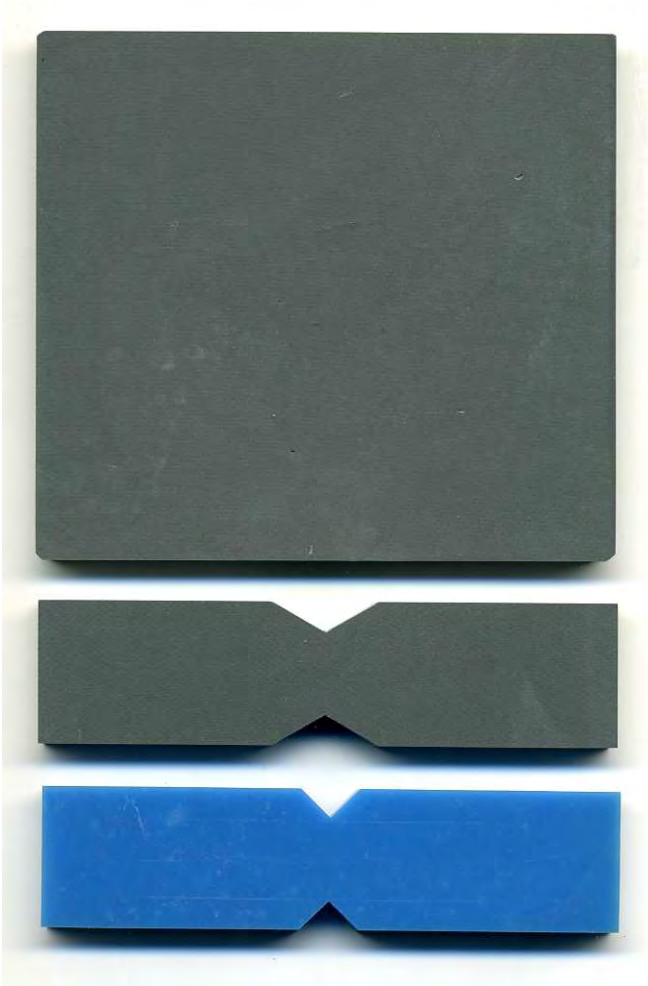

Figure 84. Bulk Adhesive Iosipescu Specimens: Uncut Casting and Finished Specimens With 120° and 90° Notches, Respectively

4.4 BONDED IOSIPESCU SPECIMEN FABRICATION.

In situ shear tests were accomplished by using a modification of the Iosipescu specimen (ASTM D 5379). The specimen was comprised of aluminum adherends bonded together between the notches to form a complete Iosipescu specimen. Specimens were fabricated with three different bondline thickness of 0.254 mm (0.01 in.), 1.27 mm (0.05 in.), and 2.54 mm (0.10 in.). All specimens featured a 120° notch angle since this angle was determined to be the optimal configuration using finite element analysis.

The aluminum adherends were CNC machined from 4.76-mm (0.1875-in) -thick 6061-T6 plate. To accommodate the three different bondline thicknesses, the length of the aluminum halves varied to maintain an overall specimen length of 76 mm (3.0 in.). The dimensions of the adherends are shown in figure 85. The dimensions of the bonding surface varied for each bondline thickness. This was necessary to maintain consistent overall specimen dimensions because the notch extended into the adhesive. The pertinent dimensions that remained constant regardless of bond length were the length of 76.2 mm (3.0 in.), the overall height of 19.1 mm (0.75 mm), the NDR of 0.20, and the notch angle of 120° (figure 86). Two holes were drilled in each specimen half to provide a means for securing each piece during the milling process. These holes were assumed to have no significant effect on the adhesive since they were located sufficiently far away from the bondline.

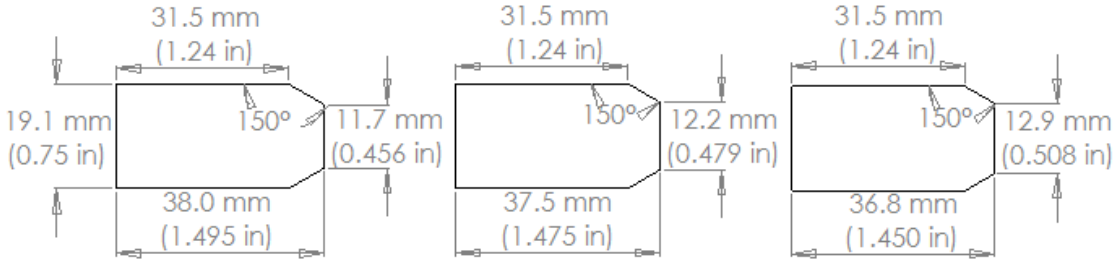

(a) (b) (c)

Figure 85. Aluminum Adherend Dimensions for Bonded Iosipescu Specimens With Bondline Thicknesses of (a) 0.254 mm (0.01 in.), (b) 1.27 mm (0.05 in.), and (c) 2.54 mm (0.10 in.)

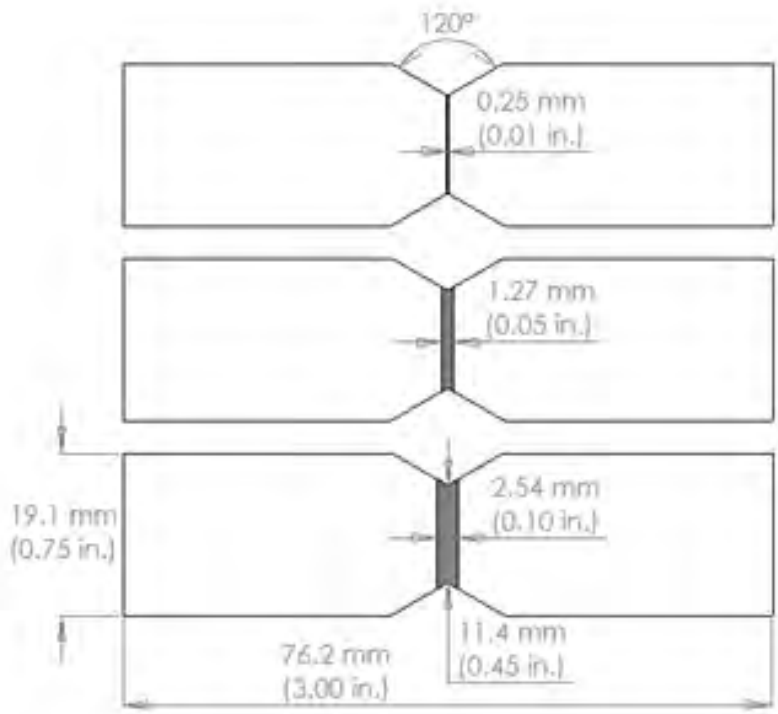

Figure 86. Bonded Iosipescu Specimen Dimensions

4.4.1 Aluminum Surface Preparation.

One of the challenges to testing adhesives with aluminum adherends is the issue of properly treating the aluminum surface so that the adhesive will form a high-strength bond. The purpose of the surface treatment was to remove the existing oxide layer from the aluminum. Initial surface treatments consisted of mechanical abrasion using sandpaper, wire brushes, and grit blasting. These treatments were found to be unsatisfactory, as the specimen consistently failed by adhesion, with the adhesive separating from the aluminum. To achieve a cohesive failure in the bondline, a chemical surface treatment was used.

Prior to adhesive bonding, all aluminum adherends were anodized with phosphoric acid according to ASTM D 3933 [27]. The anodizing process consisted of wiping all surfaces with acetone to remove any dirt, grease, fingerprints, etc. The aluminum pieces were then affixed to an aluminum anodizing rack to facilitate transfer of the pieces from one solution to the next and also to prevent any unnecessary handling of the pieces. The specimens were attached to the rack by 12-gauge aluminum wires and nylon screws (no metal other than aluminum was used to prevent any galvanic effects). The anodizing procedure consisted of several chemical solution baths and rinse tanks, as shown in figure 87). The initial anodizing step consisted of submerging the aluminum pieces for 20-25 minutes in a solution of water and lye that serviced as both an alkaline cleaner and a deoxidizer to remove any existing oxide layers. The aluminum pieces were then rinsed with tap water and placed in a bath of 30% nitric acid for 2-3 minutes to remove

any material, such as silicon, that was left on the surface during the deoxidizing. Again, the pieces were rinsed with clean water before being placed in the anodizing tank. The anodizing tank contained a solution of 7% phosphoric acid that was agitated by an air bubbler. The aluminum rack with the affixed pieces was then put into the solution and attached to a direct current (dc) power supply that maintained a potential of 10V between the pieces and two aluminum cathodes also in the solution. After 20-25 minutes in the anodizing tank, the pieces were moved into the final rinse tank of deionized water. After the final rinse, the pieces were air dried and bonded within 48 hours.

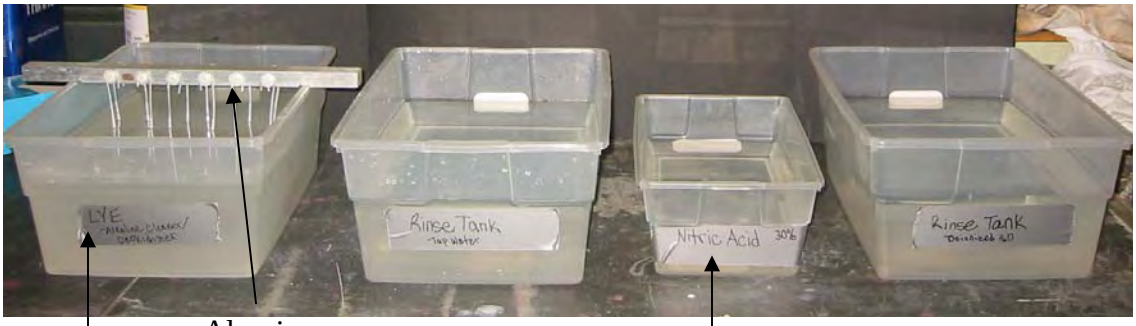

Deoxidizer Aluminum Rack Bath

(a)

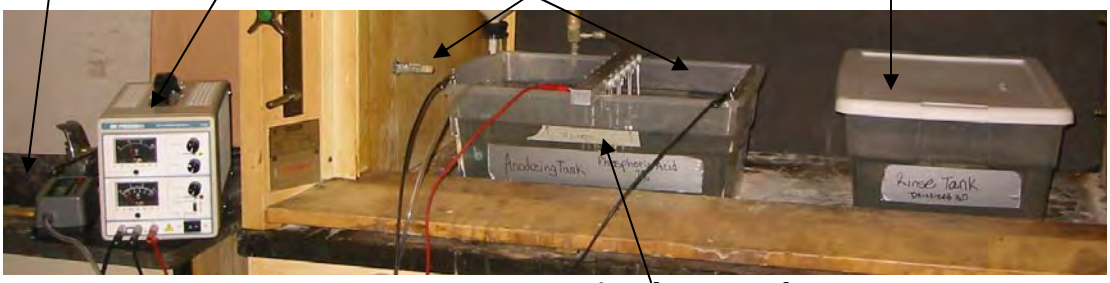

Anodizing Tank

(b)

Figure 87. Anodizing Line Setup Consisting of (a) Alkaline Cleaner/Deoxidizer, Nitric Acid Bath and (b) Phosphoric Anodizing and Water Rinse Tanks

4.4.2 Bonding Procedures.

After the aluminum adherends were anodized, they were adhesively bonded using one of the three adhesives described previously. A bonding fixture was constructed to facilitate consistent bondline thickness and to allow for variation between the three prescribed bondline thicknesses. As shown in figure 88, the bonding fixture allowed for up to six specimens to be bonded simultaneously. The fixture consisted of a flat plate with dividers (A) to separate the specimens and to ensure that the two adherends were properly aligned. Bondline thickness was controlled by using shims of the desired thicknesses. Before the adherends were anodized, they were placed in the bonding fixture and separated by the correct shim size with one adherend pressed firmly against the backstop (B). The end marker (C) was placed against the free end of the

specimen and secured. Next, the length marker (D) was positioned against the end marker and secured. Once the length marker was in place, the specimen and other fixture pieces were removed for anodizing. After anodizing, all specimen and fixture pieces were returned to their proper locations identified by corresponding labels on the specimen and fixture. The top adherend was located by placing it against the backstop (B). A small amount of adhesive was put into place between the adherends, and the bottom adherend was pushed towards the top adherend, stopping when the end of the adherend was aligned with the length marker. Finally, the dividers were pushed together to ensure that the adherends of each specimen were collinear. The adhesive was then cured for at least 7 days at room temperature.

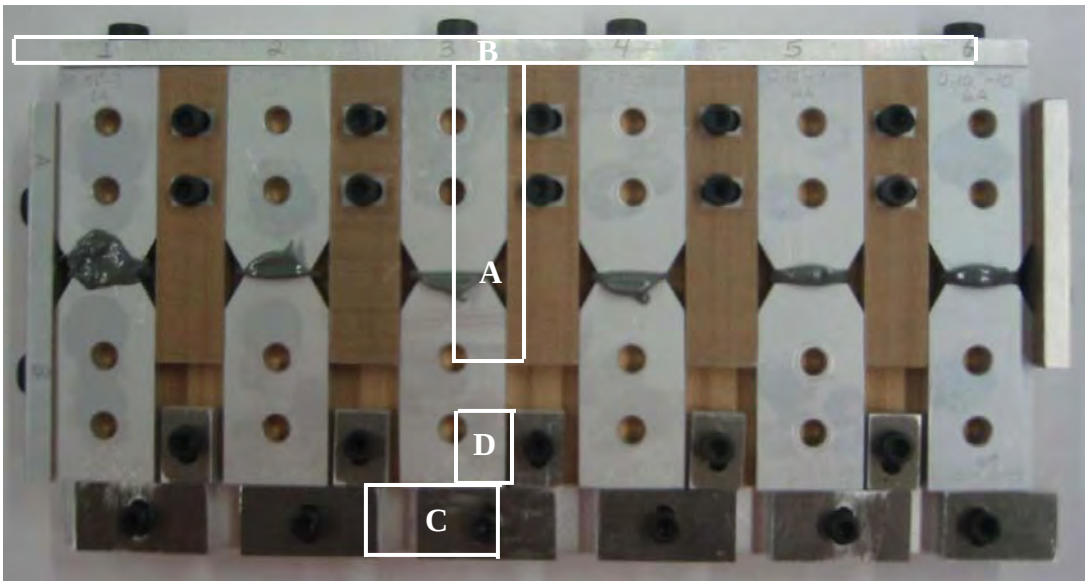

Figure 88. Bonding Fixture With Iosipescu Specimens

Adhesive application was performed using a static mixing device for the primary adhesive, EA 9394. The static mixer consisted of the two adhesive components in a prepackaged dual cartridge (Hysol EA 9394 50 mL Sempak). A mixing nozzle was attached to the cartridge which was subsequently loaded into the dispensing gun, as shown in figure 89(a). As the two adhesive components were dispensed through the nozzle, the helical flutes inside the nozzle (figure 89(b)) caused the components to thoroughly mix. The two secondary adhesives were not available from the manufacturer in prepackaged dual cartridges. Therefore, these adhesives were mixed by hand. The reason for not degassing the adhesive used for bonding was that the amount of adhesive needed for bonding was so small that the vacuum mixer was not effective on such small amounts and larger quantities were not used to avoid unnecessary waste.

After cure, the specimens were removed from the fixture by first removing all the dividers and locating pieces. Next, the specimens were lightly tapped until they came loose. All surfaces of the fixture that were in contact with the adhesive were covered with Teflon® release paper and treated with a release agent to facilitate specimen removal from the bonding fixture.

(a)

(b)

Figure 89. Static Mixer: (a) Fully Assembled Dispensing Gun and (b) Close-Up of Fluted Nozzle

4.4.3 Removal of Adhesive Flash.

The final step in fabricating the bonded Iosipescu specimens was the removal of the adhesive flash or squeeze-out. This was accomplished by using a surface grinder with a flat grinding wheel to remove the hardened adhesive from the front of the specimen. The adhesive in the notches was then removed by using a grinding wheel shaped to an angle of 120°. In order to not damage the aluminum adjacent to the adhesive layer, the grinding was stopped just short of the aluminum surface, and the thin layer of remaining adhesive was removed by medium-grit sandpaper.

4.5 BUTT TENSILE SPECIMEN FABRICATION.

In situ tensile tests were performed using butt tensile specimens. Specimens were fabricated according to ASTM D 2094. The adherends were cut from 12.7- by 12.7-mm (0.50- by 0.50-in.)-square 6061-T6 aluminum bar stock. Each adherend was initially rough cut with a band saw and then machined with an end mill to the final length of 38.1 mm (1.50 in.). A 4.76-mm (0.1875-in.)-diameter through hole was drilled in each adherend for loading purposes. The butt tensile adherend dimensions are shown in figure 90.

The aluminum adherends were anodized using the same procedure followed for the bonded Iosipescu specimens. The butt tensile specimens were fabricated with bondline thicknesses of

0.25 mm (0.01 in.), 1.27 mm (0.05 in.), and 2.54 mm (0.10 in.). Only the primary adhesive, EA 9394, was used for the butt tensile tests and thus all adhesive was dispensed using a static mixer. The adhesive flash was removed from the specimens by first using a band saw to cut away the majority of the hardened adhesive and then using medium-grit sandpaper to smooth away the remaining adhesive. The final specimens with varying bondline thickness are shown in figure 91.

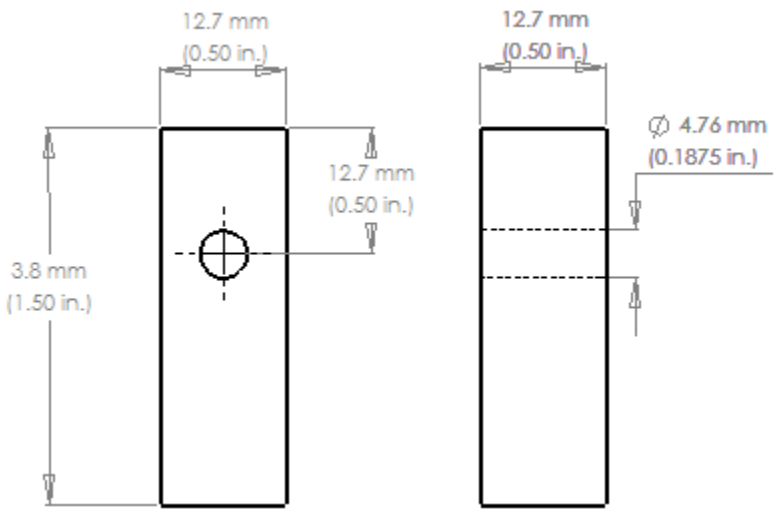

Figure 90. Butt Tensile Adherend Dimensions

Figure 91. Butt Tensile Specimens With Three Adhesive Bondline Thicknesses

4.6 IOSIPESCU TESTING METHODS.

Shear response for both bulk and in situ adhesives was evaluated using the Isosipescu shear test. Tests were performed using a computer-controlled Instron 4303 load frame, equipped with a 25kN Instron tension compression load cell. All Iosipescu shear tests were performed at room temperature.

4.6.1 Bulk Iosipescu Tests.

The fixture and specimen setup for the bulk adhesive Iosipescu tests are shown in figure 92. Iosipescu strain gages (Measurements Group, Inc., N2P-08-C032A-500) were centered between the specimen notches on both the front and back of the specimen to monitor any twisting of the specimen. A National Instruments multichannel SCXI-1000 data acquisition system attached to a Pentium® computer provided data acquisition.

The specimen was loaded into the test fixture, centered with the notch alignment tool, and the two adjustment screws were finger tightened. The specimen was loaded at a constant rate of 1.3 mm/min (0.05 in./min) until the load dropped below 220 N (50 pound force (lbf)) or the fixture bottomed out.

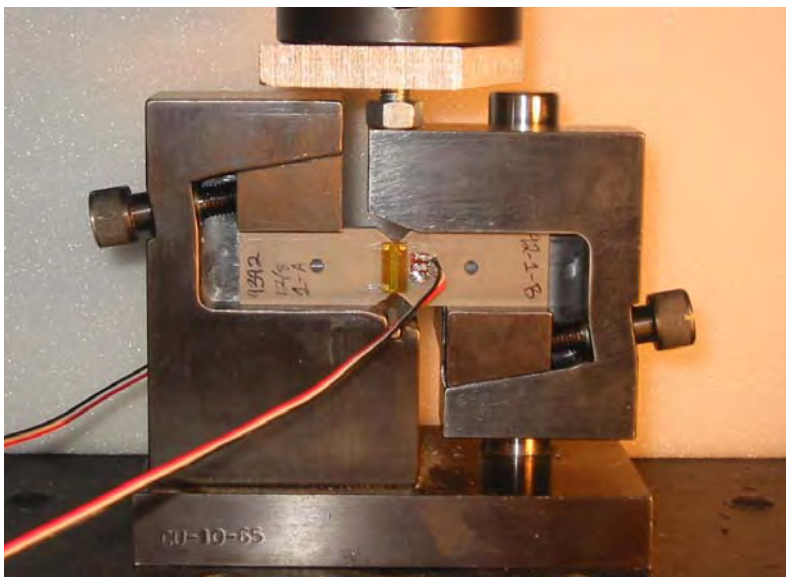

Figure 92. Bulk Adhesive Iosipescu Test Setup

Due to the relatively low modulus of the three structural adhesives, it was necessary to correct for any reinforcement effects from the bonded strain gages. Using a simplified model of the adhesive and strain gage aggregate specimen, a correction was developed for the Iosipescu shear specimens. The correction assumes that the entire strain gage and the strain gage adhesive (M-Bond 200) act as a single stiffening element with an effective stiffness and that the strain gages create a global reinforcement effect such that the strain gage influences the strain field in the entire cross-section [28].

The strain gage correction for the Iosipescu shear specimen assumes that two strain gages are bonded to the specimen (front and back) and that the gages cover the specimen from notch to notch. The assumption of constant strain between the gages and the specimen is made. The effective shear stiffness, K, is defined as

$$K = \frac{G \times A}{L} \tag{8}$$

where G is the shear modulus, A is the cross-sectional area, and L is the length between the notches. Since the cross-sectional area is the product of the length, L, and the specimen thickness, t, the stiffness reduces to

$$K = G \times t \tag{9}$$

The measured stiffness, K_m, is the combination of the specimen stiffness, K_s, and the strain gage stiffness, K_g, as

$$K_m = K_s + 2K_g \tag{10}$$

where both strain gages have been accounted for. Substituting equation 9 into equation 10 gives

$$G_m t_m = G_s t_s + 2G_g t_g \tag{11}$$

Realizing that the measured thickness, t_m, is the same as the specimen thickness, t_s, equation 11 is rearranged to solve for the specimen modulus, G_s, as

$$G_s = G_m - 2G_g \left(\frac{t_g}{t_s} \right) \tag{12}$$

When correcting for the strain gage stiffening effect, the effective strain gage thickness, t_g, was 0.053 mm (0.0021 in.), the strain gage shear modulus was 1.93 GPa (280 ksi), and the nominal specimen thickness, t_s, was 4.76 mm (0.1875 in.). On average, the strain gages were found to increase the measured shear modulus by approximately 2.5 percent.

4.6.2 Bonded Iosipescu Tests.

The bonded Iosipescu specimens were tested in a similar manner to the bulk adhesive Iosipescu specimens, except no strain gages were used (see figure 93). Due to the thin bondlines, it was not possible to attach a strain gage to obtain the shear strain in the adhesive layer. Therefore, the data collected from these tests was limited to applied load and cross-head displacement. Data was collected with Instron® series IX software on a Pentium computer. All other test parameters were identical to those used in the bulk adhesive Iosipescu tests.

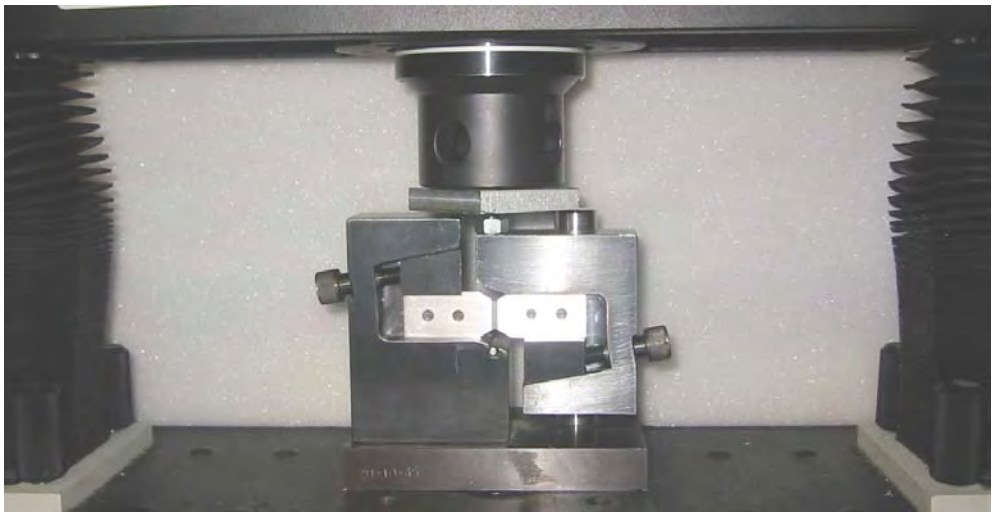

Figure 93. Bonded Iosipescu Test Setup

4.7 TENSILE TEST METHODS.

Tensile tests were performed with the primary adhesive (EA 9394) using both bulk adhesive and in situ specimens. The tests were performed on the same load frame as the shear tests under the same ambient conditions.

4.7.1 Bulk Adhesive Tensile Tests.

Since there is no ASTM standard for testing bulk adhesives, tensile tests were performed following the procedure specified in ASTM D 638 for tensile properties of plastics. The specimen dimensions are shown in figure 83. Strain gages (Measurements Group, Inc., EA-06-031CE-350) were applied to all four sides of the rectangular gage section to measure both axial and transverse strain (two axial and two transverse gages per specimen). Placing strain gages on opposing sides of the specimen allowed for monitoring of any specimen twisting during the test. Also, measuring transverse strain allowed for calculation of Poisson's ratio.

After the strain gages were applied, the specimen was loaded into the grips. Tests were performed using the same Instron load frame and National Instruments data acquisition system used for the shear tests. The specimen was loaded at a constant cross-head displacement rate of 1.3 mm/min (0.05 in./min) until fracture. The bulk adhesive tensile test setup is shown in figure 94(a).

4.7.2 Butt Tensile Tests.

Butt tensile tests were performed according to ASTM D 2095. The butt tensile specimens were pin-loaded with the top and bottom pins perpendicular to each other, as shown in figure 94(b). Tests were performed on an Instron load frame and data acquisition included data from cross-head displacement and applied load. The loading rate was a constant 1.3 mm/min (0.05 in./min) applied until fracture.

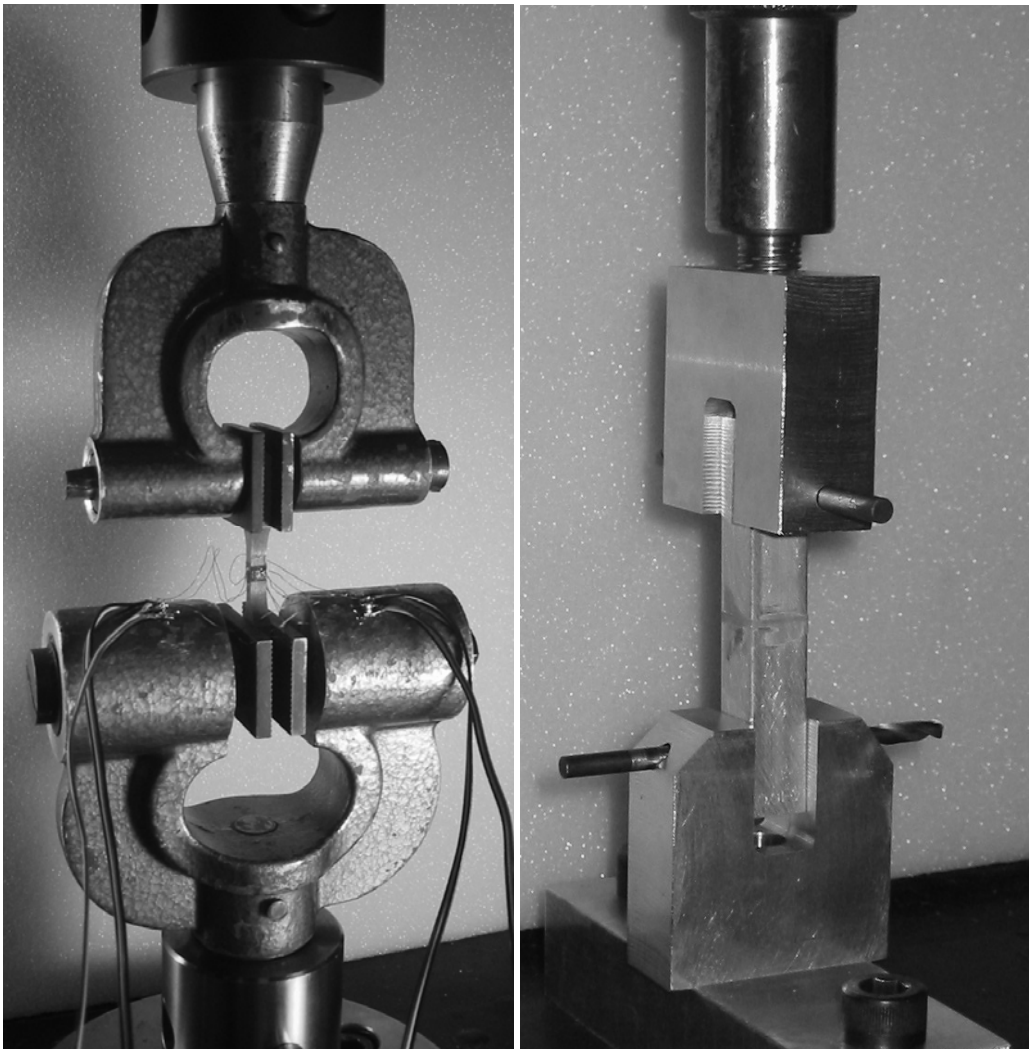

(a) (b)

Figure 94. Tensile Test Setups for (a) Bulk Adhesive and (b) Butt Tensile Specimens

Due to the relatively low modulus of the adhesive, the strain gages had a stiffening effect as described previously in regard to the bulk adhesive shear tests. The correction for tensile modulus follows the same logic as for the shear modulus correction except that the tensile test employs four strain gages, one on each side of the test specimen. The effective tensile stiffness, K, is defined as

$$K = \frac{EA}{L} \tag{13}$$

where E is the tensile modulus, A is the cross-sectional area, and L is the length of the strain gages. The measured stiffness, K_m, is the sum of the stiffnesses of the five individual components as

$$K_m = K_s + 2K_a + 2K_t \tag{14}$$

where the subscripts *s*, *a*, and *t* refer to the specimen, axial strain gage, and transverse strain gage, respectively. Substituting equation 13 into equation 14 gives

$$\frac{E_m A_m}{L_m} = \frac{E_s A_s}{L_s} + 2\frac{E_a A_a}{L_a} + 2\frac{E_t A_t}{L_t} \tag{15}$$

where the subscript *m* refers to measured values. Realizing that the measured area, A_m, is equal to the specimen area, A_s,, and also that the measured length, L_m, is equal to both the length of the axial strain gage, L_a, and the length of the specimen gage section, L_s, equation 15 is rearranged to solve for the specimen tensile modulus, E_s, as

$$E_s = E_m - 2E_a\left(\frac{A_a}{A_s}\right) - 2E_t\left(\frac{A_t}{A_s}\right)\left(\frac{L_a}{L_t}\right) \tag{16}$$

When correcting for the strain gage stiffening effect, the axial length of the strain gage, L_a, was 1.930 mm (0.076 in.); the transverse length of the strain gage, L_t, was 1.575 mm (0.062 in.); the effective thickness of the strain gages was 0.038 mm (0.0015 in.); and the nominal area of the specimen was 15.1 mm^2 (0.02 $in.^2$). The tensile modulus of the strain gage was 5.17 GPa (750 ksi) and Poisson's ratio of the strain gage was 0.33. For the bulk adhesive tensile specimens, the strain gage stiffening effect increased the tensile modulus by approximately 2 percent.

4.8 MOIRÉ INTERFEROMETRY.

High sensitivity moiré interferometry was used to measure the actual displacements in the adhesive bondline under applied load. Shear tests were performed with the bonded Iosipescu specimens and the thick adherend lap joint specimens, with bondline thicknesses of 0.25 mm (0.01 in.), 1.27 mm (0.05 in.), and 2.54 mm (0.10 in.) for both configurations.

4.8.1 Moiré Interferometry Background.

Moiré interferometry is an optical technique that produces whole-field contour maps of in-plane displacement components, U and V. A comprehensive treatment of the method is given by Post, Han, and Ifju [29]. Briefly, the test procedure consists of replicating a high-frequency, crossed-line diffraction grating on the specimen surface. In these experiments, the gratings had a frequency of 1200 lines/mm (30,480 lines/in.). The gratings were bonded to the specimen surface using an epoxy resin, PC-10C, manufactured by Measurements Group, Inc. Once bonded, the grating deformed together with the specimen surface.

The specimen grating was illuminated using a four-beam compact moiré interferometer [29]. The light originated from a 50 mW helium neon laser with a wavelength of 632.8 nm and was delivered to the interferometer through an optical fiber. By means of a series of mirrors and the interferometer's diffraction grating, the light was separated into four beams. The beams of light interacted with each other to form a virtual reference grating that in turn interacted with the specimen grating to form two interference patterns, denoted as N_x and N_y. A digital camera

connected to a desktop computer recorded still images of the interference patterns. The frequency of the of the virtual reference grating, f, is related to the frequency of the specimen grating, f_s, by the relationship

$$f = 2*f_s \tag{17}$$

The virtual reference grating frequency was therefore 2400 lines/mm (60960 lines/in.) and the sensitivity was $1/f$, or 0.417 μm (16.4 μin.) per fringe order.

4.8.2 Moiré Test Setup.

The compact moiré interferometer was configured on a vibrationally damped optical table. Since all interferometry was performed on the optical table, it was not possible to use a traditional load frame, thus, alternative loading mechanisms were devised. Loading for the Iosipescu specimens was accomplished by a stiff screw-type mechanism that could apply and hold a fixed displacement to the Iosipescu test fixture, as shown in figure 95. Included in the load train were a 4500 N (1000 lbf) force transducer attached to a Vishay Instruments Division P-3500 strain indicator to monitor applied force and a lubricated ball bearing to prevent rotation from the screw from entering the test fixture.

Loading the thick adherend lap joint specimens was accomplished by a similar screw-type mechanism that could apply a tensile force. Loading pins were inserted into the holes in the ends of the specimens. One of the loading pins was secured to the table and the other was attached to two eye bolts that could be retracted upward by tightening the bolts on top of the load frame crossbar (see figure 96). Each end of the top loading pin could be independently raised or lowered to allow for adjustment in any specimen rotation. The load cell was not incorporated into the loading apparatus for the lap joint specimens.

The complete moiré interferometry setup is shown in figure 97. The digital camera used in the test was a 12-bit Dalsa 1M30P, 1 megapixel by 1 megapixel resolution CCD camera. The camera was connected to the computer by a National Instruments image acquisition board. A field lens was placed between the interferometer and the camera to better focus the emerging fringe patterns.

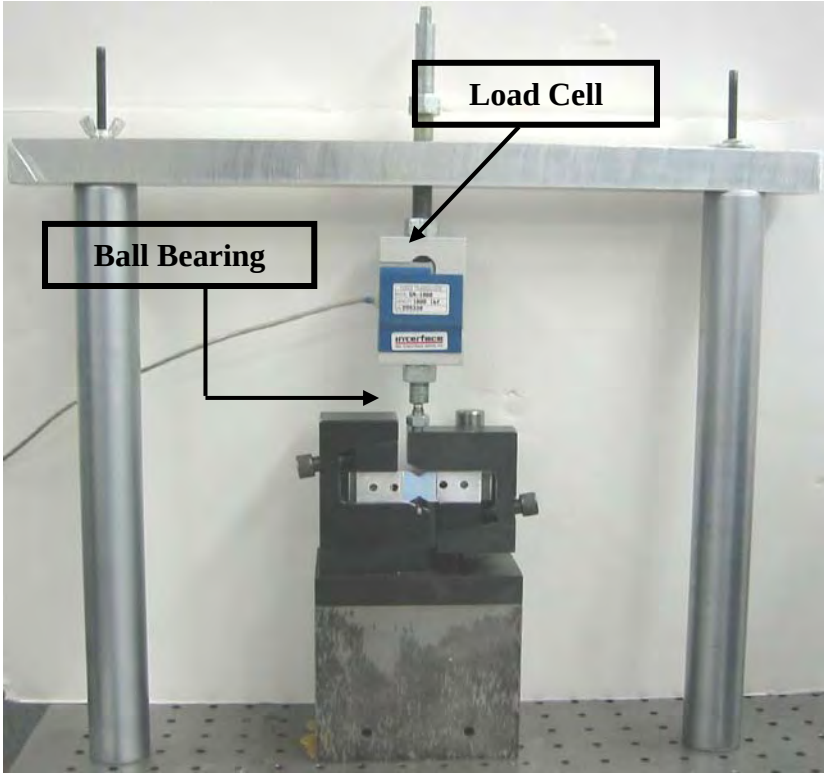

Figure 95. Loading Setup for Bonded Iosipescu Moiré Interferometry

Figure 96. Loading Setup for Thick Adherend Lap Joint Moiré Interferometry

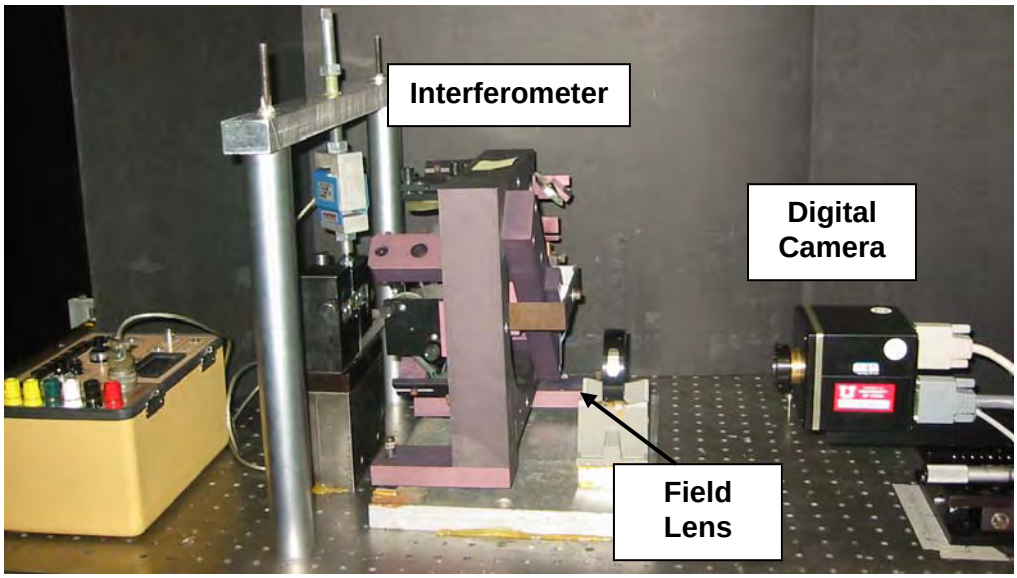

Figure 97. Complete Setup for Moiré Interferometry

5. RESULTS OF EXPERIMENTAL TESTS.

5.1 INTRODUCTION.

Shear and tensile tests were performed on bulk adhesive specimens and in situ bonded specimens according to the procedures described in section 4. The primary focus of these tests was to determine how the adhesive shear and tensile strengths varied with bondline thickness and between bulk and thin bondline forms. Shear tests were performed using three aerospace-grade epoxies (Loctite EA 9394, EA 9392, and EA 9360), and tensile tests were performed using the primary adhesive (Loctite EA 9394). Additionally, moiré interferometry was used to evaluate the strain throughout the adhesive bondlines. The results from each test are presented in the following sections.

5.2 RESULTS OF BULK ADHESIVE IOSIPESCU SHEAR TESTS.

Shear testing of the adhesives was first performed with bulk adhesive Iosipescu specimens. Bulk adhesive shear tests produced the shear stress-shear strain response for all three adhesives used. Strain values reported were the average value of the front and back strain gages and stress was calculated as the applied load, *P*, divided by the cross-sectional area, *A*, or

$$\sigma = P/A \tag{18}$$

The shear modulus of elasticity, *G*, was calculated according to ASTM D 5379 as the slope of the stress-strain curve between 1500 and 5500 με. The equation for the shear modulus calculation is

$$G = \Delta\tau / \Delta\gamma \tag{19}$$

where Δτ is the change in shear stress and Δγ is the change in shear strain. Note that the correction due to strain gage reinforcement (section 4.6.1) was used in obtaining shear modulus.

Typical shear stress-shear strain curves from bulk adhesive shear testing of the three adhesives are shown in figure 98. The primary adhesive, EA 9394, had a significantly higher apparent shear strength and shear modulus whereas the other two adhesives had larger amounts of plastic deformation before failure. The EA 9360 specimens did not fracture during the test, and thus, the tests ended when the fixture bottomed-out. Table 5 provides a summary of the apparent shear strength and shear modulus from bulk adhesive shear testing of all three adhesives. A total of 10 specimens were tested from the EA 9394 adhesive and 6 specimens from each of the EA 9392 and EA 9360 adhesives.

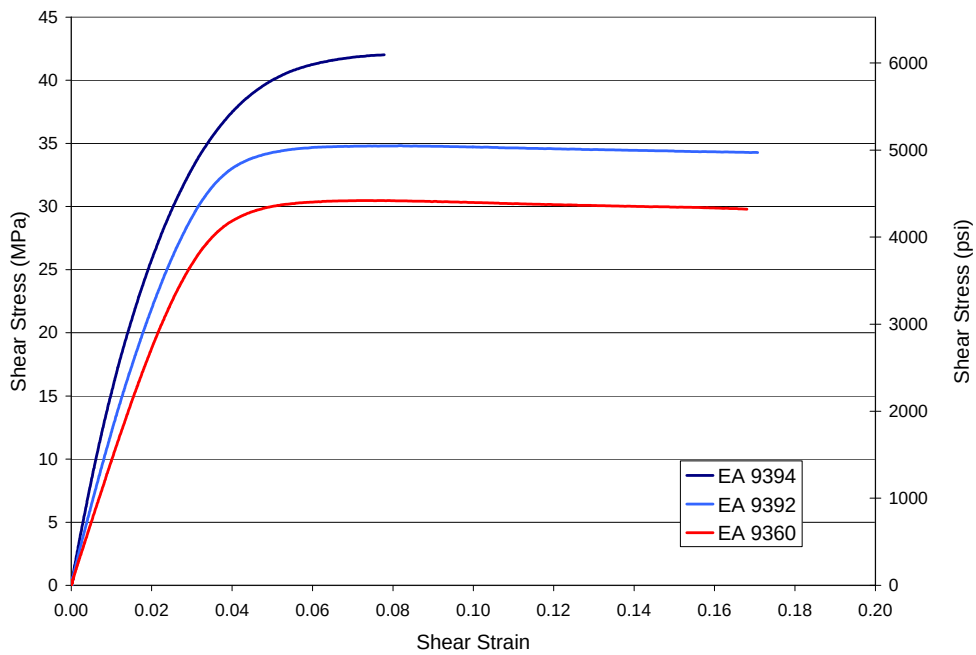

Figure 98. Characteristic Shear Stress-Shear Strain Curves for Three Adhesives

Table 5. Summary Results for Bulk Adhesive Iosipescu Tests

EA 9394			
		Apparent Shear Strength	Shear Modulus
Average	MPa	41.4	1578
	ksi	6000	229
s	MPa	1.3	45.5
	ksi	184	7
COV	%	3.1	2.9

EA 9392			
		Apparent Shear Strength	Shear Modulus
Average	MPa	34.3	1164
	ksi	4969	169
s	MPa	0.7	20.7
	ksi	99	3
COV	%	2.0	1.8

EA 9360			
		Apparent Shear Strength	Shear Modulus
Average	MPa	30.4	950
	ksi	4415	138
s	MPa	1.0	25.7
	ksi	139	4
COV	%	3.1	2.7

s = standard deviation
COV = coefficient of variation

Failure mechanisms in the bulk Iosipescu specimens for all three adhesives were very similar. For each adhesive, failure initiated near the notch tip along the notch flank, occurring asymmetrically in both the top and bottom notches. The failure then propagated perpendicular to the notch flank. For the EA 9394 and EA 9392 adhesives, the specimens fractured into three pieces. For the EA 9360 adhesive, which was much more ductile, cracks initiated in the same locations as the other adhesives but the specimens did not fracture and continued to deform until the fixture bottomed-out. Characteristic specimen failures are shown in figure 99.

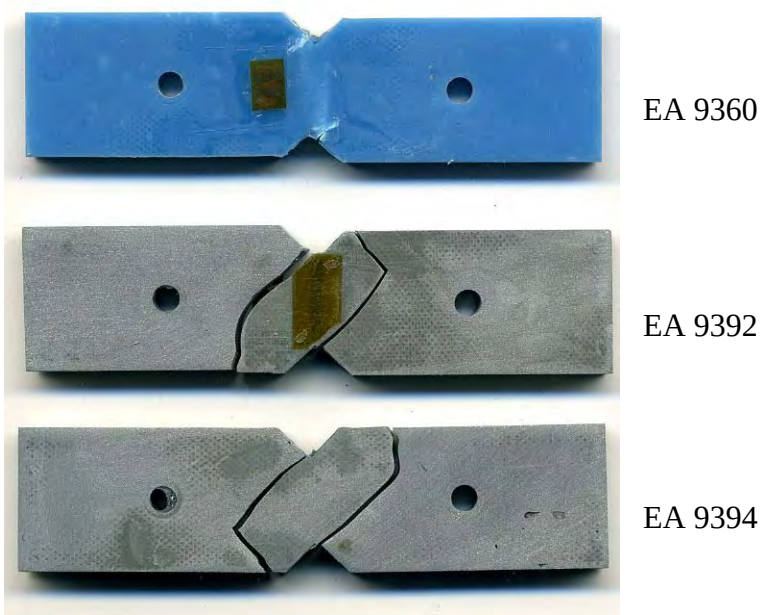

Figure 99. Characteristic Failures of Bulk Iosipescu Specimens for all Three Adhesives

5.3 RESULTS OF BONDED IOSIPESCU SPECIMENS.

The bonded Iosipescu specimen was used to determine the effect of bondline thickness on adhesive shear strength. The results of the bonded Iosipescu shear tests are plotted in figures 100, 101, and 102 for the EA 9394, EA 9392, and EA 9360 adhesives, respectively. For all three adhesives, the general trend observed was a decrease in the apparent shear strength as the bondline thickness increased, although these changes were not very dramatic. The apparent shear strength data from the bulk adhesive specimens is also included in the plots and gives very similar results within the scatter of the data.

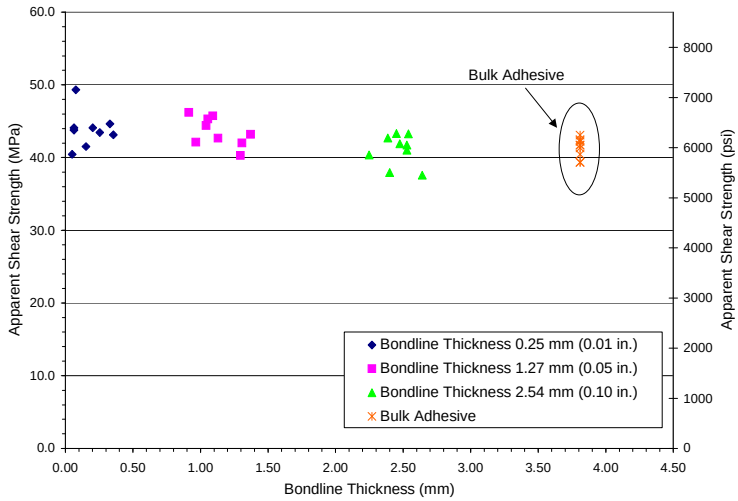

Figure 100. Apparent Shear Strength Versus Bondline Thickness for EA 9394

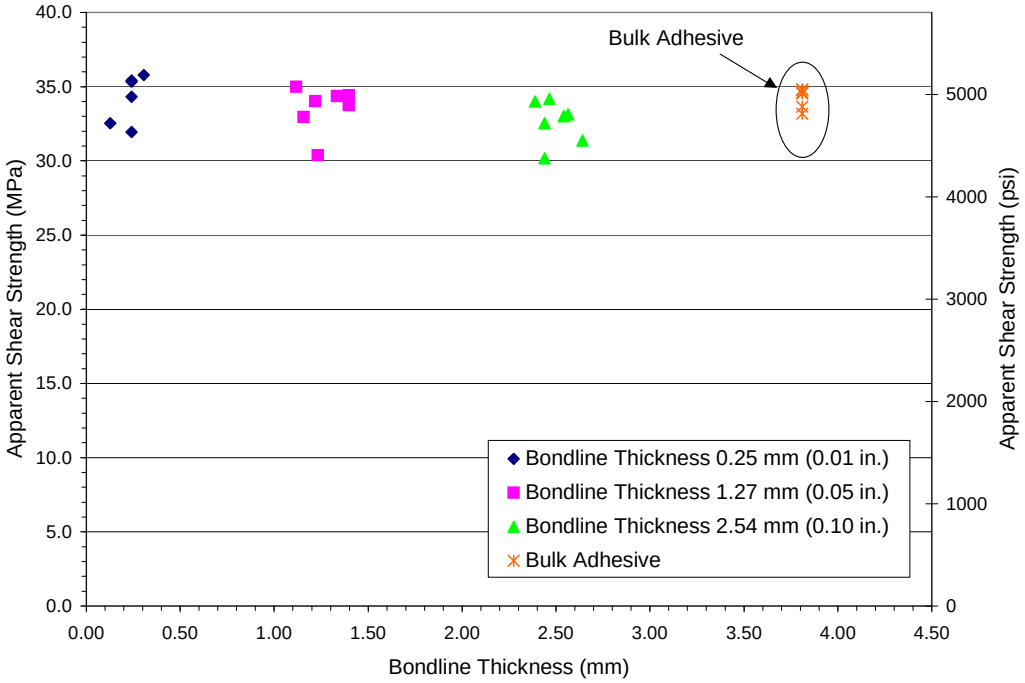

Figure 101. Apparent Shear Strength Versus Bondline Thickness for EA 9392

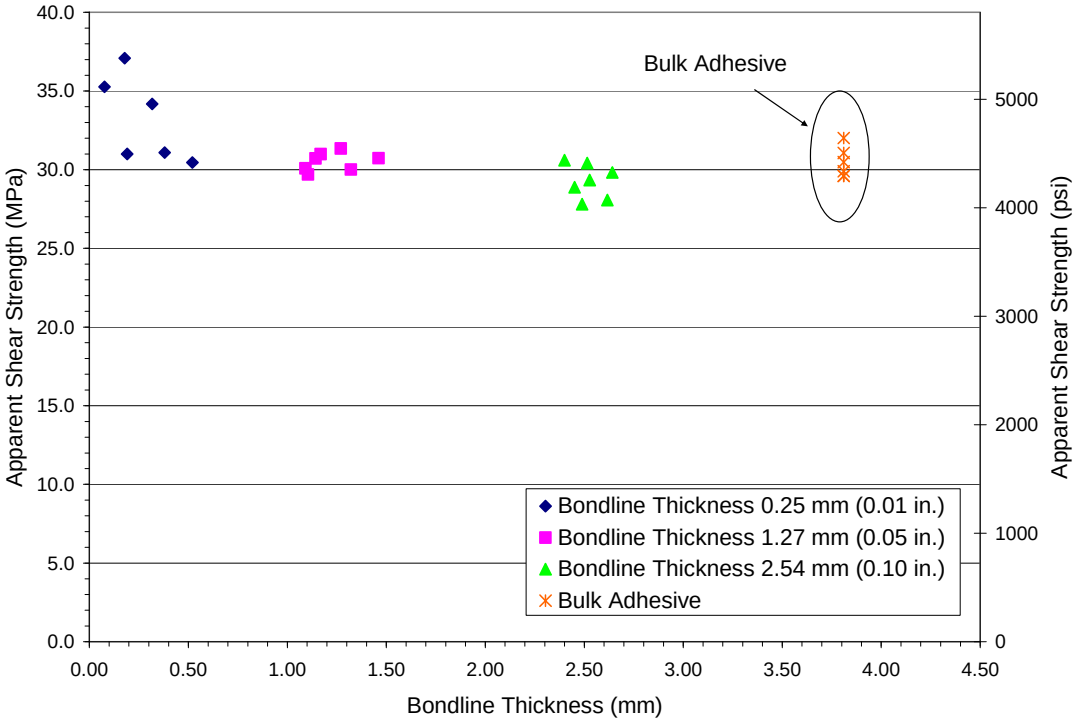

Figure 102. Apparent Shear Strength Versus Bondline Thickness for EA 9360

A summary of the bonded Iosipescu shear strength data from the previous plots is presented in tables 6-8, for EA 9394, EA 9392, and EA 9360 adhesives, respectively. For the primary adhesive EA 9394, a total of nine specimens of each bondline thickness were tested. For the other two adhesives, EA 9392 and EA 9360, six specimens with the thin bondline configuration and seven specimens for each of the intermediate and thick bondline configurations were tested. As was shown in figures 100-102, the average apparent shear strength decreases with a thicker bondline, although the change is not large. The change in apparent shear strength between the 0.25-mm (0.01-in.) and 2.54-mm (0.10-in.) bondlines is a decrease of 6%, 5%, and 13% for the EA 9394, EA 9392, and EA 9360 adhesive respectively. The apparent shear strength of the bulk adhesive lies between the thin and thick bondlines for all three adhesives.

Table 6. Summary Results for EA 9394 Bonded Iosipescu Tests

Nominal Bondline Thickness 0.25 mm (0.01 in.)				
	Bondline Thickness		Apparent Shear Strength	
	mm	in	MPa	ksi
Average	0.17	0.007	43.8	6.357
s	0.12	0.005	2.5	0.358
COV	69.4		5.6	

Nominal Bondline Thickness 1.27 mm (0.05 in.)				
	Bondline Thickness		Apparent Shear Strength	
	mm	in	MPa	ksi
Average	1.13	0.045	43.6	6.317
s	0.16	0.006	2.0	0.289
COV	14.2		4.6	

Nominal Bondline Thickness 2.54 mm (0.10 in.)				
	Bondline Thickness		Apparent Shear Strength	
	mm	in	MPa	ksi
Average	2.49	0.098	41.2	5.977
s	0.09	0.003	2.4	0.353
COV	3.6		5.9	

Bulk Adhesive		
	Apparent Shear Strength	
	MPa	ksi
Average	41.4	6.005
s	1.3	0.187
COV	3.1	

s = standard deviation
COV = coefficient of variation

Table 7. Summary Results for EA 9392 Bonded Iosipescu Tests

Nominal Bondline Thickness 0.25 mm (0.01 in.)				
	Bondline Thickness		Apparent Shear Strength	
	mm	in.	MPa	ksi
Average	0.23	0.009	34.2	4.963
s	0.06	0.002	1.6	0.235
COV	24.8		4.7	

Nominal Bondline Thickness 1.27 mm (0.05 in.)				
	Bondline Thickness		Apparent Shear Strength	
	mm	in.	MPa	ksi
Average	1.26	0.050	33.6	4.867
s	0.11	0.004	1.5	0.222
COV	8.9		4.6	

Nominal Bondline Thickness 2.54 mm (0.10 in.)				
	Bondline Thickness		Apparent Shear Strength	
	mm	in.	MPa	ksi
Average	2.50	0.098	32.6	4.733
s	0.09	0.003	1.4	0.207
COV	3.6		4.4	

Bulk Adhesive		
	Apparent Shear Strength	
	MPa	ksi
Average	34.3	4.969
s	0.7	0.099
COV	2.0	

s = standard deviation
COV = coefficient of variation

Table 8. Summary Results for EA 9360 Bonded Iosipescu Tests

Nominal Bondline Thickness 0.25 mm (0.01 in.)				
	Bondline Thickness		Apparent Shear Strength	
	mm	in	MPa	ksi
Average	0.28	0.011	33.2	4.813
s	0.16	0.006	2.7	0.395
COV	58.0		8.2	

Nominal Bondline Thickness 1.27 mm (0.05 in.)				
	Bondline Thickness		Apparent Shear Strength	
	mm	in	MPa	ksi
Average	1.22	0.048	30.5	4.425
s	0.13	0.005	0.6	0.087
COV	11.0		2.0	

Nominal Bondline Thickness 2.54 mm (0.10 in.)				
	Bondline Thickness		Apparent Shear Strength	
	mm	in.	MPa	ksi
Average	2.52	0.099	29.3	4.246
s	0.09	0.003	1.1	0.158
COV	3.4		3.7	

Bulk Adhesive		
	Apparent Shear Strength	
	MPa	ksi
Average	30.4	4.415
s	1.0	0.139
COV	3.1	

s = standard deviation
cov = coefficient of variation

5.4 RESULTS OF BULK ADHESIVE TENSILE TESTS.

Bulk adhesive tensile tests were performed on the primary adhesive EA 9394 to determine the modulus of elasticity, E, and Poisson's ratio, ν. Additionally, these tests were used to determine how the adhesive tensile strength varied with bondline thickness and between bulk and thin bondline forms. Data was collected from two strain gages aligned in the axial direction and two

aligned in the transverse direction (one strain gage on each of the four sides of the specimen). The axial strain, ε_a, and the transverse strain, ε_t, were each obtained by averaging the two opposing gages aligned in the corresponding directions. Figure 103 shows characteristic stress strain curves for both axial and transverse strain in the EA 9394 bulk adhesive tensile specimens.

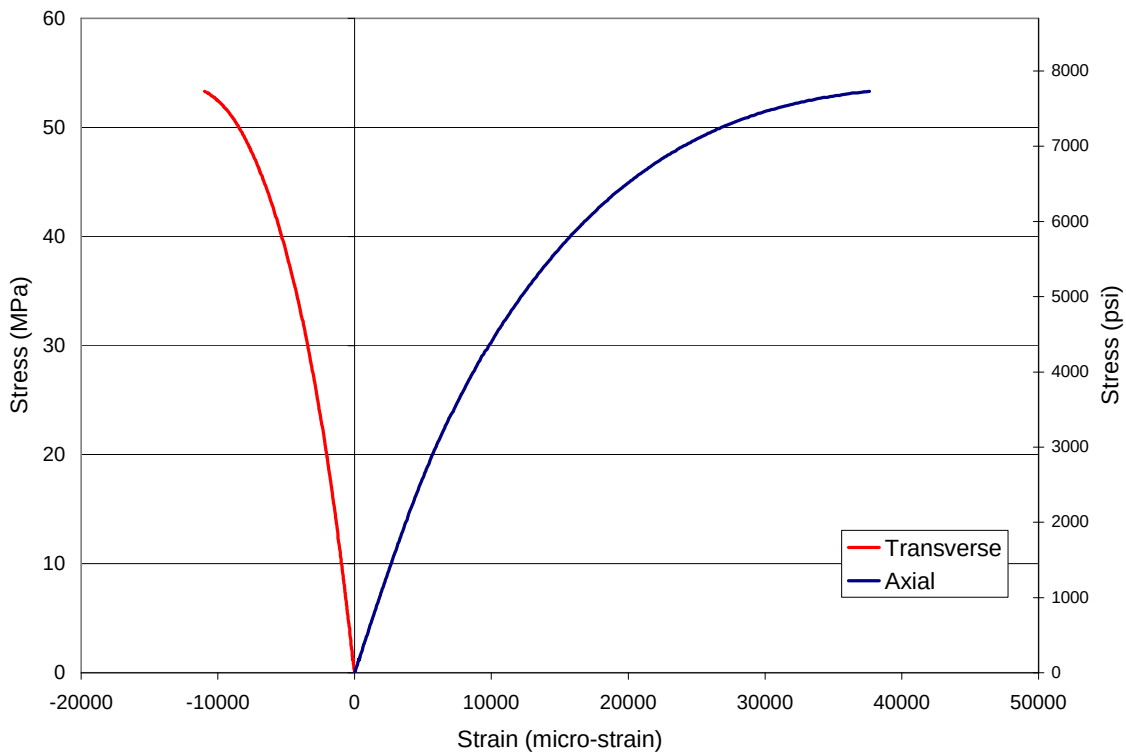

Figure 103. Characteristic Axial and Transverse Stress-Strain Curves for EA 9394

The tensile modulus of elasticity, E, was calculated as the change in stress, $\Delta\sigma$, divided by the corresponding change in axial strain, $\Delta\varepsilon_a$,

$$E = \frac{\Delta\sigma}{\Delta\varepsilon_a} \tag{20}$$

Note that the correction due to strain gage reinforcement (section 4.7.2) was used in obtaining tensile modulus. Poisson's ratio, ν, is defined as the negative ratio of change in transverse strain to the corresponding change in axial strain, or

$$\nu = -\frac{\Delta\varepsilon_t}{\Delta\varepsilon_a} \tag{21}$$

Based on data reduction using the above equations, summary results for the bulk adhesive tensile tests are presented in table 9. A total of six tensile specimens were tested.

Table 9. Summary Results for Bulk Adhesive Tensile Tests

		Apparent Tensile Strength	Tensile Modulus of Elasticity	
Average	MPa	54.6	3814	Poisson's Ratio
	ksi	7.922	553	0.340
s	MPa	2.0	95	0.029
	ksi	0.291	14	
COV	%	3.7	2.5	8.5

s = standard
COV = coefficient of variation

For a linearly elastic isotropic material, the relationship between tensile modulus of elasticity, Poisson's ratio and shear modulus of elasticity is defined as

$$G = \frac{E}{2(1+\nu)} \tag{22}$$

Thus, the shear modulus, *G*, can be calculated based on measured values obtained from bulk adhesive tensile testing. These calculated values can be compared directly to measured values of shear modulus obtained from bulk adhesive shear testing (listed in table 5). Results of this comparison are listed in table 10 for the primary adhesive EA 9394. The shear modulus values calculated from tensile test results using equation 22 are about 10 percent lower than the values obtained from shear tests.

Table 10. Summary Results for Bulk Adhesive Shear Modulus Tests

		Measured Shear Modulus	Calculated Shear Modulus	Percent Difference
Average	MPa	1578	1423	9.8
	Ksi	229	206	
s	MPa	45.5	15.3	
	ksi	7	2	
COV	%	2.9	1.1	

s = standard deviation
COV = coefficient of variation

Typical failures of the bulk adhesive tensile specimens are shown in figure 104. Specimen failure occurred perpendicular to the applied load and in the gage section adjacent to the strain gages. The location of the failure adjacent to the strain gages suggests that the strain gages may have produced a small reinforcing effect to the specimen, and thus, a small stress concentration at the edges where failure occurred.

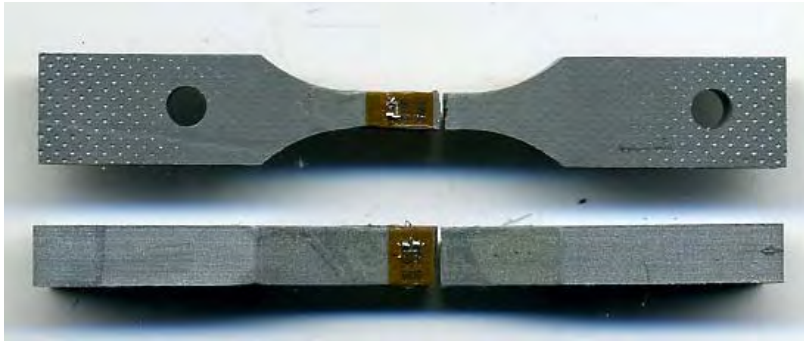

Figure 104. Characteristic Failures of Bulk Adhesive Tensile Specimens

5.5 RESULTS OF BUTT TENSILE TESTS.

Butt tensile tests were conducted using the primary adhesive EA 9394. Aluminum adherends were bonded together to produce bondline thicknesses of 0.25 mm (0.01 in.), 1.27 mm (0.05 in.), and 2.54 mm (0.10 in.). Figure 105 shows the relationship between bondline thickness and apparent tensile strength. These results show that as the bondline thickness increases, the apparent tensile strength decreases. This finding is in agreement with results obtained from the butt tensile finite element analysis that showed the tensile stress throughout the bondline becoming less uniform with greater bondline thicknesses. In fact, results from finite element analysis showed that the thicker bondline specimen had tensile stresses that were significantly higher than the average tensile stress. Therefore, the experimentally obtained change in apparent tensile stress can be explained by the variations in stress distribution throughout the adhesive bondline. Figure 105 also shows the apparent tensile strength of the bulk adhesive tensile specimens. The tensile strength values of the bulk adhesive specimens are between that of the thin and intermediate bondline thicknesses. Table 11 summarizes the results for the adhesive tensile tests. A total of six specimens were tested for each of the three bondline thicknesses.

Failures of butt tensile specimens were relatively consistent, as shown by the characteristic failures of each bondline thickness in figure 106. The failures were almost entirely cohesive for all specimens.

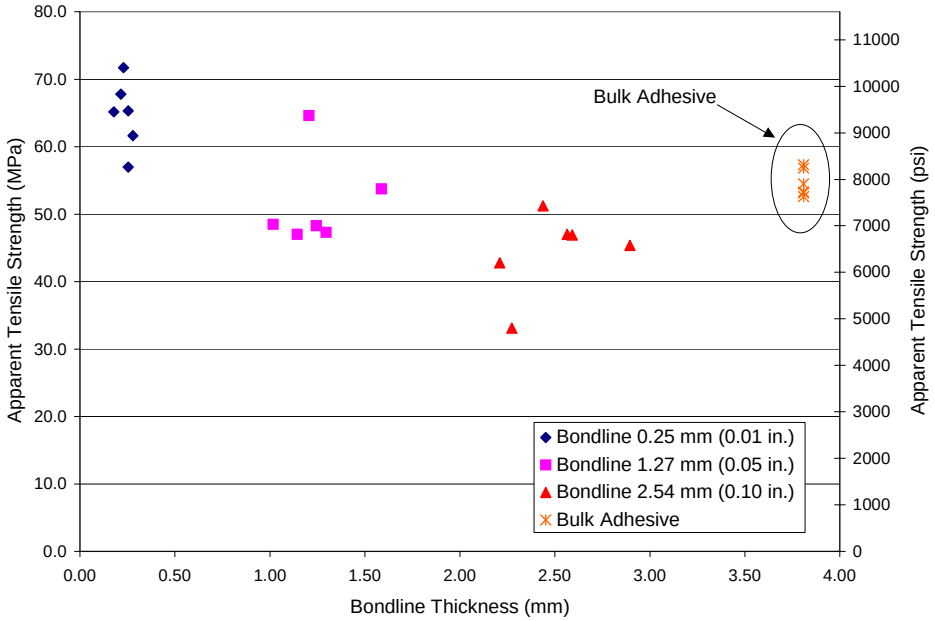

Figure 105. Apparent Tensile Strength of EA 9394 Butt Tensile Specimens

Table 11. Summary Results for EA 9394 Butt Tensile Tests

Nominal Bondline Thickness 0.25 mm (0.01 in.)				
	Bondline Thickness		Apparent Tensile Strength	
	mm	in.	MPa	psi
Average	0.23	0.009	64.8	9394
s	0.04	0.001	5.1	735
COV	15.2		7.8	

Nominal Bondline Thickness 1.27 mm (0.05 in.)				
	Bondline Thickness		Apparent Tensile Strength	
	mm	in.	MPa	psi
Average	1.25	0.049	51.6	7480
s	0.19	0.008	6.8	992
COV	15.4		13.3	

Nominal Bondline Thickness 2.54 mm (0.10 in.)				
	Bondline Thickness		Apparent Tensile Strength	
	mm	in.	MPa	psi
Average	2.50	0.098	44.4	6437
s	0.25	0.010	6.2	895
COV	10.0		13.9	

Bulk Adhesive		
	Apparent Tensile Strength	
	MPa	psi
Average	54.6	7922
s	2.0	291
COV	3.7	

s = standard deviation
COV = coefficient of variation

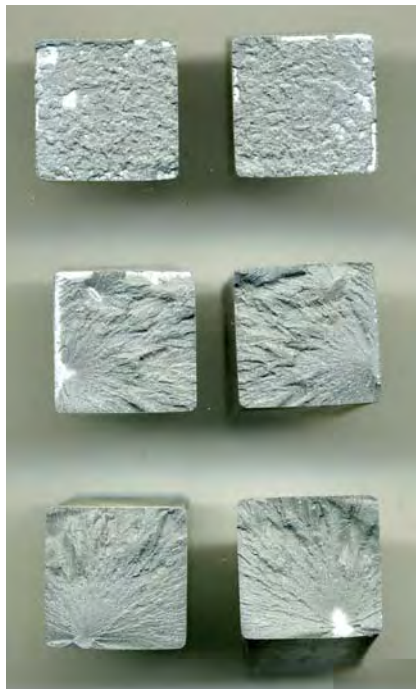

Bondline Thickness:

0.25 mm
(0.01 in.)

1.27 mm
(0.05 in.)

2.54 mm
(0.10 in.)

Figure 106. Characteristic Failures of Butt Tensile Specimens

5.6 IOSIPESCU MOIRÉ RESULTS.

High sensitivity moiré interferometry was performed on bonded Iosipescu shear specimens for each of the three bondline thicknesses using the primary adhesive EA 9394. The use of moiré interferometry allowed for the accurate measurement of the deformation across the entire surface of the adhesive bondline.

Moiré interferometry was performed on one specimen from each bondline thickness. All three specimens were loaded with 356 N (80 lb) of applied force, and the in-plane displacement fringe patterns were recorded with a digital camera. The U (horizontal)-displacement field was recorded first, and the V (vertical)-displacement field was recorded shortly after. The applied stress of 6.5 MPa (950 psi) was well within the linear elastic region of the shear stress-shear strain data from bulk adhesive tests.

Strains may be obtained from the displacement fringe patterns according to the relations

$$\varepsilon_x = \frac{1}{f}\frac{\partial N_x}{\partial x} \tag{23}$$

$$\varepsilon_y = \frac{1}{f}\frac{\partial N_y}{\partial y} \tag{24}$$

$$\gamma_{xy} = \frac{1}{f}\left(\frac{\partial N_x}{\partial y} + \frac{\partial N_y}{\partial x}\right) \tag{25}$$

where f = 2,400 lines/mm (60,960 lines/in.) and N_x and N_y are the fringe orders in the U- and V-displacement fields. Thus, the in-plane strains are proportional to the gradients in the fringe patterns. Details of strain calculations from the displacement fringe patterns are provided in Post, et al. [29].

The U- and V-displacement fields for the 0.25-mm (0.01-in.), 1.27-mm (0.05-in.) and 2.54-mm (0.10-in.) bondline specimens are shown in figures 107, 108, and 109, respectively. Note that for a state of perfect shear strain, both normal strain components ε_x and ε_y should be equal to zero. For the normal strain ε_x to be zero, the U-field fringe gradient in the x-direction should be zero. Thus, the U-field fringes should be oriented horizontally for ε_x to be zero. Likewise, for the normal strain ε_y to be zero, the V-field fringes should be oriented vertically such that the gradient in the vertical (y) direction is zero. Note that for all three specimens, the normal strains ε_x and ε_y appear to be zero in the central region of the adhesive bondline (midway between the notches). Additionally, the fringe density in the U-and V-fields appear to be approximately constant in the central region of the adhesive bondline, indicating that the magnitude of the shear strain is approximately constant throughout this region. However, all three specimens display an increase in transverse strain, ε_x, near the notch tips relative to the central region of the adhesive bondline. This increase is visible as an increased fringe density in the U-field within these regions. Additionally, a slight increase in axial strain, ε_y, visible as an increased fringe density in the V-field, is present near the notch tips. Note that these observations are consistent with results obtained from finite element analysis.

The in-plane shear strain is calculated using both the U- and V-displacement fields according to equation 25. To compare the shear strain distributions for the three different adhesive bondline thicknesses, the shear strain was calculated through the thickness of the bondline at a location midway between the notches. To provide a better comparison between the three different specimens, the shear strain distributions were each normalized with respect to the shear strain in the aluminum adherends at a specified point sufficiently distant from the adhesive interface. Figure 110 shows the shear strain distributions across the bondline thickness, normalized as

$$\gamma_{xy} \Big/ \gamma_{xy,adherend} \tag{26}$$

The results show that the shear strain is relatively constant across the bondline thickness in the central region of the specimen. Note that data near the adhesive/adherend interface are not presented due to uncertainty in identifying the exact location of the interface and problems with obtaining the fringe order derivatives in these regions. At the midpoint of the bondline thickness, the largest normalized shear strain occurs in the thin bondline, followed by the intermediate and thick bondlines. This trend is consistent with the finite element results (see figure 77), suggesting that the variation in shear strain between the different bondline thicknesses is due to the slight variations in stress state rather than a difference in the adhesive shear modulus.

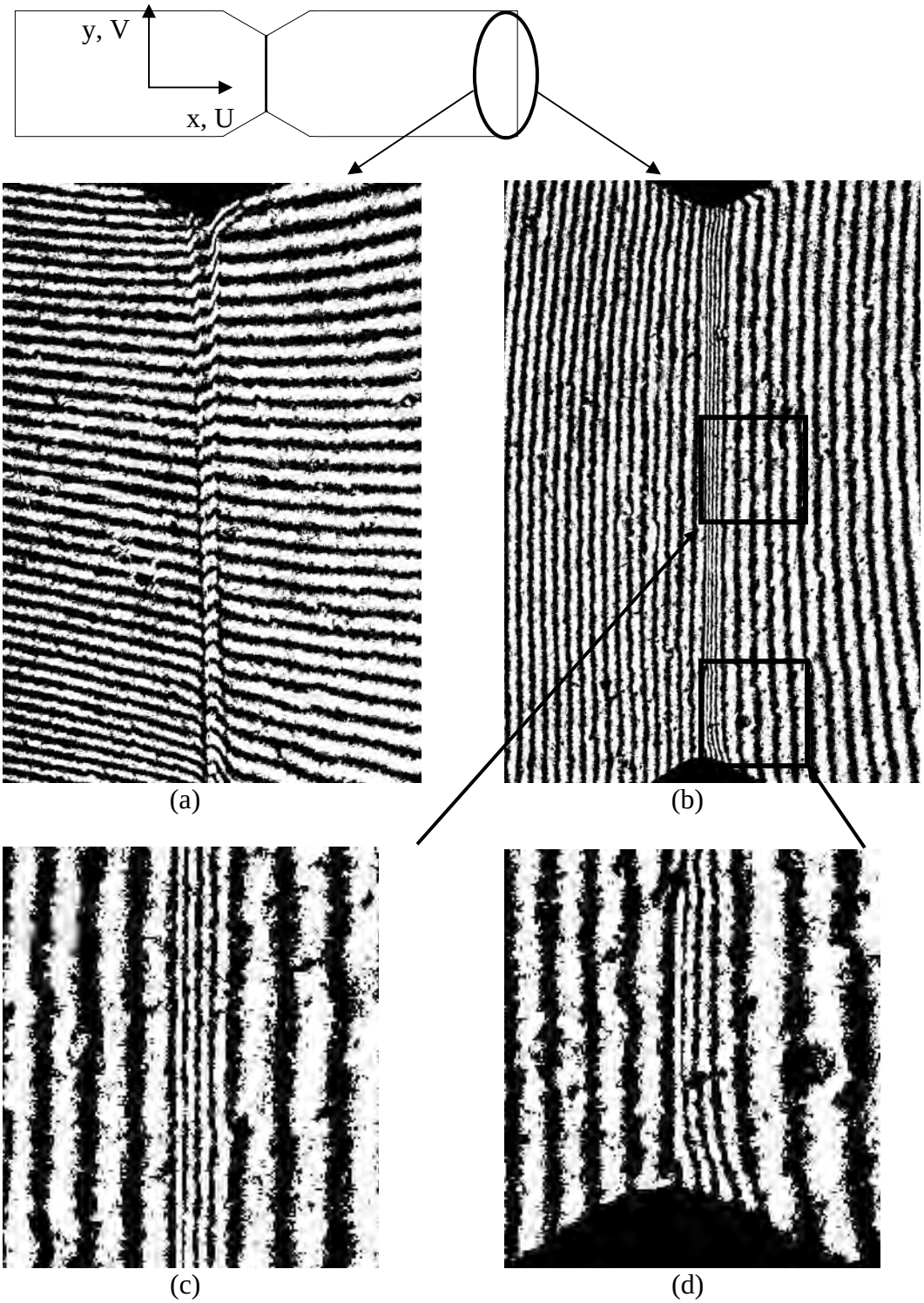

Figure 107. The (a) U- and (b) V-Displacement Fields for Bonded Iosipescu Specimen With 0.27-mm (0.010-in.) Bondline. Inserts are Enlarged Views of the V-Field at (c) the Center and (d) Around the Notch Tip of the Adhesive Bond

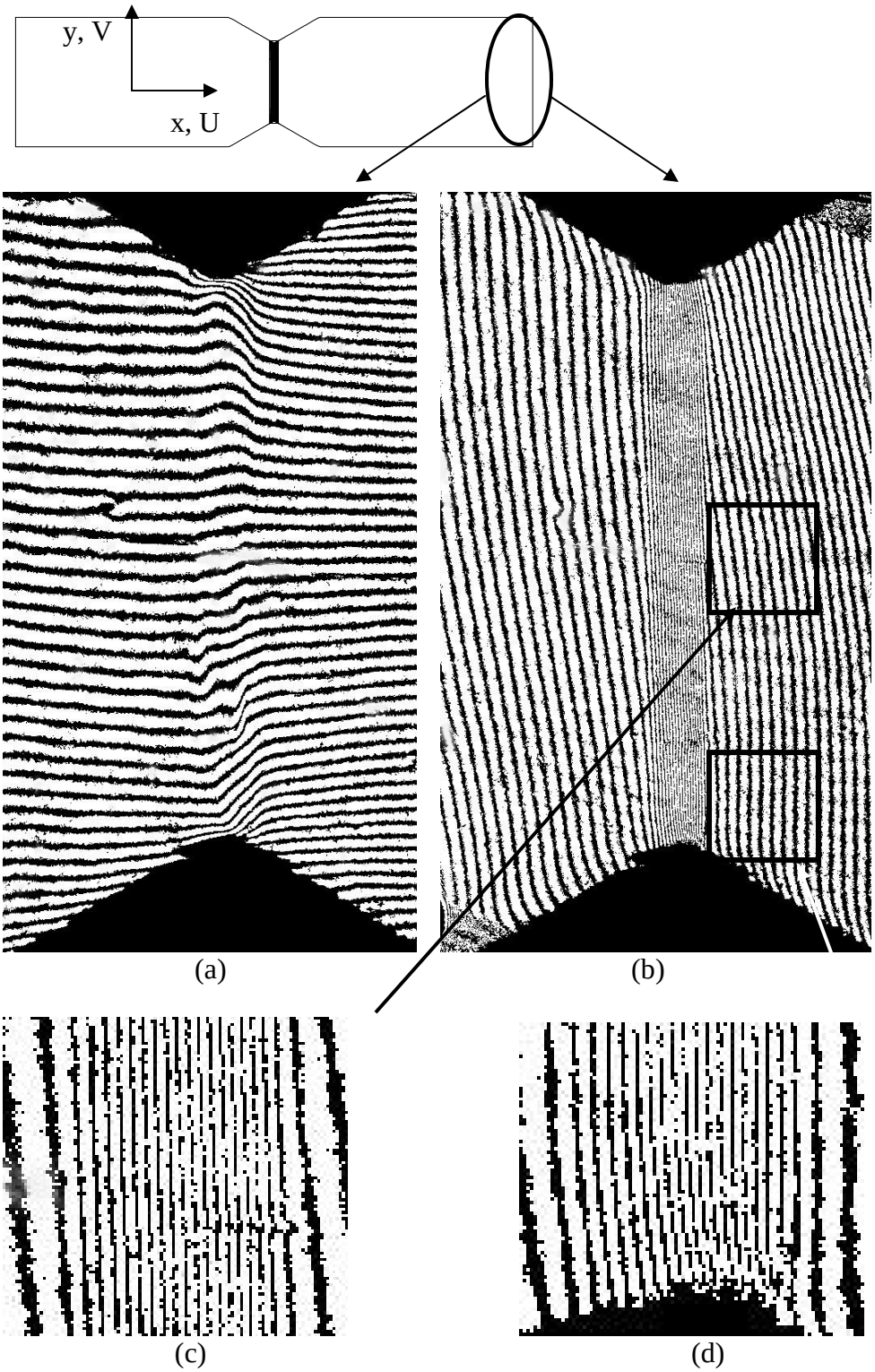

Figure 108. (a) U- and (b) V-Displacement Fields for Bonded Iosipescu Specimen With 1.19-mm (0.047-in.) Bondline. Inserts are Enlarged Views of the V-Field at (c) the Center and (d) Around the Notch Tip of the Adhesive Bond

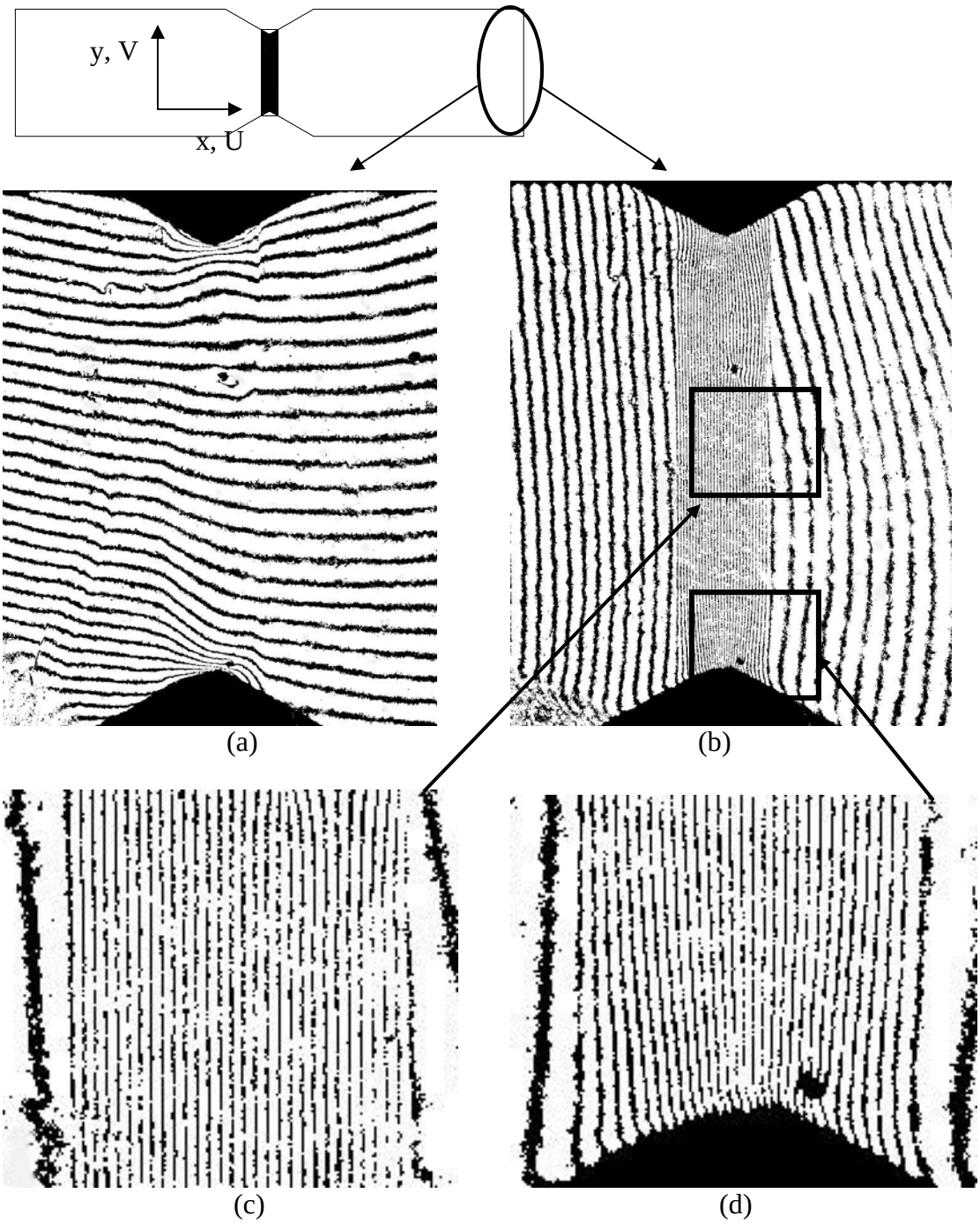

Figure 109. (a) U- and (b) V-Displacement Fields for Bonded Iosipescu Specimen With 2.54-mm (0.100-in.) Bondline. Inserts are Enlarged Views of the V Field at (c) the Center and (d) Around the Notch Tip of the Adhesive Bond

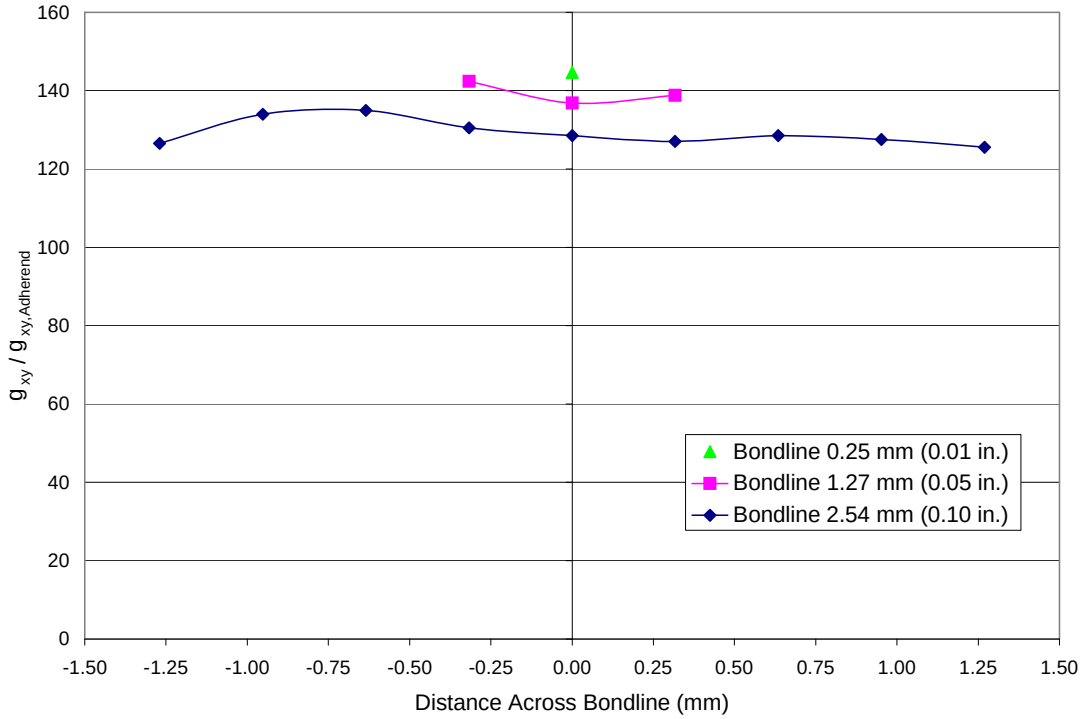

Figure 110. Shear Strain Across Adhesive Bondline (Normalized With Respect to Adherend Shear Strain)

5.7 THICK ADHEREND LAP JOINT MOIRÉ RESULTS.

The previous section described how moiré interferometry was used to quantify bondline deformation due to shear loading. In addition to the bonded Iosipescu specimens, moiré interferometry was also used to analyze adhesive shear behavior in a different loading configuration, the thick adherend lap joint. This lap joint test induces a shear loading into the adhesive by applying tension to the aluminum adherends. The fringe patterns for the lap joint are shown in figure 111 for the 0.25-mm (0.01-in.) bondline, figure 112 for the 1.27-mm (0.05-in.) bondline, and figure 113 for the 2.54-mm (0.10-in.) bondline. The same relationships between fringe order and strain that applied to the analysis of the bonded Iosipescu specimens also apply to the thick adherend lap joint. Note that the improvised loading configuration for the lap joint test on the optical table did not allow for the applied load to be monitored. As displacement was applied through a screw mechanism, however, it was possible to apply approximately the same load to each specimen. Even without knowledge of the exact load magnitude, the moiré results provide a quantitative comparison of the strain distribution throughout each adhesive test section and a qualitative comparison between the different bondline thicknesses.

The three specimens tested with different bondline thicknesses all displayed similar deformation patterns. Of the two shear strain components (dN_x/dy and dN_y/dx), dN_y/dx is zero throughout most of the adhesive test section. This is evidenced by the horizontal nature of the fringes in the V-displacement field. However, dN_y/dx is negative adjacent to the ends of the adhesive bondline, reducing the magnitude of γ_{xy} in these regions. The dominant shear strain component

is dN_x/dy, represented by the y direction fringe gradient in the U-displacement field. Note that this gradient is relatively uniform across the bondline thickness and throughout a majority of the adhesive. Approaching the ends of the lap joint, however, the dN_x/dy component of shear strain increases, indicating an increase in γ_{xy} near the ends of the bondline. Together, these observations suggest that although the magnitude of γ_{xy} is relatively constant throughout the central region of the adhesive bondline, the shear stress increases near the ends of the bondline and subsequently decreases immediately adjacent to the ends. These findings are in agreement with finite element results shown in figure 78.

For all three bondline thicknesses, the axial (horizontal) normal strain, ε_x, is zero throughout most of the test section. This result is evidenced by the nearly horizontal fringes in the U-displacement field. Note, however, that a small amount of axial strain exists at the ends of the lap joint. In contrast, the region of largest transverse strain, ε_y, occurs in the central region of the adhesive bondline and decreases near the ends. This strain component is obtained from the y direction fringe gradient in the V-displacement field. These results from moiré interferometry are consistent with those obtained from finite element analysis and support the concerns that transverse normal stresses throughout the test section as well as the concentrations of normal and shear stress at the lap joint ends may produce test results that are not representative of the actual adhesive shear properties.

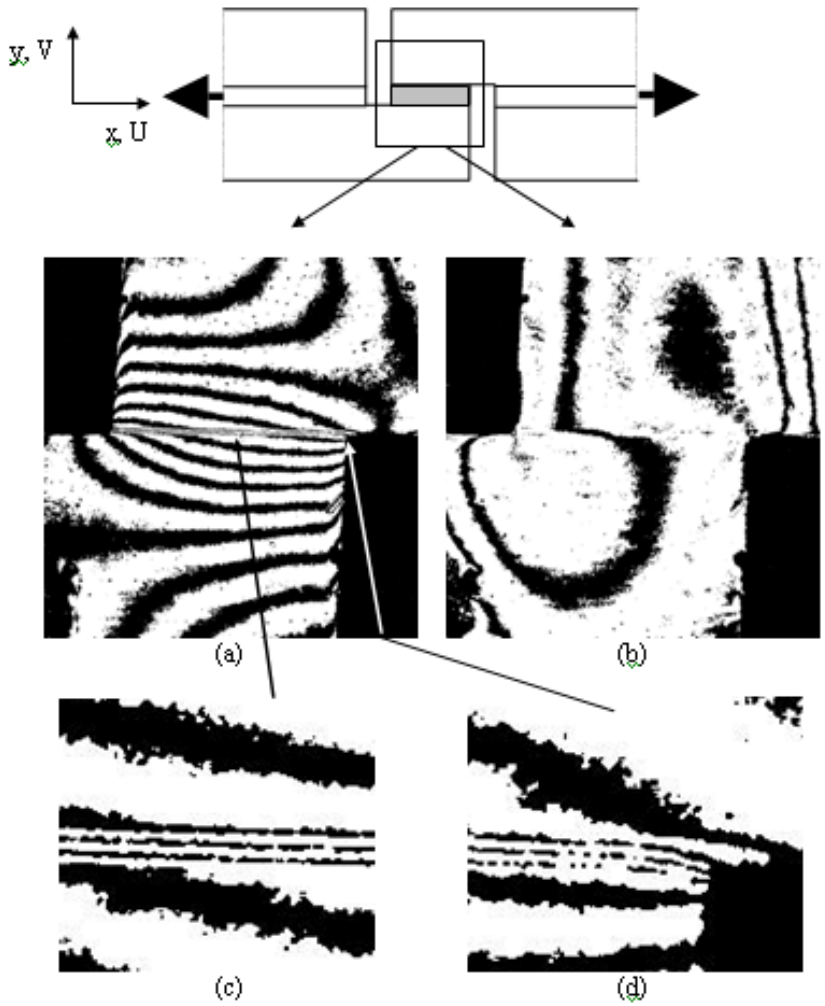

Figure 111. (a) U- and (b) V-Displacement Fields for Thick Adherend Lap Joint Specimen With 0.25-mm (0.010-in.) Bondline. Inserts are Enlarged Views of the U-Field at (c) the Center and (d) End of the Lap Joint

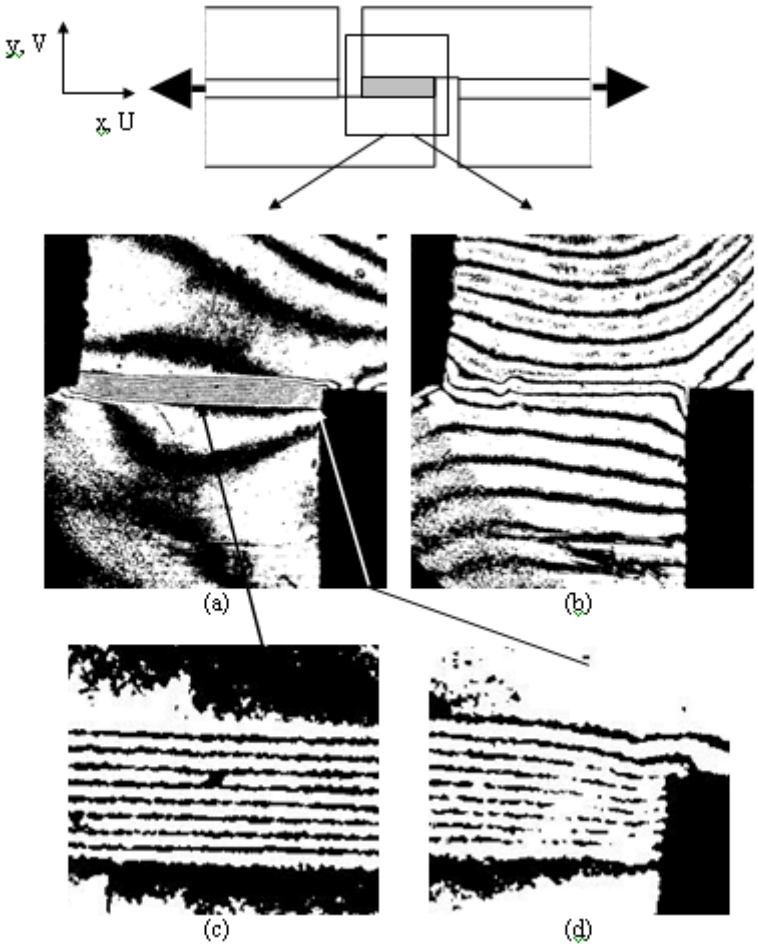

Figure 112. (a) U- and (b) V-Displacement Fields for Thick Adherend Lap Joint Specimen With 1.27-mm (0.050-in.) Bondline. Inserts are Enlarged Views of the U-Field at (c) the Center and (d) End of the Lap Joint

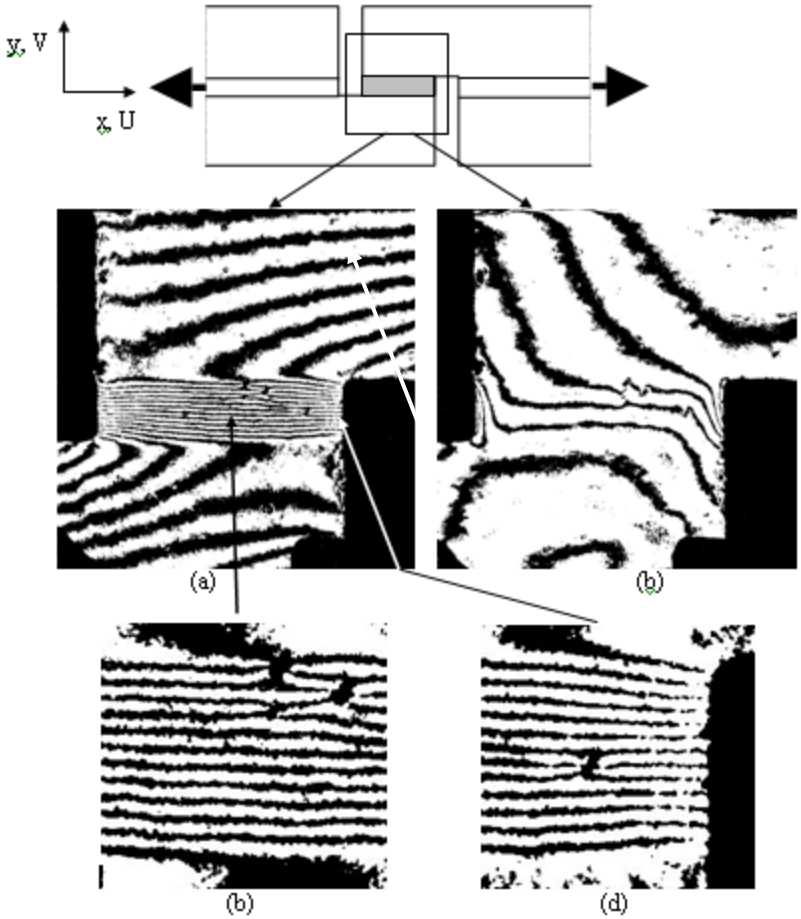

Figure 113. (a) U- and (b) V-Displacement Fields for Thick Adherend Lap Joint Specimen With 2.54-mm (0.100-in.) Bondline. Inserts are Enlarged Views of the U-Field at (c) the Center and (d) End of the Lap Joint

6. SUMMARY AND CONCLUSIONS.

The objective of this research investigation was to determine if the material properties of structural adhesives differ between their thin-film in situ and bulk forms. Both the tensile and shear properties of adhesives were investigated using a combined numerical and experimental approach. In situ and bulk adhesive specimens were modeled using finite element analysis, and experimental tests was performed. For in situ adhesive analysis and experiments, three bondline thicknesses were investigated: 0.25 mm (0.01 in.), 1.27 mm (0.05 in.), and 2.54 mm (0.10 in.). Three aerospace-grade adhesives were used: Loctite EA 9394, EA 9392, and EA 9360, with EA 9394 serving as the primary adhesive in the investigation. Shear testing focused on the V-notched Iosipescu shear specimen. Additionally, the thick adherend lap joint test configuration was evaluated. Tensile testing focused on adhesively bonded butt joint specimens as well as bulk adhesive bar specimens.

Extensive linear-elastic finite element analysis was conducted on the adhesively bonded Iosipescu specimen to determine the notch geometry producing the most desirable shear stress state in the adhesive bondline. Several different U-notch and V-notch geometries were considered. The results of these analyses indicated that the preferred notch geometry for the in situ specimens was a 3.8-mm (0.15-in.) deep V-notch (producing a notch-depth-ratio (NDR) of 0.20) and a notch angle of 120°. For the bulk adhesive Iosipescu specimens, the same 3.8-mm (0.15-in.)-deep V-notch was selected, but with a notch angle of 90°. For both the in situ and bulk adhesive specimens, all other specimen dimensions were the same as the standard Iosipescu specimen specified in ASTM D 5379. These geometric features provided an optimal state of stress in the specimen by reducing the magnitude of the normal stresses in the test section, reducing stress concentrations associated with the notches, and creating a uniform shear stress distribution throughout the adhesive test section.

The results obtained from this investigation suggest that the adhesive properties obtained from bulk adhesive specimens are valid for use in structural analysis of in situ thin-film adhesives. The results from in situ shear testing showed that as the bondline thickness increased, the apparent shear strength decreased slightly. This finding was consistent with the results obtained from finite element analysis, which showed that the shear stress concentration increased slightly as the adhesive bondline thickness increased. Additionally, shear strengths obtained from bulk adhesive testing were comparable to shear strengths obtained from in situ testing. This result was expected, since the shear stress concentrations predicted in the bulk adhesive shear specimens were approximately equal in magnitude to those from the intermediate-thickness bondline specimens. The results from moiré interferometry confirmed that the strain variations in the adhesive bondlines corresponded to variations predicted using finite element analysis. Additionally, the moiré interferometry results showed that there is no significant difference in adhesive shear modulus between the three thicknesses investigated. Combined, these results suggest that the shear strength and shear modulus of the adhesives investigated do not differ when tested in their thin-film in situ and bulk forms. Additionally, these results show that the Iosipescu shear test configuration is well suited for both in situ and bulk adhesive shear testing.

Finite element analyses and moiré interferometry experiments were also performed for the thick adherend lap shear test, ASTM D 5656. Finite element results showed that a relatively

nonuniform state of shear stress exists throughout the adhesive bondline and that the stress state changes significantly as the bondline thickness increases. All three bondline thicknesses investigated produced large normal stress concentrations at the interface corners. The results from moiré interferometry were consistent with those obtained from finite element analysis and supported the concerns that transverse normal stresses throughout the test section as well as the concentrations of normal and shear stress at the lap joint ends may produce test results that are not representative of the actual adhesive shear properties.

The results of butt tensile tests showed that as the bondline thickness increased, the apparent tensile strength decreased. This finding was in agreement with results obtained from finite element analysis, which showed the distribution of tensile stress throughout the bondline becoming less uniform with greater bondline thickness. Therefore, the experimentally obtained decrease in apparent tensile stress appears to be produced by variations in stress distribution throughout the adhesive bondline. The apparent tensile strength obtained from bulk adhesive tensile testing was between the values of apparent tensile strengths obtained for the thin and intermediate bondline thicknesses. These results suggest that the apparent variation in tensile strength as a function of bondline thickness is a result of variations in the adhesive stress state, not variations in the tensile strength of the adhesive.

While the Iosipescu shear test configuration appears to be well suited for both in situ and bulk adhesive shear testing, some precautions must be taken during specimen preparation. For in situ shear testing, care must be taken to ensure that the two specimen halves are coplanar when bonding. Additionally, since the bonded Iosipescu adherends are machined to final dimensions before bonding, the use of an alignment fixture is required to achieve the desired bond thickness. Similar specimen alignment precautions are necessary when preparing in situ butt tensile specimens. While the in situ shear specimen may be used to obtain adhesive shear strength data, the test specimen does not accommodate the measurement of shear strain using a bonded resistance strain gage. Thus, this test methodology is not capable of producing a stress versus strain curve or the shear modulus of the adhesive without the development of a specialized extensometer or the use of an optical technique.

Using bulk adhesive specimens for either shear or tensile testing allows for the measurement of strain using bonded resistance strain gages, and thus the determination of elastic properties. Due to the relatively low modulus of adhesives, it is necessary to correct for any reinforcement effects when using bonded strain gages. Additionally, the fabrication of bulk adhesive specimens requires special care to minimize void formation within the specimen. However, adhesive degassing methods, including the mixing of the adhesive under vacuum or in a static mixer, may be used with relatively high-viscosity, two-part adhesives.

7. REFERENCES.

1. Standard Test Method for Apparent Shear Strength of Single-Lap-Joint Adhesively Bonded Metal Specimens by Tension Loading," ASTM D 1002, *Annual Book of ASTM Standards*, Vol. 15.06, ASTM International, West Conshohocken, PA, 2001.

2. "Standard Test Method for Strength Properties of Adhesives in Shear by Tension Loading of Single-Lap-Joint Laminated Assemblies," ASTM D 3165, *Annual Book of ASTM Standards*, Vol. 15.06, ASTM International, West Conshohocken, PA, 2001.

3. Tomblin, J., Seneviratne, W., Kim, H., and Lee, J., "Characterization of In-Plane, Shear Loaded Adhesive Lap Joints: Experiments and Analysis," FAA report DOT/FAA/AR-03/21, May 2003.

4. Yang, C., Tomblin, J., and Guan, Z., "Analytical Modeling of ASTM Lap Shear Adhesive Specimens," FAA report DOT/FAA/AR-02/130, February 2003.

5. "Standard Test Method for Thick adherend Metal Lap-Shear Joints for Determination of the Stress-Strain Behavior of Adhesives in Shear by Tension Loading," ASTM D 5656, *Annual Book of ASTM Standards*, Vol. 15.06, ASTM International, West Conshohocken, PA, 2001.

6. Kassapoglou, C. and Adelman, J.C., "KGR-1 Thick Adherend Specimen Evaluation for the Determination of Adhesive Mechanical Properties," *Proceedings of the 23rd International SAMPE Technical Conference*, Society for the Advancement of Material and Process Engineering, Covina, CA, 1991, pp. 162-176.

7. "Standard Test Method for Shear Properties of Composite Materials by the V-Notched Beam Method," ASTM D 5379, *Annual Book of ASTM Standards*, Vol. 15.03, ASTM International, West Conshohocken, PA, 2001.

8. Adams, D.O., Moriarty, J., Gallegos, A., and Adams, D.F., "Development and Evaluation of the V-Notched Rail Shear Test for Composite Laminates," FAA report DOT/FAA/AR-03/63, September 2003.

9. Dolev, G. and Ishai, O., "Mechanical Characterization of Adhesive Layer In situ and as Bulk Material," *Journal of Adhesion*, Vol. 12, No. 4, 1981, pp. 283-294.

10. Chai, H., "Deformation and Failure of Adhesive Bonds Under Shear Loading," *Journal of Materials Science*, Vol. 28, No. 18, January 1993, pp. 4944-4956.

11. Peretz, D., *Journal of Adhesion*, Vol. 9, 1978.

12. Lilleheden, L., "Mechanical Properties of Adhesives In situ and in Bulk," *International Journal of Adhesion and Adhesives*, Vol. 14, No. 1, 1994, pp. 31-37.

13. Tomblin, J., Yang, C., and Harter, P., "Investigation of Thick Bondline Adhesive Joints," FAA Report DOT/FAA/AR-01/33, June 2001.

14. Knollman, G.C., "Variation of Shear Modulus Through the Interfacial Bond Zone of an Adhesive," *International Journal of Adhesion and Adhesives*, Vol. 5, No. 3, 1985.

15. Roche, A.A. and Bouchet, J., "Formation of Epoxy/Metal Interphases," *Proceedings of Structural Adhesives in Engineering VI*, Institute of Materials, 2001.

16. Wycherley, G.W., Mestan, S.A., and Grabovac, I., "A Method for Uniform Shear Stress-Strain Analysis of Adhesives," *Journal of Testing and Evaluation*, Vol. 18, No. 3, May 1990, pp. 203-209.

17. Grabovac, I. and Morris, C.E.M., "The Application of the Iosipescu Shear Test to Structural Adhesives," *Journal of Applied Polymer Science*, Vol. 43, 1991, pp. 2033-2042.

18. Ding, S., Erdinc, I., Buchholz, F., and Kumosa, M., "Optimization of the Adhesive Joint Iosipescu Specimen for Pure Shear Test," *International Journal of Fracture*, Vol. 76, 1996, pp. 1-20.

19. Ignjatovic, M., Chalkley, P., and Wang, C., "The Yield Behaviour of a Structural Adhesive under Complex Loading," Defence Science and Technology Organisation Report DSTO-TR-0728, September 1998.

20. Asundi, A., "Deformation in Adhesive Joints Using Moire Interferometry," *International Journal of Adhesion and Adhesives*, Vol. 7, No. 1, January 1987, pp. 39-42.

21. Post, D., Czarnek, R., Wood, J.D., and Joh, D., "Deformation and Strains in a Thick Adherend Lap Joint," *Adhesively Bonded Joints: Testing, Analysis, and Design, ASTM STP 981*, W.S. Johnson, ed., American Society for Testing and Materials, Philadelphia, 1988, pp. 107-118.

22. ANSYS, Version 6.0, ANSYS, Inc., Canonsburg, PA, 1994.

23. Surfer – Surface Mapping System, Version 7.04, Golden Software, Inc., Golden, CO, 2001.

24. "Standard Test Method for Tensile Properties of Plastics," ASTM D 638, *Annual Book of ASTM Standards*, Vol. 8.01, ASTM International, West Conshohocken, PA, 2001.

25. "Standard Practice for Preparation of Bar and Rod Specimens for Adhesion Tests," ASTM D 2094, *Annual Book of ASTM Standards*, Vol. 15.06, ASTM International, West Conshohocken, PA, 2001.

26. "Standard Test Method for Tensile Strength of Adhesives by Means of Bar and Rod Specimens," ASTM D 2095, *Annual Book of ASTM Standards*, Vol. 15.06, ASTM International, West Conshohocken, PA, 2001.

27. "Standard Practice for Preparation of Aluminum Surfaces for Structural Adhesives Bonding (Phosphoric Acid Anodizing)," ASTM D 3933, *Annual Book of ASTM Standards*, Vol. 15.06, ASTM International, West Conshohocken, PA, 2001.

28. Ajovalasit, A. and Zuccarello, B., "Local Reinforcement Effect of a Strain Gauge Installation on Low Modulus Materials," *Journal of Strain Analysis*, Vol. 40, No. 7, 2005, pp. 643-653.

29. Post, D., Han, B., and Ifju, P., *High Sensitivity Moire: Experimental Analysis for Mechanics and Materials*, Springer-Verlag, New York, 1994.